VitalSensors - New wearable sensors for monitoring First Responders

João Manuel Figueira da Silva

Master Thesis

Supervisor: PhD João Paulo Cunha

Collaborator: Nuno Ferreira, Biodevices SA

MSc in Bioengineering

December, 2015

Resumo

Os sistemas de monitorização vestíveis são extremamente úteis para a monitorização dos profissionais de primeira resposta, enquanto os mesmos se encontram em ação. Como estes operam frequentemente em ambientes hostis, importa monitorizar tanto parâmetros vitais como ambientais, bem como providenciar os dados recolhidos aos chefes de equipa em comando das operações, pois essa informação pode permitir maximizar a eficácia operacional e minimizar os riscos a que os profissionais de primeira resposta estão sujeitos, tendo potencial para, no futuro, ajudar a reduzir o número de vitimados durante as operações.

A presente tese é focada nos agentes de primeira resposta, e tem como objetivo dar mais e melhor informação aos mesmos, através de melhorias, diretas ou não, num sistema vestível já existente, o VitalResponder. Para tal, foi adotada uma estatégia a três passos, onde o primeiro passo visa dar mais informação, através da introdução de novos sensores, o segundo visa a seleção da informação mais relevante a partir dos dados adquiridos, bem como a sua transmissão de modo eficiente aos chefes de operações, e o terceiro visa dar informação fisiológica importante, que não pode ser medida com sensores, de forma intuitiva aos chefes de operações.

O VitalResponder é uma versão melhorada do VitalJacket® - uma t-shirt da Biodevices SA que grava sinais eletrocardiográficos com qualidade clínica, bem como de actigrafia - que possui uma maior gama de sensores capazes de medir parâmetros vitais e ambientais. Por outro lado, existe ainda o VitalLogger, que expande as capacidades do VitalJacket® ao introduzir sensores de saturação de oxigénio, temperatura ambiente e humidade relativa. Como o VitalLogger pode ser integrável no VitalResponder, o desenvolvimento do VitalLogger expande, por si só, as potencialidades do VitalResponder.

No primeiro passo desta tese, o firmware e SDK do VitalJacket foram expandidos para o VitalLogger, de modo a aceitar os novos sensores, e, a pensar nas necessidades futuras em adicionar novos sensores, uma nova versão do firmware para o VitalLogger foi desenvolvida de modo a funcionar numa arquitetura modular. No segundo passo foi criado um sistema que analisa os dados medidos pelos sensores e seleciona apenas a informação relevante a enviar, com o objetivo de reduzir a redundância dos dados. Este sistema foi implementado no firmware do VitalLogger apenas para controlo da temperatura ambiente. Para além disso, foi adicionado a uma aplicação de teste já existente, para Android, um sistema de alarme que alerta quando a temperatura ambiente passa os níveis considerados seguros. No terceiro passo, para fornecer informação que não pode ser medida diretamente com sensores, foi criado um sistema para prever a temperatura corporal a partir do ritmo cardíaco, sendo essa temperatura usada para calcular um índice de stress e fadiga, o PSI.

Como resultado desta tese obteve-se um sistema com funcionalidades acrescidas, o VitalLogger, que está ainda em fase de protótipo. O sistema de previsão de temperatura corporal não se encontra ainda finalizado, pelo que não foi integrado no sistema, mas, com melhorias futuras, é possível obter um sistema concorrente dos que existem no mercado.

Abstract

Wearable monitoring technologies are extremely useful to monitor first responders whilst in action. As first responders frequently operate in hazardous environments, it is of critical interest to monitor both vital and environmental parameters, and to provide that information to the commanding entities in charge of operations, as this information might be used to enhance first responders' efficacy while minimizing their own risk, presenting potential to diminish on duty casualties.

The present thesis is focused on first responders, and its objective is focused on giving, not only more, but better information to first responders, by improving, directly or not, an existing wearable system, VitalResponder. For that purpose, a three step work plan was adopted, where the first step aims to provide more information by implementing new sensors, the second step aims to intelligently select only the most relevant information from acquired data, as well as conveying it more efficiently to the chiefs in charge of operations, and the third one aims to provide important physiological indicators, that cannot be acquired directly with sensors, intuitively to chiefs in charge of operations.

VitalResponder is an improved version of VitalJacket® - a t-shirt from Biodevices SA which acquires actigraphy and clinical quality electrocardiogram (ECG) signals - that possesses a wider range of sensors capable of sensing both vital and environmental parameters. Moreover, there exists VitalLogger, which expands the capabilities of VitalJacket® by introducing sensors for oxygen saturation, ambient temperature and relative humidity. Since VitalLogger can be integrated in VitalResponder's system, the development of VitalLogger also leads to an increase in VitalResponder's potentialities.

In the first step of this thesis, VitalJacket's firmware and SDK were expanded for VitalLogger, in order to accept the newly implemented sensors, and, with future necessities in terms of adding new sensors in mind, a new version for VitalLogger's firmware was developed, which prepares the system to work in a modular architecture. In the second step, a system that selects important information from sensed signals was developed with the objective of reducing data redundancy. This control system was implemented in VitalLogger's firmware, to control ambient temperature. Moreover, an alarm system was added to an existing test application, for Android, which alerts when ambient temperature leaves what is considered the safe zone. In the third step, with the objective of providing important physiological data that cannot be sensed directly, a core temperature predictor that uses only heart rate measurements was created, with core temperature predictions being further used to compute a strain index, PSI.

As a result from this thesis' work, a system with augmented functionalities was obtained - the VitalLogger - which is still in prototype stage. Furthermore, the core temperature estimator implemented during this thesis is not complete yet, therefore this version of the estimator was not integrated in VitalLogger. However, with future work, a system that can rival with those that exist in the market can be obtained.

Agradecimentos

Primeiro que tudo, quero agradecer à minha família por todo o seu apoio ao longo desta "curta" mas marcante viagem que foi o meu percurso universitário. Para alguém que cai redondo, e a sós, numa realidade diferente e distante da qual estava habituado, o vosso apoio tornou tudo imensamente mais fácil, principalmente na fase inicial. Nesse sentido, deixo o meu terno agradecimento aos meus pais, irmão, avós e padrinhos, que sempre acreditaram em mim e me incentivaram a ambicionar por mais.

Deslocalizando os meus agradecimentos de Leiria para o Porto, quero começar por agradecer ao Professor Doutor João Paulo Cunha, pelo seu apoio e por me ter dado a oportunidade de ser parte integrante de um projeto aliciante, que mais do que um mero projeto, poderá num futuro mais ou menos próximo constituir uma solução real a ser comercializada. Seguidamente, quero agradecer ao Professor Doutor Miguel Velhote Correia pela arguência da presente tese, bem como por todas as sugestões fornecidas com o intuito de melhorar a mesma. Para além disso, quero agradecer a oportunidade de trabalhar em colaboração com a Biodevices SA, onde pude aprender bastante com o Nuno Ferreira, Vitor Castro e Catarina Ricca. A todos vós deixo o meu sincero obrigado. Quero ainda deixar uma palavra de apreço a todos os membros do BRAIN-LAB com quem pude trabalhar e conviver, e ao Dustin que me deu feedback extremamente valioso ao longo desta tese.

Passo agora aos agradecimentos a quem me acompanhou ao longo destes 5 anos passados na bela cidade do Porto (por quem fiquei a nutrir também um carinho especial), tendo contribuído em maior ou menor parte para o meu crescimento profissional, mas acima de tudo pessoal. Nesse sentido, quero começar por agradecer aos meus companheiros de casa, Tiago e Fábio que, tal como eu, iniciaram esta etapa uns putos, e acabaram por terminar como algo mais próximo daquilo que um homem deve ser. Um enorme obrigado também à Inês e à Mariana, que com todas as suas palhaçadas me conseguiram animar em vários dias enfadonhos. Sem ordem de preferência, deixo ainda o meu obrigado ao Freixo, João Costa, Miguel, Pedro, Dinis, Frederico, Bruna, Jéssica.

Por fim, e porque considero dignos de um obrigado "especialmente" especial por tudo o que passámos, agradeço agora aos que dificilmente cairão no meu esquecimento, com aquele cunho pessoal que vocês bem conhecem.

Em primeiro lugar deixo um obrigado ao Nuno, que para além de ter sido também companheiro de casa, se tornou como que um segundo irmão com quem partilho muito do que sou (tantos momentos de telepatia não podem ter sido apenas sorte. Como diria uma certa pessoa, "uncanny").

Ao Duarte, pela grande amizade que tenho com ele, pelos muitos e bons momentos que passámos juntos, e pelo seu incalculável dom de moralizar os outros, refazendo as pessoas das cinzas. Como cada um tem aquilo que merece, tu só poderás ter mesmo um futuro risonho.

Ao Jorge ... ao Jorge, por aquilo que foi, não é, mas espero que volte a ser.

Ao Hugo, pelo seu sentido de humor mais clínico que as cotoveladas do Slimani, e mais natural que os mergulhos do Gaitán (vamos ser factuais: não é difícil), pela sua franja de clubite e apartidarite que dão azo a algumas das melhores discussões que já pude presenciar, e por tudo o que me ajudou e ensinou ao longo destes anos.

Ao meu grande amigo Daniel, por todo o seu discUrso fanático pelo seu clube do coração, que me proporcionou belos momentos de diversão. A mim... e ao RGS, porque mesmo ele consegue ter alguma noção. Mas contra factos não há argumentos, e quando a discussão é centrada em alguém dotado de rigor como só tu o consegues, não existe autocarro que resista às investidas do Tacuara. Obrigado pela disponibilidade para o que fosse preciso (qual farmácia 24/7), por seres das pessoas mais únicas e indiferentes às opiniões de outrem (leia-se: por não seres um Daniel vai com os outros), e por isso mesmo teres reservado um lugar no Panteão do meu hipocampo e estruturas anatómicas vizinhas.

Por fim, e porque os últimos são os primeiros, neste caso literalmente, quero agradecer ao António, o primeiro verdadeiro amigo que fiz pelos ares do norte. Uma amizade que começou pelos trabalhos de grupo, mas que rapidamente transcendeu tudo isso. Por toda a companhia que me fizeste, pelos conselhos que me deste, pelos momentos que me aturaste, pela tua tamanha prestabilidade e lealdade, não tenho verdadeiramente meios como te agradecer pela pessoa que foste, e ainda hoje és, neste curto excerto de texto.

A todos vós, e aos que me esqueci (ironias do destino), deixo mais uma vez o meu obrigado, e a promessa de que vos manterei por muitos e muitos anos comigo, ou até à doença de Alzheimer aparecer (bate na madeira e espera que um de vocês encontre a cura para a doença, porque o karma vai bater à porta).

João Manels

"Isto não vem nos livros"

Jorge Jesus

Contents

List of Figures

List of Tables

List of Abbreviations

6LoWPAN	IPv6 over Low power Wireless Personal Area Networks
ANS	Autonomic Nervous System
BAN	Body Area Network
BANC	Body Area Network Coordinator
BP	Blood Pressure
BPV	Blood Pressure Variability
BR	Breathing Rate
BSN	Body Sensor Network
BT	Body Temperature
CO	Carbon Monoxide
CO_2	Carbon Dioxide
CRC	Cyclic Redundancy Check
CT	Core Temperature
ECG	Electrocardiogram
EEG	Electroencephalography
EMG	Electromyography
FFT	Fast Fourier Transform
FPF	False Positive Fraction
GPS	Global Positioning System
GSR	Galvanic Skin Response
HMM	Hidden Markov model
HR	Heart Rate
HRV	Heart Rate Variability
IG	Inner Garment
IP	Inductive Plethysmography
I/O	Input/Output
LED	Light Emitting Diode
MEMS	Microelectromechanical Systems
MINDS	Miniaturized, Integrated, Networked, Digitalized and Standardized
NN	Neural Network
OG	Outer Garment
PCG	Phonocardiography

PHS	Personal Health Systems
PSD	Power Spectral Density
PSI	Physiological Strain Index
PTT	Pulse Transit Time
PWV	Pulse Wave Velocity
RFID	Radio-frequency Identification
RMSE	Root Mean Square Error
ROC	Receiver Operating Characteristic
SDK	Software Development Kit
SPI	Serial Peripheral Interface
SpO_2	Blood Oxygen Saturation
SVM	Support Vector Machine
TEB	Thoracic Electrical Bioimpedance
TPF	True Positive Fraction
VL	VitalLogger
WHS	Wearable Health Systems
WSN	Wireless Sensor Network

Chapter 1

Introduction

1.1 Background and Context

Technologic advances are constantly redefining healthcare, being personalized healthcare the latest revolution in the healthcare domain. Ubiquitous computing and electronic textiles, with the former resulting from the merging of two distinct areas, have led to the development of wearable systems capable of monitoring both vital and environmental parameters. However, these systems face the enormous challenge of monitoring physiological status in a continuous, non-invasive and real-time manner. Moreover, these systems need to be integrated in communication network structures in order to enable control at a greater scale (e.g. multi-individual real-time monitoring).

While wearable technologies have been mostly designed for vital sign monitoring for clinical applications, these technologies are also useful to monitor first responders whilst in action. As first responders frequently operate in hazardous environments, it is critical to monitor both vital and environmental parameters, and to provide that information to the leaders in charge of operations. This information can make the difference by increasing tactical awareness and supporting critical decision making, allowing first responders to maximize their efficacy while minimizing their own risk [1].

VitalResponder project is an example of a wearable monitoring system designed for first responders. Being an evolution of VitalJacket®, VitalResponder has a wider range of embedded sensors and accepts different external sensors that enable the measurement of not only vital but also environmental parameters, making it a resourceful tool capable of delivering reliable monitoring for first responders. VitalLogger is a prototype of a wearable health device that seeks to expand the sensing capabilities of the VitalJacket, and that can therefore be integrated in VitalResponder in the future.

Work developed in this thesis is part of a greater project, which has contributions from two other MSc students. The aim of this greater project is to aggregate data from diverse vital signs and environmental parameters. Figure 1.1 presents a basic view of this project, where the hardware and low-level firmware part of VitalLogger will be developed

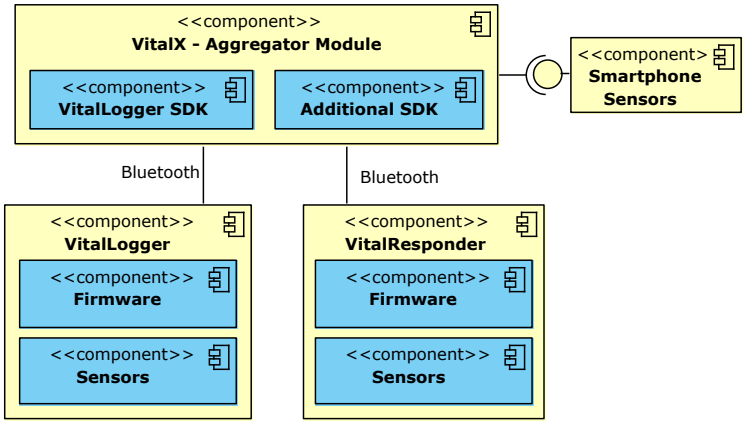

Figure 1.1: Basic overview of the component architecture where this thesis is inserted.

by another student's Master Thesis, and the aggregator module that condenses data from all devices, VitalX, will also be developed in another student's Master Thesis. This Master Thesis is focused on the high-level firmware and SDK for VitalLogger, with the aim of being integrated in the future in other systems such as in the VitalResponder. This will be explained in more detail in Chapter 3.

This Master Thesis was developed in the Faculty of Engineering of the University of Porto and INESC TEC Porto, in collaboration with Biodevices SA. Work developed in this thesis dealt with existing wearable health devices as well as with prototypes, and had the objective of upgrading those systems according to the specific needs of First Responders. This work was included in an I&D group hosted at INESC TEC, the Biomedical Research and INnovation LABoratory (BRAIN-LAB), and supervised by Professor Ph.D. João Paulo Cunha.

Furthermore, during the time of this thesis, a three month undergraduate internship was completed at Carnegie Mellon University, Pittsburgh, in the Human Sensing Lab (Robotics Institute), with a small evaluation report from this internship being provided in Appendix A.

1.2 Motivation

Wearable health devices is a growing market that is attracting a lot of attention. Among its various areas of interest, one of the most renowned is that of clinical applications, where these solutions enable continuous monitoring vital signs in a more comfortable and practical way than the commonly used solutions.

Despite existing considerable availability of wearable monitoring solutions for clinical environments, there is a market gap for solutions directed at first responders. First responders can be split into diverse working groups, such as civil protection rescuers, firefighters, paramedics and police officers. As each group has specific user needs, implemented solutions have to be either too generic, where the systems have a wide range of sensing

capabilities to cover most of the needs of the different first responders, or be specific, being designed according to the specific needs of a given group of first responders.

Since this is an area of Biomedical Engineering that I find specially interesting, this Master Thesis is a great opportunity to apply my knowledge, even more when there is collaboration with a portuguese company that works on biomedical system solutions, Biodevices SA.

Work developed in this thesis has the objective of implementing a new wearable health device, that can be used as an extension of the existing solutions, and using that system to build new features that suit the specific needs of First Responders, more specifically those of firefighters. As firefighters are exposed to enormous stress and hazardous conditions while working, which can put their life at risk, this wearable device aims to make their job more secure, while also enabling them to improve their performance.

1.3 Objectives

In this thesis, it is proposed to work with VitalLogger, in collaboration with a portuguese company which works on Biomedical Engineering solutions, which is Biodevices SA. Work developed on the VitalLogger is expected to increase VitalResponder's scalability, as by integrating, in the future, the new functionalities of VitalLogger in VitalResponder, will make VitalResponder a more capable and intelligent system.

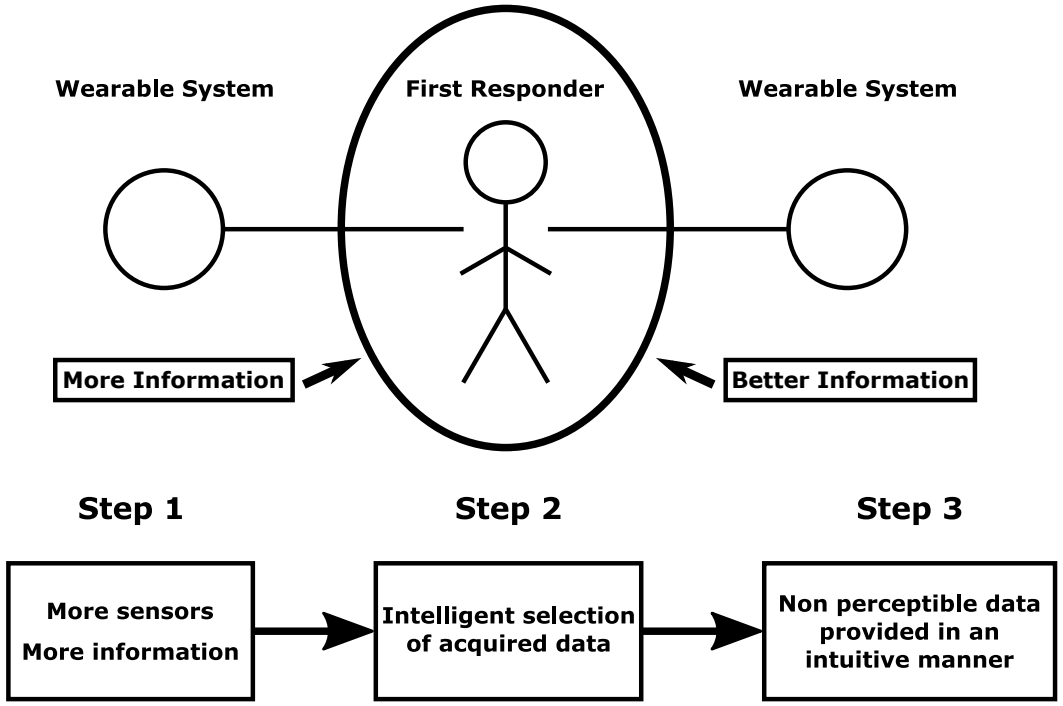

Figure 1.2: Workflow of the work to develop in this Master Thesis, in order to accomplish the defined objective of having a system that provides first responders with not only more, but better information, that suits their user requirements

The objective of this thesis is centered on first responders, more specifically on firefighters, and it is to provide them not only with more information, but also better information that suits their specific requirements as a target group of wearable health systems. Since first responders already use existing wearable solutions, such as VitalResponder, the objective of this thesis can be accomplished by intervening on those wearable solutions, improving their sensing capacities, and the way they provide information to first responders. As these wearable solutions are used by groups of first responders, in the case of VitalResponder by groups of 5 firefighters, a lot of data is sent to the fire chief who is commanding the firefighters, therefore it is crucial to provide only the necessary information, and in the most intuitive way possible. A schematic representation of the objective of this thesis is presented in the top part of Figure 1.2.

In order to meet these objectives, a workflow was designed to address different issues of the final objective, and it is presented in Figure 1.2. This workflow was divided in three steps. The first step consists in adapting a wearable system to newly implemented sensors, which enable the acquisition of novel physiological and environmental data, thus rendering more information.

Naturally associated with a system that senses more variables and gathers more data, comes the problem of having enormous amounts of information to provide to the first responders. Since it is important to provide only the most relevant information to the Fire Chief commanding the units, the second step aims to implement a system that intelligently selects data being acquired by the sensors, so that data redundancy is minimized and only the important information is given to the Fire Chief. Also in this step, and due to the requirements of first responders, information is provided in a more intuitive way to the Fire Chief.

Finally, there is important information on the physiological status of first responders that is very hard, or even impossible to acquire using sensors, namely fatigue indexes. While this information can be extracted from other physiological parameters, easily sensed with the current wearable system, this information is not perceptible for the user, so it must be provided in an intuitive approach. Therefore, step 3 aims to implement a system that extracts important, non perceptible information from currently measured data, that can be provided to the Fire Chief in a way that can be intuitively analysed, and used to manage human resources more efficiently.

With the final improved system, it is expected to be able to monitor more efficiently first responders' stress and fatigue, while these operate in critical scenarios.

1.4 Structure

This Master Thesis is structured in four chapters, including the present chapter of introduction. The second chapter contains a review of the state of the art. The first part of the state the art presents an overview of common wearable health systems (WHS), shows

some of the existing wearable solutions, either in prototype phase or as a final product available in the market, both for clinical scenarios and for first responders. Moreover, this part explores the specific needs of first responders in what concerns WHS and presents a brief vision of the WHS market.

Still in the second chapter, the second part of the state of the art presents a description of the most important vital signs to be measured, and its respective sensing techniques. Finally, in the third part of the state of the art, VitalJacket® technology and the VitalResponder project are explained.

In the third chapter, the development phase of this thesis is presented. This chapter goes through the three steps of the workflow presented in Figure 1.2. The first step describes the adaptation of a wearable health system, VitalLogger, to newly implemented sensors, and also the preparation of the system for the addition, in the future, of other sensors that might be needed. The second step describes the implementation of a system that intelligently selects data acquired by sensors, so that only important information is used. This step reduces data redundancy, and, also in this step, selected data is provided to Fire Chiefs in a more intuitive way. Finally, the third step describes the development of a system that extracts important measures for first responders that are hard to, or even cannot be acquired with sensors, but instead by exploring the relations between other physiological signals that are currently measured by the existing wearable solutions. These extracted measures can be used to provide relevant information about physiological status of the first responders, in a more intuitive approach.

In Chapter 4, which is the final chapter of this thesis, conclusions on the work developed during this thesis are presented, as well as some suggestions for future work that can help improving even further the wearable sensing solutions that are VitalLogger and VitalResponder.

1.5 Main Contributions

This thesis had two main contributions, with the first one being related to the improvement of personal skills and knowledge, and the second one with the achievement of a more capable and intelligent wearable system, that will hopefully, in the future, be placed in the market as a biomedical engineering solution that is useful for first responders.

In what concerns the personal component, this thesis was a completely new challenge that presented many difficulties during its course, specially because it dealt with unknown areas that were not explored during the course of my studies. The opportunity to work with employees from Biodevices SA was definitely a major asset, as it gave me the opportunity to work with experienced people that used their experience to help me learning and improving. Their full support and commitment was crucial to help me understanding their systems, so that I could successfully develop my work. Moreover, the chance to leave

the academia context, transition to the "real world", and work on a product that might be used by other people in the future, greatly stimulated my personal growing.

In what regards the second contribution, the work developed in this thesis helped creating a new system that can be integrated with the existing ones, evolving them and making them more capable and intelligent. Hopefully, the implemented solution can, on the one hand, provide firefighters with the necessary tools to make their job safer and increase their performance. On the other hand, it is hoped that the implemented solution can help Biodevices SA expanding as a company in the future.

It must be referred that the collaboration with Biodevices SA was only possible because of the non-disclosure agreement with INESC TEC. This thesis was developed at INESC TEC, enabling greater proximity between INESC TEC and Biodevices SA, which in turn enabled easier knowledge transfer with Biodevices SA during this thesis.

Chapter 2

State of the Art

The development of innovative technologies and solutions is fostering progress in the concept of personalized healthcare. Due not only to the open-minded and technology consuming nature of our society, but also to increasing interest in active health monitoring (self-tracking or quantified self) [2], citizens often avail of these developments as new technologies end up being incorporated in a wide range of devices (e.g. smartphones).

Personal health systems (PHS), which is a recent concept (introduced in the 1990s), started being deployed due to the personalized healthcare approach. PHS are about placing the individual citizen/patient right in the centre of the healthcare service, increasing his power and likewise his responsibility in the management of his own health. The main goal with PHS is to improve quality of care whilst reducing healthcare cost by having a proper and efficient use of technological capabilities [3].

Since its introduction, PHS have evolved and new specific categories were defined, namely wearable health systems. Wearable technologies possess particular interest and are herein explored as they may play a central role in the "quantified self" movement, and are a major asset in the personalized health challenge [4].

Wearable systems can be used to measure a wide range of signals, being it vital signs or even environment related variables (e.g. ambient temperature, humidity, etc). These systems enable the acquisition of enormous amounts of data, from which precious information can be extracted directly. However, data sets can often be underexploited, as more complex information cannot be retrieved through the common, intuitive approaches. In order to explore data sets closer to their full extent, approaches based on data mining and machine learning must be deployed.

In this chapter, a brief definition and overview of WHS will be presented, as well as some existing products in the market, that are either targeted at healthcare or first responders market segments. Then, some of the most important vital signs that can be acquired with wearable systems will be presented and explained, followed by a brief overview on the fields of data mining and machine learning. Finally, VitalResponder, which is the system used in the work herein presented, will be briefly explained.

2.1 Wearable Health Systems

2.1.1 What are WHS?

Wearable systems can be defined, in a broad extent, as mobile electronic devices that can be embedded, unobtrusively, in pieces of clothing and accessories, presenting the advantage of being operational and accessible without interfering with user activity [5]. While these systems can vary from micro sensors seamlessly integrated in textiles to head mounted displays [5], natural trend aims for miniaturized, integrated, networked, digitalized and standardized (MINDS) devices [6].

These systems are extremely versatile and can be designed and developed specifically targeting health related applications, thus fitting in the branch of WHS. Initial interest in WHS originated from the need to provide healthcare services outside hospitals and monitor patients over extensive periods of time, whilst enabling patients to carry their normal life during the process [3]. With WHS enhancing healthcare services away from medical facilities, a new paradigm in remote patient monitoring emerged.

Concerning current standards, monitoring devices can only be accepted and used for remote health monitoring if there is a comfortable sensing interface and easiness of use and customization. Moreover, the interface must combine continuous and real-time remote control with perfect integration with users' daily activities, without causing any interference whatsoever [7]. Textile approach, where sensors are embedded in pieces of clothing, allows long-term monitoring of patients at low cost, with the additional advantage of enabling customization of sensor configuration according to each user needs [7]. While implantable devices must be made with biocompatible materials in order to prevent rejection by biological tissue, on-body devices are less prone to biocompatibility constraints and have more flexibility in terms of materials. However, in order to provide safe long-term usage, it is recommended that on-body devices are also built with biocompatible materials [8].

In more advanced systems, which can be called intelligent WHS, integrated systems are not only able to sense, process and communicate biomedical, biochemical and physical parameters, but also capable of carrying out actions for the user, in case necessary [3]. These systems increase user's level of awareness and allow a better control of his own health status by providing direct feedback, which is a crucial aspect when monitoring professional workers engaged in extreme environmental or stressful conditions, as is the case of first responders [1, 7].

While there are some hurdles posed by technology that restrain implementation of WHS, namely energy supply, power consumption, price and size of the devices, seamless connectivity or even interoperability [9], current progress has managed to partly address some of these issues. Regarding energy supply, which is currently a major handicap, devices

capable of harvesting energy from the surrounding environment have already started to be studied and developed [10].

2.1.2 Communication in WHS

2.1.2.1 Networks in WHS

WHS are usually integrated in complex systems that comprise much more than wearable sensing technology. For instance, the increasing amount of sensors to be worn or implanted on the users, quite often at several different body parts, triggered the need to develop a networking system capable of connecting this sensing "infrastructure" [10]. These networks are responsible for the data routing from sensors to the required destination [11]. In order to fully understand how a WHS works, it is necessary to explore the networking domain where some interrelated notions arise, such as Body Area Network (BAN), Body Sensor Network (BSN) and Wireless Sensor Network (WSN).

On the most general level, WSNs usually involve large numbers of low-cost, low-power and tiny sensor nodes, with each node having a predefined set of components: sensors, microcontroller, memory and radio transceiver [12]. This set of components grants each node sensing, computing, storage and communication capabilities [8]. WSNs can be deployed for environmental and health monitoring, battlefield surveillance, etc [12].

When various physiological and biomedical sensors are placed around the human body and interconnected through a network, a BAN is established. If each node from the connecting network possesses a sensor or medical device with a sensing unit, we can then refer to it as a BSN rather than a BAN [10, 12]. Connecting all sensors by means of a network presents clear advantages, as it enables centralization of data gathered from different sensors, which can be sent to external networks for remote processing. Furthermore, it enhances control, scheduling and programming of the whole system, which allows the system to adapt according to present body condition and external environment. These advantages culminate in an optimization of resource usage [10].

Wireless communication is a key asset, and mandatory if we want systems to go mobile and ubiquitous. There is, however, a significant trade-off between energy consumption and data volume to exchange, distance to communicate and needed uptime. The more demanding the three former aspects, the lower is the expected battery life time, thus communication protocol selection is an important task that must be thoroughly analysed for each situation [9].

Nevertheless, future prospects in next-generation WSNs are bright since they will have two significant features: massive use of energy-efficient nodes that extend networks' working time, and dramatically increased network throughput that allows, for example, streaming of multiple high definition videos captured by optical sensors. These will prove useful for applications aimed at first responders, such as large scale emergency rescues during natural disasters [13].

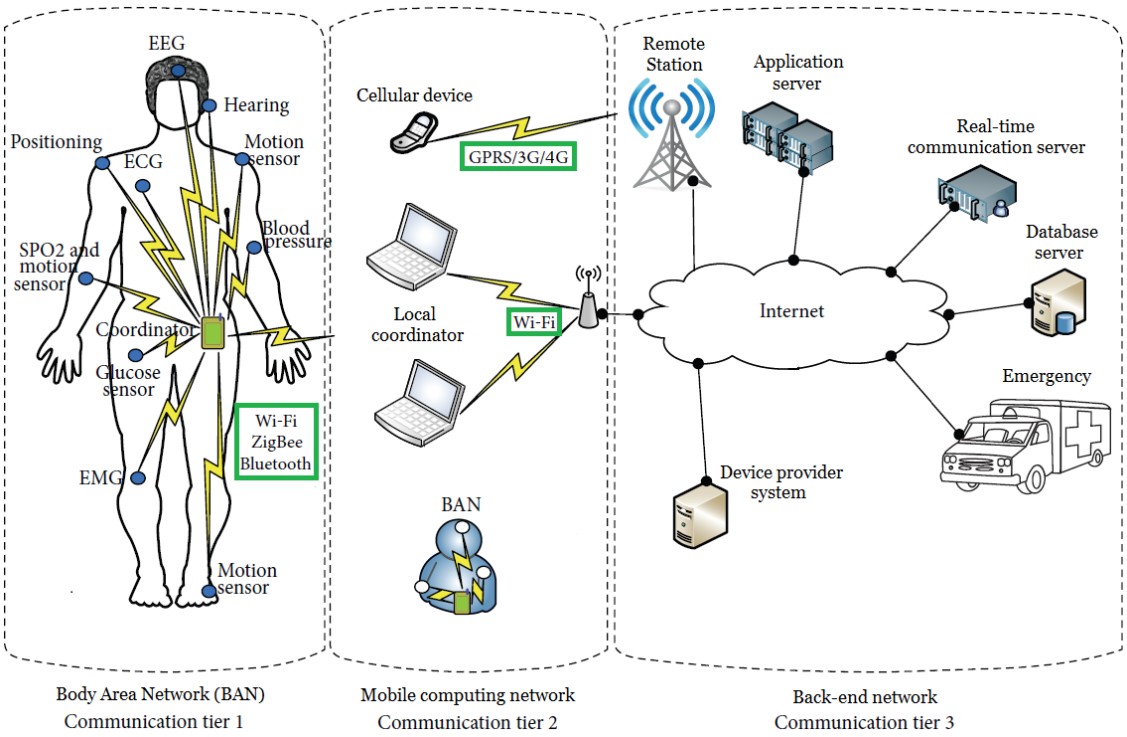

Figure 2.1: A three-tier system architecture of a BAN communication framework. Adapted from [8, 11].

Bear in mind that WSNs designed for health related solutions, such as WHS, need special care in certain aspects, when compared to "general-purpose" WSNs. Some of the most important aspects to take into account are: devices have a very small form factor, which limits available energy resources; transmit power per node must be low to minimize interference and to cope with health concerns; devices must be robust against frequent changes in network topology and channel variability, since these devices are located on the human body, where motion is frequently a reality; manipulated data is critical thus high reliability and low latency are required and, finally, devices are heterogeneous due to its different requirements in terms of resources, namely in data rate, power consumption and reliability [8].

2.1.2.2 System Architecture: A hierarchical view

When analysing WSNs regarding its organization, a hierarchical perspective of systems' architecture can be adopted. Most WSNs can be decomposed in a three-tier system architecture [8, 11], as depicted in Figure 2.1. Evidently, tier composition may differ slightly from the one in the presented scheme, with changes occurring according to the purpose of the designed WSN (i.e. military WSNs differ from healthcare directed WSNs).

The lowest tier (tier 1) connects all sensor nodes within the BAN to a local collector, usually called BAN coordinator (BANC), where information collected from sensors is

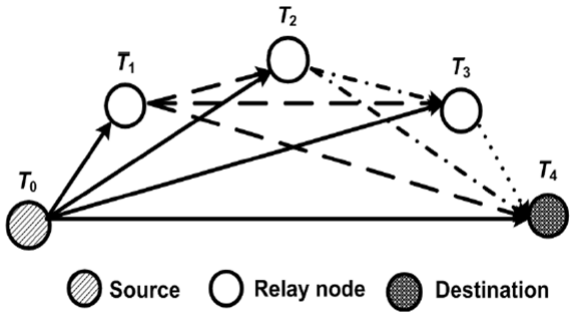

Figure 2.2: Representative scheme of a multihop communication process. Retrieved from [14].

centralized. The coordinator can be a device such as a smartphone or PDA [8]. Since sensors in a BAN tend to have tiny dimensions and limited energy resources, it is wise to route data into a coordinator with better technical resources, since it boosts systems' energy efficiency. During this routing procedure, nodes can forward information from and to other nodes, instead of sending it directly to the coordinator [11]. This process is called multihop communication and can be observed in Figure 2.2.

Some of the commonly used communication protocols in this tier are Bluetooth, Wi-Fi and ZigBee [8, 9]. ZigBee wireless technology operates on IEEE 802.15.4 and is a standard for robust, low-cost and low-power mesh networks [15, 16, 17]. This standard is widely accepted and deployed as it enables multihop communication, thus being useful for BAN applications as aforementioned. It should be noted that, in this tier, communication protocol selection is paramount as it must take into account sensor heterogeneity, whilst securing reliable communication within the network.

In the intermediate layer (tier 2), the BANC can connect to multiple mobile computing platforms, such as cellular devices, gateways and local coordinators. At this level, data can be processed in structures such as the local coordinators, where relevant information can be extracted to assess and control tier 1 structures. It is also possible for BANCs to connect to other BANCs, but in this case data cannot be forwarded to tier 3 unless the receiving BANC connects and sends the data to a local coordinator, gateway or cellular device. In what concerns communication protocols, data can be routed through Bluetooth, Wi-Fi and ZigBee protocols [8, 11].

The last and upper level (tier 3) is considered the long distance communication level. Information is routed from tier 2 structures mainly through Wi-Fi protocol, but also through GPRS, 3G and more recently 4G. Routed data is placed in IP-based networks where different structures can access, process and analyse it in real time [8, 11]. Relevant data can be explored in order to control lower tier infrastructures.

Due to constant technologic evolution, wireless communication protocols described within this architecture are not immutable, and other protocols such as Radio-frequency Identification (RFID) and IPv6 over Low power Wireless Personal Area Networks (6LoW-

PAN) can also be used [9]. More recently, great interest has been placed on IEEE 802.11ac, which is a standard of the Wi-Fi family. This new standard allows increased link throughput up to 1 Gigabits per second, bringing exciting prospects for next-generation WSNs [13].

Some frameworks go even further and categorize devices in the communication framework considering their energy levels, with type 1 devices being directly connected to power sources, type 2 having replaceable batteries and type 3 non replaceable batteries [11].

2.1.3 Current Solutions

WHS are used in a broad scope of applications, comprising healthcare and military applications, or even personal usage considering the wide spreading paradigm of the quantified self. A list of various wearable biomedical measurement systems can be seen in [18]. Herein, some of the existing WHS solutions implementing different measurement systems, either in prototype stage or already in the market, are briefly presented.

2.1.3.1 Prototypes

ANTREC Project

ANTREC Project is an ongoing project developed in the scope of the Spanish Future Combatant Program (ComFut), a program created by the Spanish Ministry of Defense. This project seeks to develop a set of sensorized garments capable of measuring, non-invasively, galvanic skin response (GSR), body temperature (BT), ECG, thoracic electrical bioimpedance (TEB) and voice recording for speech analysis, in order to assess through real-time monitoring the stress levels of combatants [19].

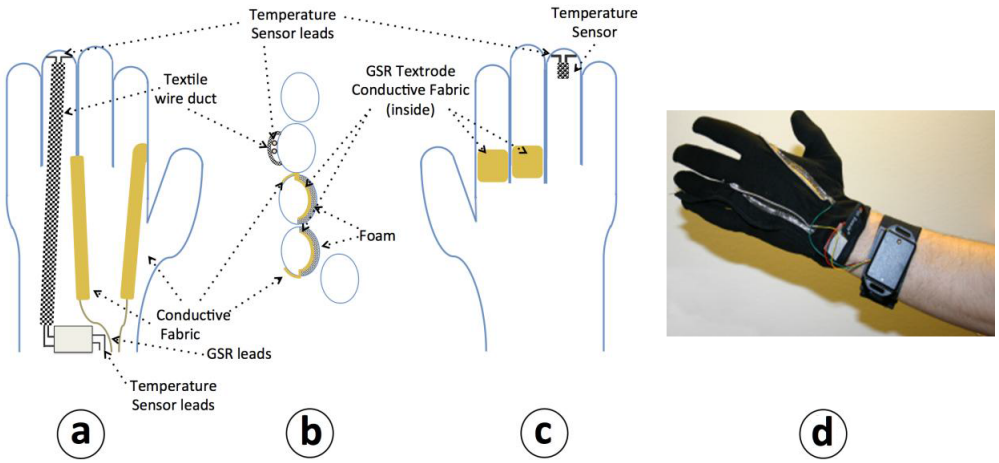

Figure 2.3: Schematics of the sensorized glove. (a) Upper view. (b) Cross-sectional view of the glove at the proximal phalanx in a perpendicular plane to the palm. (c) Palm view. (d) Prototype of the sensorized glove connected to the measuring unit fastened to the wristband. Adapted from [19].

(a) Upper arm strap.

(b) Chest strap system for ECG and TEB electrodes.

Figure 2.4: Chest and arm strap monitoring systems. Adapted from [19].

This prototype system is based on several different measurement systems. By combining them with different sensorized garments, it was possible to change the position and modalities of the different sensors, creating various distinct measurement configurations.

Three measurement devices were created to assess different physiological signals. The first piece of garment is a sensorized glove that has two textiles electrodes (textrodes) integrated on the inside of the glove, used to measure GSR, and a temperature sensor placed at the tip of the ring finger, used to measure peripheral skin temperature [19]. GSR textrodes and temperature sensors are cabled to a measuring device that is fastened to a wristband. The glove can be seen in Figure 2.3.

The second device is an upper arm strap with two textrodes to sense GSR, and a digital thermometer integrated in the inner lining of the strap to measure skin temperature [19]. The prototype version of this strap can be observed in Figure 2.4a.

The third piece of garment is a chest strap with repositionable textrodes. Two textrodes are used to record 1-lead ECG, and four are used to measure tetrapolar TEB. Textrode placement can be changed around the thorax and abdomen to manipulate cardiac and respiratory components, thus it is possible to perform "single" or multi-parametric signal recordings [19]. The chest strap is presented in Figure 2.4b.

Finally, as this project includes voice recording for speech analysis, a water and shock resistant smartphone was used, running a customized Android application that was specifically designed and programmed for this purpose. Speech recordings are stored in an SD card.

SQUID

SQUID is a sensorized shirt with smartphone interface that is targeted at exercise monitoring and home rehabilitation. The smart shirt has 6 vibration motors, a compression shirt with holes and wirings for 13 surface EMG electrodes, a wireless HR detector on the torso, and embedded wirings connecting the sensor mesh [20].

SQUID system acquires muscle activity, with a six-channel EMG, and HR data, storing data in an online database for more complex evaluations. Regarding EMG, 12 electrodes

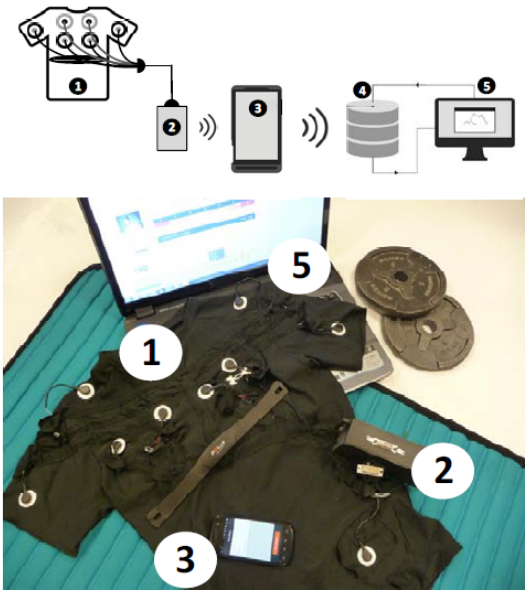

Figure 2.5: SQUID system's schematic and physical components: 1- Smart shirt, 2- Electronic case for the data amplification and acquisition circuit, 3- Smartphone, 4- Online database, 5- Personal computer. Retrieved from [20].

are used in the six-channel EMG, with the extra electrode being used as reference to reject offset voltage from skin-electrode resistance.

The system does also deliver effective haptic and audiovisual biofeedback to the user through two mechanisms: vibration motors integrated in the shirt and a smartphone graphical user interface. Since auditory (beeping) and visual (LED indicators or graphs on displays) feedback can be distracting to people nearby or to the user, vibration motors were integrated. These motors are triggered when peak EMG activity is below a given threshold. The developed smartphone application connects to the shirt via Bluetooth, stores data received from the shirt, and presents it to the user. The application is used to calibrate the EMG sensors, and does also send data to the online platform, where it can be accessed by users. As home rehabilitation is one of the domains SQUID is aimed at, the online platform can be used by physicians to control patient exercising and recovery, hopefully increasing rehabilitation success in the process [20].

2.1.3.2 Marketed Solutions

EQ02 LifeMonitor

This monitoring system, produced by Equivital^{TM}, is marketed as the world's leading multi parameter, ambulatory monitoring device. This device uses a modular approach and, in order to measure physiological signals, different external sensors must be connected to the central module either by wired or wireless connection. The system supports external Equivital^{TM} sensors and third party complementary sensors.

Figure 2.6: EQ02 LifeMonitor, a multi parameter ambulatory monitoring device by Equivital^{TM}. Retrieved from [21].

In terms of data, this system can monitor 2-lead ECG, HR, R-R interval, respiratory rate, skin temperature, acceleration in X/Y/Z axes, body position, motion status (with fall detection), oxygen saturation (SpO_2), GSR and even localization through GPS. Except for SpO_2, GSR and localization, all channels of data can be output simultaneously. The system does also have alarms to alert the subject when necessary.

EQ02 LifeMonitor can save data streams in its memory for later access, or transmit it in real time into other platforms. Regarding its key features, this device has very high data quality, is lightweight and optimised for long wear comfort, and has flexible software platforms so that third party application developers can create new modules. This device is certified and has clearance by FDA and CE Marking [21].

BioHarness^{TM} 3

BioHarness^{TM} 3 is a compact physiological monitoring module produced by Zephyr^{TM}, a global leader in real-time physiological and biomechanical monitoring, or Physical Status Monitoring (PSM) solutions for mHealth, Defense, First Responders, Training and Research markets [22].

Figure 2.7: Three different garment solutions, produced by Zephyr^{TM}. Each garment is specifically designed for the BioHarness^{TM} 3. Adapted from [22].

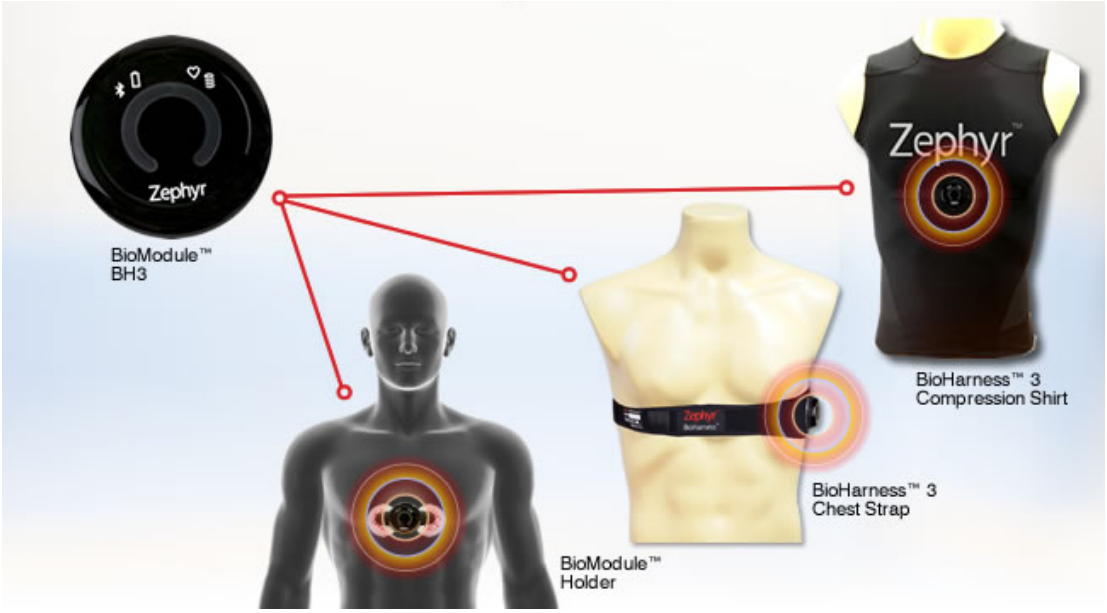

Figure 2.8: BioHarness^{TM} 3, a BioModule with three versatile harnessing solutions. Retrieved from [22].

The compact and rechargeable monitoring module can be harnessed in three different ways: on a module holder with standard ECG electrodes placed on the sternum [23], on a chest strap with a module holder and on Zephyr^{TM} designed shirts that also possess a holder where the module can be placed. These three solutions can be observed in Figure 2.8. Since this module can be used in a wide range of situations, Zephyr^{TM} designed different types of garments for distinct situations and environments [22]. Currently available garments are shown in Figure 2.7.

In what concerns measuring capabilities, the basic module is capable of measuring HR, R-R interval, breathing rate (BR), posture, activity level and peak acceleration. An additional GPS module can be integrated with the shirt solutions, as they have a specific pocket created for that purpose. GPS data can be used to obtain additional measurements such as speed, data and localization. However, solutions targeted at specific markets, such as that of First Responders, expand their capabilities beyond the previously referred set of measuring capabilities. For instance, the system aimed at First Responders can provide non-invasive core temperature (CT) estimations, using an algorithm based on a Kalman Filter and heart rate measurements [24].

Regarding connectivity, measurements are sent to a mobile platform through Bluetooth, where they can be processed and analysed. This mobile platform can work as a central monitoring station, to whom more than 50 monitoring modules can connect, thus BioHarness^{TM} 3 is a useful solution when team management is a concern [22].

2.1.4 First Responders

First responders are a specific market segment of WHS and BSNs, therefore specific user needs must be taken into account when designing solutions for them. Herein, a brief description of first responders' user needs and of two of the most relevant existing solutions is provided.

2.1.4.1 User Needs

First responders frequently operate in dangerous scenarios, where they cannot be directly monitored [1]. For instance, the United States Fire Administration estimated that 50% or more of firefighter line of duty deaths are caused by stress and overexertion [25, 26]. Therefore, the development of systems capable of remotely monitoring first responders' activity and alerting them in case of emergency is paramount. Due to the harsh nature of environments where first responders operate, these systems must fulfil various criteria, including high mobility, reliability, fast response, tight security, low energy consumption, among others [12]. Since first responders' health status depends on the environmental conditions, created solutions must integrate physiological and environmental sensors.

As previously mentioned, first responders are a specific market segment that presents specific user needs. However, first responders can be further divided in different groups, where user needs in terms of variables to be monitored, operative conditions, and compliance to European Standards are even more specific. Three of the most important and representative groups are civil protection rescuers, urban firefighters, and forest firefighters. Each of the previous groups had its requirements thoroughly analysed in [1].

Civil protection authorities marked current drawbacks in interventions management as their major problem. Therefore, they requested improvements in remote transmission of information to identify the actual entity of the emergency, such as in real-time localization of numerous rescuers in large intervention areas. These areas may have no pre-existing communication networks, thus communication protocols must be carefully selected [1].

Forest firefighters' authorities share the aforementioned request, as they mostly operate in large areas with no available communication networks. Moreover, detection of environmental threats, such as the presence of high concentrations of toxic gases, is needed to launch immediate alarms to the rescuers. Monitoring of operators' vital signs is also very important, in order to prevent possible conditions of physiological distress due to harsh working conditions. In case of emergency, the system must be able to launch an alarm to the intervention managers, who coordinate first-line rescuers from command posts located near the affected area [1].

Urban firefighters mainly operate in small operative areas, with smaller working teams where workers can often be visually monitored, hence their requirements are different from those previously mentioned. Environmental sensing is a prime concern as working conditions can be critical, with the presence of fire, toxic gases and possible explosions.

Figure 2.9: Garment solutions developed during the 3rd generation of the ProeTEX project. From left to right: fireproof t-shirt or inner garment; boots; jacket or outer garment. Retrieved from [28].

Consequently, a real-time monitoring of these variables must be performed in order to trigger alarms to the rescuers and command posts in case of emergency. Urban firefighters do already use commercial toxic-gas sensors and activity monitors (to detect extended periods of immobility), however the former produce false alarms that can interfere with normal working activity. In this line of sight, urban firefighters request more accurate systems that can reduce the existing number of false alarms [1].

2.1.4.2 Current Solutions

ProeTEX Project

ProeTEX is a project that was carried out by a consortium of 23 partners from eight European countries [27]. This project was designed to have three generations, with a new version of the set of smart protective garments, for firefighters and civil protection rescuers, being developed in each generation. These garment sets are capable of acquiring physiological activity and environmental parameters, whereas the information transmission infrastructure allows remote data communication, relevant data detection, and generation of feedback to the users [1].

Each set of garments is composed by a pair of boots, a fireproof t-shirt or inner garment (IG) and a jacket or outer garment (OG). The third generation of the produced garments is shown in Figure 2.9. Each set has measuring systems that can measure HR, BR, BT, SpO_2, environmental temperature, concentration of toxic gases such as carbon monoxide (CO) and carbon dioxide (CO_2), operator's activity and absolute position and speed.

The IG is targeted at the monitoring of operators' physiological signals, and has sensors for the measurement of HR, BR, BT, SpO_2 and dehydration. As this garment is in direct contact with users' skin, operator comfort is a key requirement. Therefore, sensors are embedded in the textile. This t-shirt has two main sections: an elastic region where all textile sensors are included, and a region containing detachable on-board electronics.

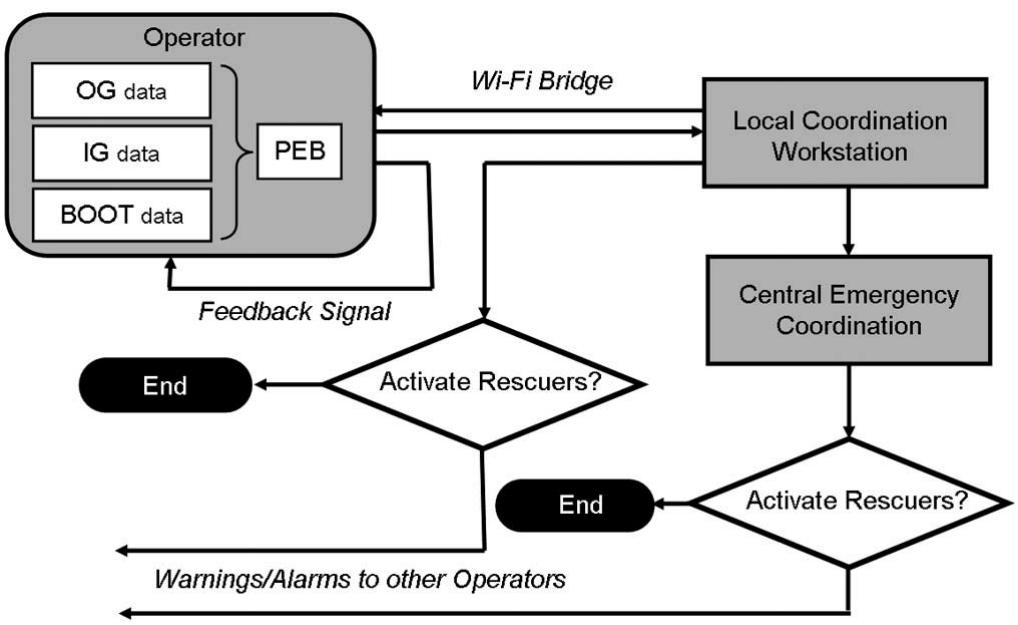

Figure 2.10: Information management network used in ProeTEX project. Retrieved from [1].

Textile-conductive cables are integrated in the shirt to connect the textile sensors and electrodes to the electronic modules. The detachable on-board electronics acquire signals from the sensors, which are then forwarded into a BANC placed in the OG [1, 28, 29].

The boots satisfy EU standards and have integrated sensors and energy harvesting elements. A CO_2 sensor is placed in an electronic module in the boots as this gas is heavier than air, and starts to accumulate at ground level. The CO_2 module processes acquired data and sends it to the BANC through a ZigBee module [1, 28].

The OG includes the measuring systems for assessing operator activity status and monitoring the surrounding environment. This piece of garment is produced in three configurations depending on the targeted users: civil protection rescuers, forest firefighters and urban firefighters. All configurations possess two triaxial accelerometers, a textile motion sensor, a CO sensor and an external temperature sensor. Since CO is an extremely toxic gas with density comparable to air, the CO sensor module is placed near the user's mouth and nose, in the OG lapel. Forest firefighters and civil protection rescuers have an integrated GPS module, whereas urban firefighters do not. As urban firefighters operate inside buildings, where reliable GPS signals are rarely available, there is no point in integrating a GPS module in their garments. Additionally, a heat-flux sensor was included in urban and forest firefighter's OG, to prevent operators' sudden uniform burning, and an alarm module was also integrated to launch visual and acoustic warnings when critical situations are detected by the sensors. Gathered data is sent to the BANC, which is placed in the OG. Finally, the OG has two antennas that are connected to the BANC. These antennas are responsible for the wireless transmission of the data acquired by the

sensors [1, 28, 29].

In what concerns the communication network, the professional electronic box (PEB) is the system core that collects data from all sensors, working as a BANC. This BANC transmits the acquired data (with Wi-Fi protocol) through the two antennas placed in the OG. This data is received by the local coordination workstation, and by self-powered bridge modules placed in the intervention area that receive and remotely rebroadcast data coming from operators, in real time. A second node, similar to the former one, is connected to the emergency coordination workstation and receives the information. Monitoring software running in the local coordination workstation processes data provided from the operators' sensors. This data is used as feedback for the operators, triggering alarms when dangerous contexts are detected, hence the bidirectional information flow between the operator and the local coordination workstation. Furthermore, alarms can be triggered for other operators, in order to alert them of emergency situations. A scheme of the global communication infrastructure can be seen in Figure 2.10 [1, 28].

WASP^{TM} – Wearable Advanced Sensor Platform

WASP is an integrated system, created by a multi-disciplinary team, led by Globe, consisting of Zephyr Technology (physiological monitoring module), TRX Systems (position tracking module), Propel (textile development), Skidmore College Health and Exercise Sciences (physiology science) with support from the US Army Natick Soldier Research, Development and Engineering Center [25].

Figure 2.11: WASP^{TM} system composed of: 1- a flame-resistant, moisture wicking, semi-fitted, base layer shirt; 2- adjustable chest strap, embedded in the shirt, where the physiological sensors are mounted; 3- belt with the TRX location unit; 4- Zephyr BioHarness^{TM} 3, a small electronic module that is attachable to the adjustable strap; 5- a Windows-based monitoring station; 6- a wheeled hard case where the WASP^{TM} system can be stored, recharged and transported. Adapted from [25].

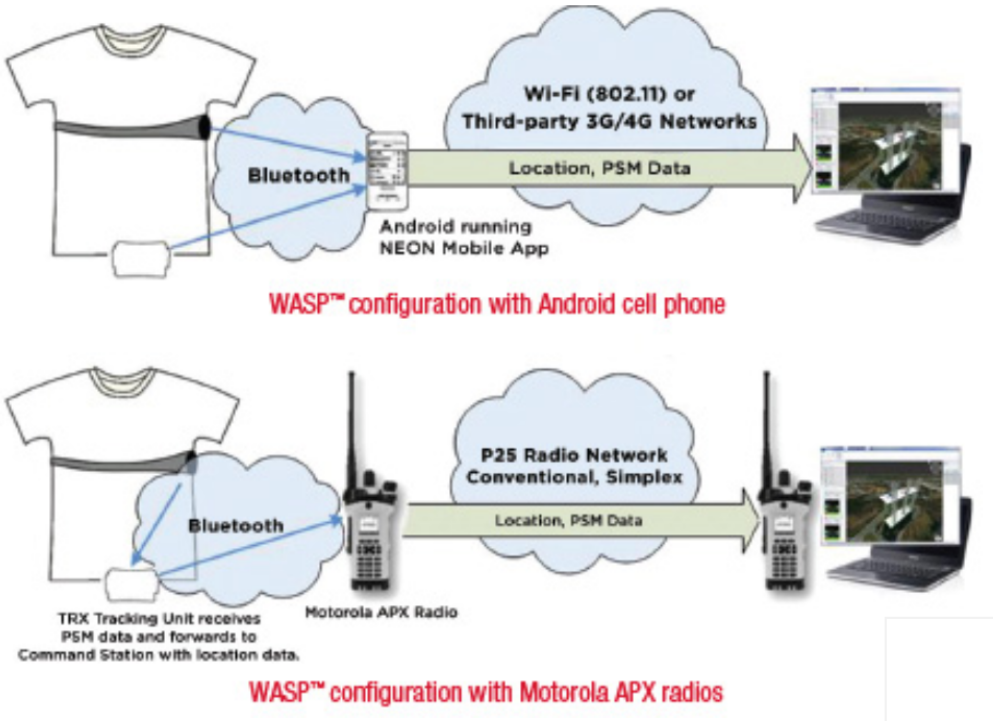

Figure 2.12: Possible networking configurations used in WASP^{TM}. Retrieved from [25].

WASP was designed to address two critical problems that were identified on the Inter-Agency Board's R&D Priority List: first responder wearable integrated electronics system development, and 3 dimensional tracking of operators [30]. The resulting tool grants commanders the ability to track the location of team members, used to improve situational awareness, and has the potential to shorten needed time for a Rapid Intervention Team to rescue a downed firefighter.

The system consists of a comfortable, flame-resistant shirt with sensing modules, and a monitoring station that receives data from shirts. The shirt has physiological monitoring technology due to the integration of the Zephyr BioHarness^{TM} 3, a small, sensing module that measures HR, heart rate variability, BR, activity levels, posture, among other physiological parameters. This module is attachable to an adjustable chest strap where the physiological sensors are embedded. Moreover, a TRX location unit, which is worn on a belt at the waist, provides positional data in 3D in indoor environments where GPS systems are usually a nonviable solution. The location unit permits ready integration with Motorola APX radios and Android smartphones. Finally, a Windows-based monitoring station, which can receive data from multiple WASP^{TM} wearable systems simultaneously, processes physiological and location data in real time and displays it on an easy to understand graphical user interface. The overall system is presented in Figure 2.11 [25, 26].

Finally, in what respects to WASP^{TM}'s communication network, two different approaches are possible. In both configurations the garment connects to a BANC, which can be an Android smartphone running a programmed application or a Motorola APX radio,

through a Bluetooth connection. These two approaches are represented in Figure 2.12.

If the BANC is an Android smartphone, both the TRX unit and Zephyr BioHarness^{TM} 3 can connect directly to the BANC. Location and physiological data is sent from the sensing modules to the BANC, which can then forward data to the monitoring station via Wi-Fi or 3G/4G protocols.

However, if the coordinator is a Motorola APX radio, Zephyr's module has to forward its data to the TRX location unit, which can then send location and physiological data to the BANC. In order to communicate with the monitoring station, data must be sent from the BANC to another Motorola APX radio, at the monitoring station, via P25 radio network [25, 26]. Project 25 (P25) is the standard for the design and manufacture of interoperable digital two-way wireless communications products, and has worldwide acceptance for public safety, security, public service and even commercial applications [31].

2.1.5 Market Analysis

Wearable technologies possess plenty of potential, having raised interest from diverse fields such as that of augmented reality. While the concept of augmented reality through wearable technologies is relatively recent, being discussed since the late 1990s, this area has already experienced significant developments, with particular focus on the shift from bulky devices to lightweight and mobile systems [32].

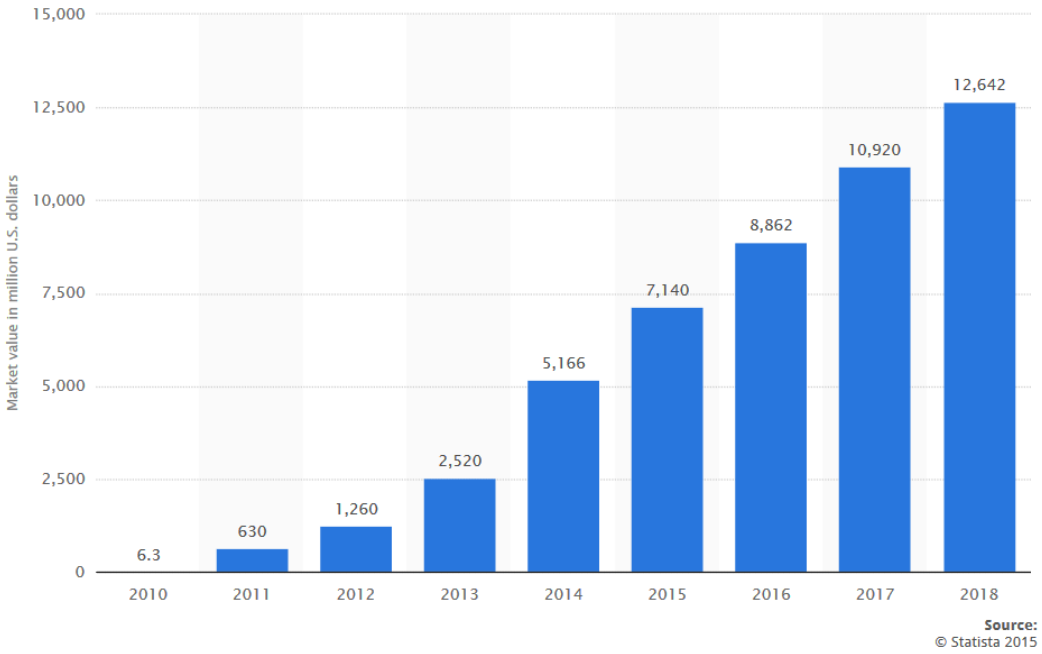

Figure 2.13: Wearable device market value from 2010 to 2018 (in million US dollars). Retrieved from [33].

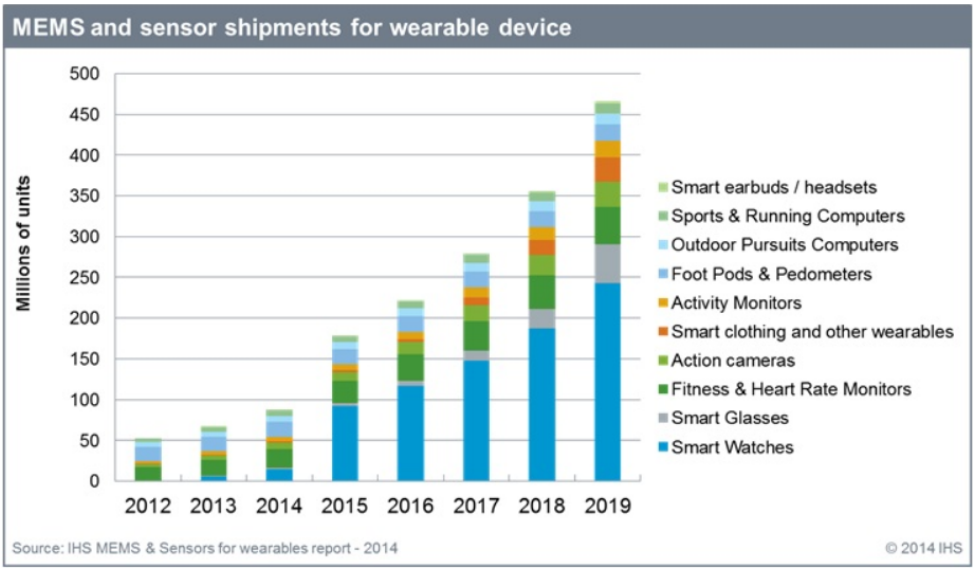

Figure 2.14: Projected sales of MEMS and sensors for wearable devices, until the year of 2019. Sales are distributed per category of wearable device. Retrieved from [34].

The area of wearable technologies has been surrounded with increasing hype, mainly due to its exciting market prospects. The market value of wearable devices is forecasted to raise from 5.1 thousand million US dollars, in 2014, to a value just above 12.5 thousand million US dollars, by 2018, as shown in Figure 2.13. This significant increase in market value is expected to be driven by the introduction of influent products, such as the Apple Watch, in the consumer market [33, 35]. Some analysts go even further, predicting that wearable devices will surpass market expectations by a long margin, becoming the fastest ramping consumer technology device to date [36].

These kind of devices are embedded with numerous electronic components, being considered the next big wave for microelectromechanical systems (MEMS) and sensors in consumer electronics after smartphones and tablets [34]. Since systems tend to grow more complex and resourceful in order to fulfil the upcoming needs of the different consumer groups, wearable devices must follow the trend by incorporating increasing numbers of MEMS and sensors [37]. Sales projections of MEMS and sensors specifically targeted at wearable electronic solutions, up to the year of 2019, are presented in Figure 2.14 and clearly illustrate the growth potential of this market.

Regarding the types of MEMS and sensors included in the above referred wearable solutions, these mostly possess motion sensors, MEMS and sensors for user interfaces, health sensors and environmental sensors. While motion sensors are currently the dominating technology, the entry of new products in the market, such as the Apple Watch, is expected to increase market representation of sensors for user interfaces and health sensors. Moreover, the entry of products like the Apple Watch is expected to accelerate the market for sensors in wearables as a whole, greatly contributing to the growth of this area's market potential [37].

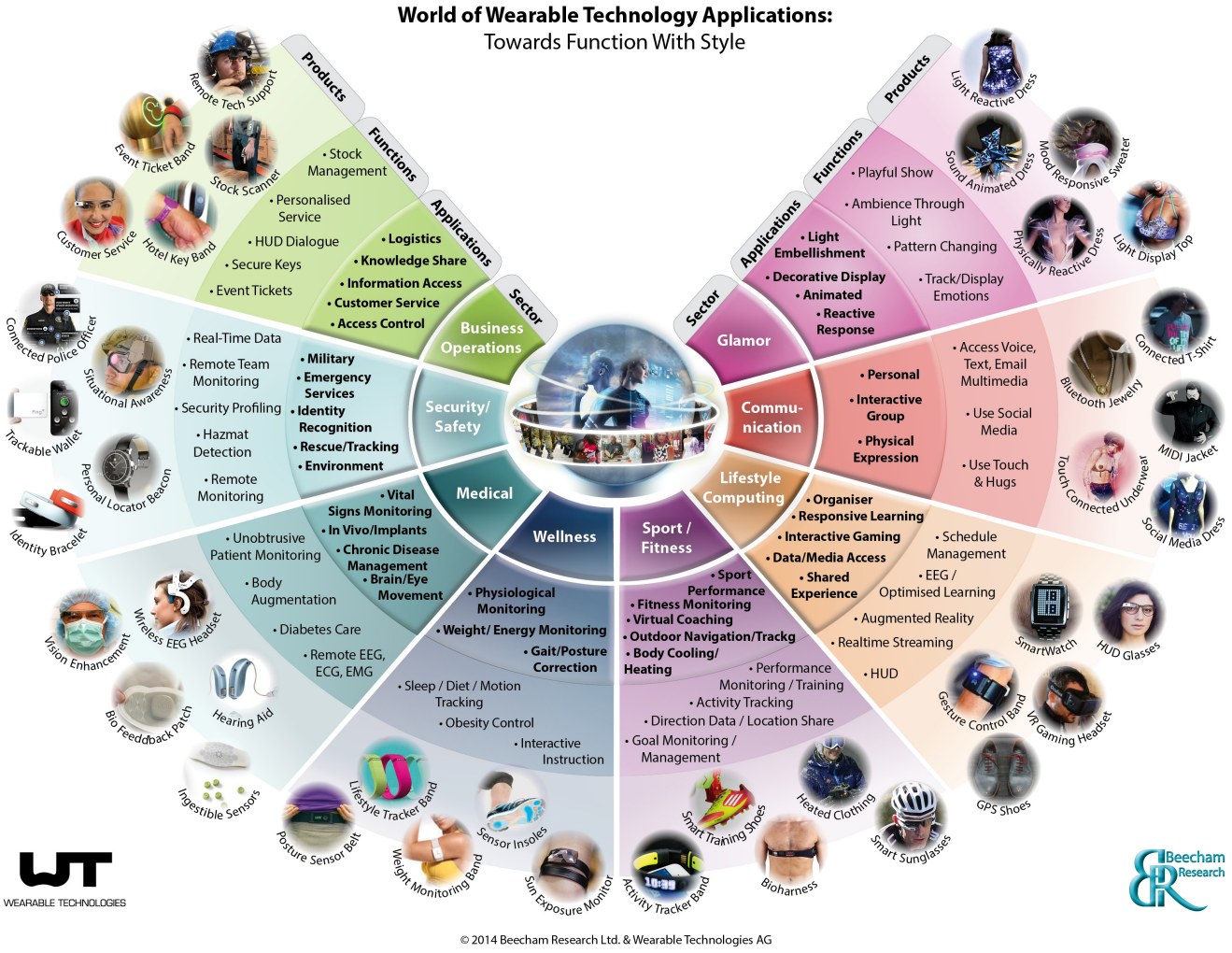

Figure 2.15: Spectrum of applications for wearable technologies. Retrieved from [38].

More recently, wireless charging technologies have been developed that allow the charging of batteries wirelessly, naturally presenting utmost interest for the domain of wearable monitoring devices. While this technology might take some time to effectively get into the market, the integration of such technology in wearable electronic devices is expected to further increase this field's market potential [35, 39].

In what concerns possible applications for wearable technologies, these are already deployed in various fields of interest. Figure 2.15 summarizes the most important sectors, applications, functions and products in wearable technologies. In spite of having security (military applications) and medical fields as the most relevant sectors until recent years, latest technological developments have shifted the spotlight to consumer market, which mostly comprises the areas of sports, fitness and infotainment [32].

In this work, interest is focused on first responders' market segment, which fits in the security/safety sector. While no values regarding market size of wearable technologies for first responders were found in literature, the market size for first responders and law enforcement robotics, which is related to that of wearable technologies, is said to be growing to 3.7 billion dollars by 2016 [40]. Since market value of the wearable device market has been increasing, and is predicted to explode in the near-future, this work presents increased importance, for it addresses a great business opportunity.

2.2 Vital Signs

The recent paradigm of pHealth (personalized health) has brought portable and wearable technology to the domain of medical systems, and with the shaping of personalized healthcare, new requirements arose. Current and future systems have to be able to monitor users' health condition on a continuous and non-invasive basis, whilst providing feedback to users and/or medical professionals when these systems are used in a medical context [10].

Depending on the intended purpose, a person's health status can be measured through the monitoring of various vital signs. The most important vital signs for medical systems, as well as those required in first responders' systems, are identified and briefly explained in this chapter.

2.2.1 Vital Signs in the Medical Context

Wearable health systems face the everlasting challenge of measuring physiological parameters through non-invasive and continuous approaches. Current monitoring systems manage to acquire diverse vital signs non-invasively, with major vital signs being HR, ECG, BP, BR, SpO_2 [10] and BT [41]. Gathered information can be used for possible disease prediction or prevention [10].

Emerging technologies open prospects for new possibilities, thus leading to the development of new monitoring approaches to assess a person's health condition. One of these

relatively recent areas attracting great interest is non-invasive biochemical measurement of body fluids such as blood, saliva, tears and sweat [42].

2.2.1.1 Cardiac Activity - HR and ECG

Cardiac activity's main characteristics can be captured through various physiological signals and parameters, which depend on the type of model considered. For instance, the heart can be modelled as an electrical generator, a moving muscle, a pump or a noisy pump [43].

Among the various cardiovascular parameters, HR, which is the number of heartbeats per unit of time, is one of the simplest and, yet, most informative ones, thus being considered a major vital sign. Other signals, such as heart rate variability (HRV), which is the variation in the time interval between each heartbeat (also known as beat-to-beat interval), have attracted increased attention as indicators of cardiovascular system's health condition [10], but aren't as deeply explored as HR and ECG.

As abovementioned, heart can be seen through multiple viewpoints. When considering it an electrical generator, heart functioning is assessed through its electrical activity which is recorded in the ECG signal. In order to measure it, electrodes are placed in direct contact with skin [10]. While conventional practices use wet-contact gel-based silver/silver-chloride electrodes, these are not suitable for certain applications. Recent developments have led to the creation of dry electrodes and non-contact electrodes. Dry electrodes can be based on rubber, fabric or foam, which is more appealing in terms of usability and comfort. Choice may fall on softer materials as these conform more easily against the skin, increasing comfort and contact area. Furthermore, dry electrodes have the advantage of being integrable into clothes, constituting an unobtrusive way to acquire ECG signal. These aspects make dry-contact electrodes more suitable for long-term monitoring purposes [44, 45].

If the second approach is followed, considering heart a moving muscle, cardiac activity can be measured with microwave sensors (Doppler transceivers), which are not in direct contact with the skin. Systems with these sensors use Doppler effect to detect heart movements, and can only acquire data about the rhythmic activity of the heart, lacking the detailed morphology of ECG signal [10, 46]. The obtained signal can be used to determine HR.

In the third viewpoint, where heart is seen as a pump, variations in blood volume can be detected and quantified by sensing changes in the electrical resistance of the body through sensors placed on the skin. Two different techniques can be used: impedance plethysmography and photoplethysmography. The first one measures electrical resistance in different parts of the body, whereas the second one uses a light emitting diode (LED) specifically placed at peripheral sites, such as the fingertips and earlobes, to measure transmitted or reflective light via a photodiode. This technique detects variations in

blood volume since light absorption varies, according to Lambert-Beer law, as blood flow changes [10], enabling the determination of HR and SpO_2.

Finally, when heart is considered a noisy pump, the solution relies on phonocardiography (PCG). PCG consists in the acquisition of sound signals with a highly sensitive microphone (in a PCG sensor), which are then filtered and processed in order to obtain quantitative measurements of HR [10, 47].

2.2.1.2 Blood Pressure (BP)

Blood pressure is the pressure that blood exerts against the arterial wall, and is influenced by cardiac output, peripheral vascular resistance, vessel wall elasticity, blood volume and viscosity. As a major vital sign, BP provides a reflection of blood flow during heart contraction (systole) and relaxation (diastole), and is one of the various indicators of cellular oxygen delivery [41]. Moreover, BP is a vital sign that requires attention in every individual since most subjects affected with hypertension are asymptomatic. Some studies even point out blood pressure variability (BPV) as an independent indicator of morbidity and mortality due to cardiovascular disease [41], thus it is of utmost interest to have monitoring systems capable of continuously measuring BP.

Many wearable systems have been developed for BP measurement, either recurring to conventional measurement techniques, such as the oscillometric method, or novel techniques, such as arterial tonometry that captures radial pulse waveform [10]. Systems using the latter technique do not need to be placed on the brachial artery, as is the case of watch-type monitors which perform measurements over the radial artery at the wrist [10, 48].

While conventional apparatus require cuffs, those based on novel techniques are heading for a cuff-free environment [48, 49, 50]. These systems still need an external pressure exerted on the wrist and its measurements are location-sensitive. Furthermore, these systems have yet to evolve in terms of being wearable and unobtrusive [10]. Regarding functioning, cuffless systems estimate BP from the transit time (PTT) and velocity (PWV) of a pulse travelling along an artery [48, 50].

2.2.1.3 Breathing Rate (BR)

Breathing rate, or respiratory rate, is one of the most sensitive pointers for critical illness. Abnormal BR can indicate respiratory distress, hypoxemia, and even be a predictor of harmful events such as cardiac arrest [41].

Breathing acts on chest kinematics, leading to changes in thoracic volume in two different compartments: the rib cage and the abdomen. The conventional method to measure BR is direct spirometry, which does not allow monitoring outside medical institutions due to technical equipment issues. However, as chest wall is divided in two compartments, sensors can be placed in each compartment to measure changes in lung volume. This

method is unobtrusive and has three variants that assess: changes in electrical impedance, changes in electrical inductance and piezoelectric changes [51].

Inductive plethysmography (IP), which measures changes in electrical inductance, is the gold standard method for assessing BR unobtrusively, and consists on the measurement of changes in self-inductance of two conductive wires, placed around the rib cage and abdomen, caused by motions of the chest wall [10].

Recent developments in the area of piezoelectric solutions have led to the creation of wearable yarn-based piezo-resistive sensors. Measuring BR with this method is simple, inexpensive, and more comfortable, thus these systems are considered the substitute for conventional sensors [10, 51].

2.2.1.4 Blood Oxygen Saturation (SpO_2)

Blood oxygen saturation measures the percentage of haemoglobin bound with oxygen, and is a very important vital sign since human beings cannot survive for much time without constant oxygen supply to the brain. Although it presents special interest for military and space applications where gravity changes and other sources of stress can result in fatigue, and ultimately, in blackouts, SpO_2 can also be used to monitor aerobic efficiency of users undertaking exercise routines, enhancing maximization of athletic performance [10].

The most frequently used devices to monitor both continuously and unobtrusively SpO_2 are pulse oximeters. These are often ring shaped and can also measure HR [10, 52]. Recent advances in textile electronics enabled sensor embedding in fabric, leading to the development of more comfortable solutions such as the one described in [53].

It must be noted that in order to measure SpO_2 effectively, pulse oximeters require adequate peripheral blood flow, which can be impaired by many factors such as patient movement or vasoconstriction. Moreover, pulse oximeters must be used with caution as SpO_2 measurements on anaemic users can be misleading, since these users can have normal SpO_2 levels despite having a lowered potential to carry oxygen [41].

2.2.1.5 Body Temperature (BT)

Body temperature is a vital sign that controls thermoregulation, for it presents the balance between heat production and heat loss in the body [10]. Since human bodies have many elements in its composition that are defunctionalized above certain temperatures (e.g. proteins denature and lose function above certain temperatures), controlling BT is paramount.

BT can be divided into core temperature and skin temperature, and values between these two temperatures usually differ. Skin temperature varies within a wider range of temperatures than core temperature, as the body's thermoregulation mechanisms regulate core temperature. A factor that can affect skin temperature is blood circulation, as higher blood circulation leads to an increase in skin temperature, hence skin temperature is also

related with other vital parameters such as HR and metabolic rate [54, 55, 56]. Physical exertion is linked to these factors, and is very important as it triggers the following cascade: exercise leads to a demand for oxygen in the muscles, HR goes up to increase oxygenated blood supply, and an increased metabolic rate leads to heat production that can be either stored (increasing CT) or dispersed. This regulatory mechanism is viable within a 3 to 4 degrees Celsius temperature range. When exercise continues and heat is progressively stored, the body increases blood circulation to the skin so that heat can be lost through evaporative or convective processes, and in order to get this increase in blood circulation the body has to increase HR beyond the levels needed for oxygen supply to muscles [57]. External factors such as air circulation, ambient temperature and humidity play an important role in this body temperature regulation mechanism [54, 55].

Different wearable systems have been developed to measure both temperatures, such as skin-like arrays of precision temperature sensors or wearable adhesive devices to continuously measure temperature [58, 59, 60]. However, measuring CT through non-invasive approaches still remains a huge challenge. Nowadays, rectal temperature is still considered the gold standard for CT measurement, and while other techniques like the telemetric pill allow for better usability, they face technical issues that influence the CT measurements. For instance, telemetric pill's measurements are greatly influenced by the ingestion of hot or cold fluids, and while the pill is considered a less invasive approach than measuring CT with a rectal probe, it still is not completely non-invasive and has the problem of being inside the human body for a short period of time, which creates a logistical burden [56, 61].

It is very important to refer that while it is not possible to define a correlation between core temperature and skin temperature in normal conditions, when thermoregulation mechanisms start failing, as described in the aforementioned physiological cascade, variables like heart rate and skin temperature correlate more directly with core temperature [55]. Therefore, when skin temperature rises to values above 36°C, it can be used as a proxy for core temperature prediction [54].

2.2.1.6 Biochemical Measurements

Human body has several vital analytes, such as blood glucose or lactate, which can be non-invasively/mini-invasively measured in order to extract important information [10]. Chemical sensors and biosensors, such as optical, piezoelectric and electrochemical transducers have proved to be an attractive alternative for clinical diagnostics due to their high performance, portability, simplicity and low cost, being electrochemical transducers the dominating force. Electrochemical transducers do, however, pose the problem of relying on blood samples, which hampers continuous monitoring [42].

These systems can be used for various purposes, ranging from optimum diabetes management, to continuous assessment of fitness level during trainings or even real-time detection of pathogens in biofluids. Due to intensive study and research, sensors capable of extracting information from saliva, tears and sweat have already been developed. As

monitoring solutions are increasingly focusing on the non-invasiveness attribute, sweat is one the most deeply explored biofluids [42].

Sweat possesses lots of information about a person's health status as, for example, sodium and lactate levels in sweat are, respectively, indicators of electrolyte imbalance and physical stress. Wearable non-invasive electrochemical sensors for monitoring sweat can be split into two main types: fabric/flexible plastic-based devices and epidermal-based sensors.

Fabrics are in constant contact with skin and provide large surface area for embedded electronics, being an excellent platform for these wearable sensors. Their major adversity is the fact that intimate contact with the skin is restricted to certain regions. In what regards its integrated sensors, these are mostly potentiometric sensors, but fabric-based conductometric sensors for measuring the extent of dehydration have already been developed [42].

Epidermal-based sensors allow direct sensing on the skin as the tattoo-based electrochemical sensors are placed on the epidermal layer of the skin, enhancing measurement efficiency. Tattoo sensors are designed to resist skin deformation and, similarly to the fabric based sensors, are mostly based on potentiometric technology. More importantly, these systems are capable of monitoring analyte levels in a continuous manner [42].

2.2.2 Vital Signs in First Responders

First responders are subjected to harsh conditions that affect their physiological response. In the specific case of firefighters, major factors that influence physiological response are: individual health condition, fitness level, medication, hydration level, exertion of work performed, elevated thermal environments, wearing heavily insulated protective clothing, carrying heavy equipment and the exposure to extreme hazards during emergency responses [25, 26].

Since first responders are frequently exposed to extreme scenarios, it is crucial to continuously monitor their vital signs to increase tactical awareness and enhance personnel safety. According to end-user requirements acquired through the enquiry of civil protection and firefighter entities, the most important vital signs to be continuously monitored are HR, BR, SpO_2 and BT [1]. Whilst BT can be split in core temperature and skin temperature, core temperature is harder to obtain, specially in ambulatory environments such as those where first responders are deployed [56].

Furthermore, there exist strain indexes which can provide insight on the fatigue and strain experienced by first responders [54, 62]. Since it is frequent for first responders to be engaged in physically demanding tasks while in high heat strain environments, the Physiological Strain Index (PSI) is an interesting index to take into account [63]. PSI is an index of heat strain that only requires measurements from core temperature and heart

rate, and can be computed through Equation 2.1, where values with a 0 in the subscript represent initial values for the given variables [54, 63].

$$PSI_{(t)} = 5\frac{T_{core(t)} - T_{core(0)}}{39.5 - T_{core(0)}} + 5\frac{HR_{(t)} - HR_{(0)}}{180 - HR_{(0)}} \tag{2.1}$$

In what regards its analysis and interpretation, PSI values are considered safe when comprehended in the range between 0 and 7.5, with 7.5 being defined as the risk threshold for PSI. Values above this threshold represent potential risk situations [54, 63].

Besides monitoring physiological signs, due to the direct effect of environmental factors in operators' physiological response, it is relevant to continuously monitor the surrounding environment as well. This can be performed by using systems with integrated sensors capable of measuring environmental temperature, concentration of toxic gases such as CO or CO_2, and operator activity, speed and position [1].

Despite having a consolidated group of vital signs that is pre-established as a system requirement, new findings keep discovering connections between vital signs and physiological responses. For instance, stress can be assessed through the analysis of autonomic nervous system (ANS) activity, as ANS controls body's reaction to both internal and external stimuli. ANS activity can be evaluated non-invasively by monitoring several physiological parameters, such as the previously referred HR, BR and BT, but also GSR and electroencephalographic activity (EEG signal) [19]. As the assessment of mental stress during stressful and dangerous tasks is a very pertinent aspect to control, future solutions for first responders might start integrating GSR and EEG sensors in their systems.

2.3 VitalResponder - pHealth for First Responders

VitalResponder is a first responder oriented project that consists in a monitoring system specifically designed according to firefighters' requirements, and that is capable of continuously monitoring both vital and environmental signs. This project results from the application and adaptation of a wearable monitoring solution, the VitalJacket®, for different purposes, such as the monitoring of public transportation drivers and first responders.

Herein, VitalJacket®, which is the base platform of these studies, will be first explained. Since the proposed work is focused on the segment of first responders, the VitalResponder system will also be further explained.

2.3.1 VitalJacket®

VitalJacket® is a wearable vital signs monitoring system commercialized by Biodevices SA. It is designed to be a usable practical approach for different clinical scenarios, being a reliable monitoring system whether used in hospitals, at home or on the move [64]. This system is capable of monitoring vital signs continuously and with high signal quality.

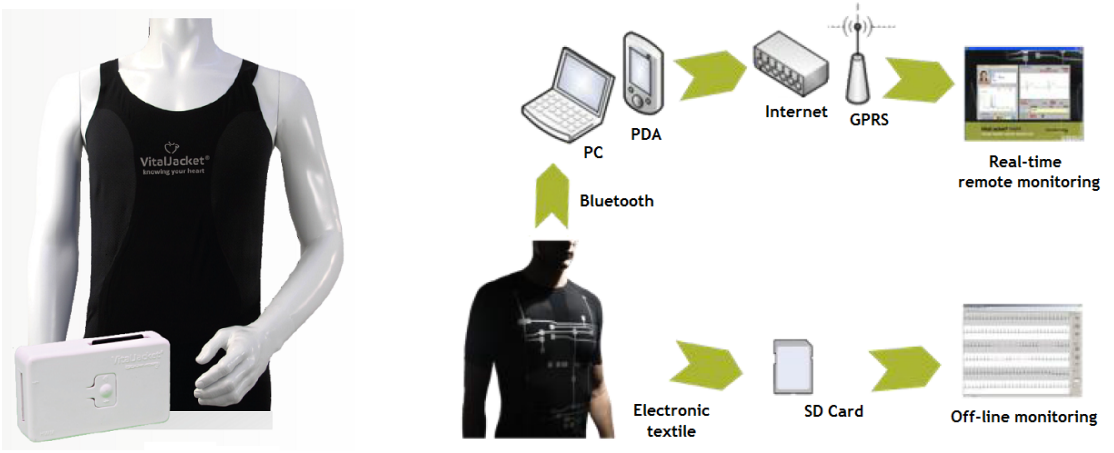

(a) Wearable monitoring shirt and recording box where data is stored/sent to other platforms.

(b) Monitoring possibilities in VitalJacket®. Data can be stored for off-line analysis or sent through a wireless connection for real-time monitoring.

Figure 2.16: VitalJacket® monitoring system by Biodevices SA. Adapted from [4, 65].

In what concerns certification, VitalJacket® is certified according to standards ISO9001 and ISO13485, and is approved as a medical "Ambulatory ECG device" according to the MDD directive 42/93/CE which regulates medical devices in Europe, being granted with CE1011 mark [4, 64, 65]. Moreover, similar certification has already been attained in Brazil, Colombia and Israel, making VitalJacket® a potential key player in the market of ambulatory cardiac monitoring systems [4]. VitalJacket® is the first certified medical device to combine mainstream biomedical engineering solutions with wearable solutions [66].

VitalJacket® has two main versions: VitalJacket® 1L, which is a 1 lead ambulatory ECG for long term use, and VitalJacket® 5L, which is a 5 lead Holter system. The first one is aimed at cardio training or cardiac rehabilitation exercise monitoring, whilst the second is targeted at cardiac screening in patients with arrhythmias. Other versions such as VJ Kids and VJ Baby have recently been developed, in order to enable the usage of this monitoring technology in younger age groups [65].

While VitalJacket® 1L is a basic version used for single lead ECG, VitalJacket® 5L does also possess a triaxial accelerometer, making it the only Holter system with an embedded accelerometer. In order to acquire the ECG signal, both systems require ECG electrodes to be placed directly on the skin. By connecting some cables on the shirt to the electrodes, ECG signal can be acquired and sent to a recording box. This small box, which is placed in a dedicated pocket inside the t-shirt, has an SD card where data is stored for off-line monitoring, and a Bluetooth transmitter that can be used to transmit data to a PC or PDA in real time. These platforms can send data remotely to other locations through Internet connection or GPRS/3G/4G mobile data networks [4, 65].

In Figure 2.16 it is possible to observe an example of a VitalJacket® shirt with the

recording box (Figure 2.16a), as well as a scheme of the communication network used in this WSN (Figure 2.16b). Similarly to the WSN architecture previously described in Chapter 2, VitalJacket® implements a three-tier architecture with a BAN (shirt) and BANC (recording box) – tier 1, local coordinator (PC or PDA) – tier 2, and server or IP-based network – tier 3.

In order to process and analyse acquired data, software suites were developed for each solution, being VJ Rehab used with VitalJacket® 1L and VJ Holter Pro with VitalJacket® 5L. Both suites extract plenty of information from the ECG signal, namely ECG, HR and HRV signals. However, VJ Holter Pro is a more resourceful platform, being able to automatically analyse, identify and separate ECG signal by class and morphology, and to correlate information between ECG and patients' level of activity due to the integration of the triaxial accelerometer in VitalJacket® 5L [4, 65].

2.3.2 VitalResponder

VitalResponder 2.0, or VR2 for short, is an ongoing interdisciplinary research project involving various institutions, and is the natural evolution of two successful projects: VitalResponder and FUMEXP [67, 68]. VitalResponder project came up from the idea of evolving VitalJacket® technology into some innovative pHealth projects, namely for the study of health and fatigue of first responders. The goal of the original Vital Responder project was to "explore the synergies between innovative wearable technologies, scattered sensor networks, intelligent building technology and precise localization services to provide secure, reliable and effective first-response systems in critical emergency scenarios" [4, 67]. VR2 gives the next step in this process, with its goal being to address "the specification, development and deployment of an ICT platform for intelligent management of critical events of stress, fatigue and smoke intoxication in forest firefighting" [68].

As first responders can be subdivided into different groups with different requirements, VitalResponder was designed targeting firefighters as its main end-user. Studies show that almost 50% of the deaths of firefighters that occur while they are on duty, are caused by heart disease. This prevalence is twice as high as that for other types of first responders such as police officers, and three times as high as the average prevalence for normal working population. Risk of death from coronary heart disease also increases during fire suppression, reaching a whopping 10 to 100 times higher risk than in non emergency events. Heart condition is, thus, one of the most life threatening conditions for firefighters, and should be closely monitored together with the factors that directly influence it, such as stress and fatigue [4].

Firefighters are frequently exposed to harmful environments that impose strict requirements in the used systems, thus VitalJacket® had to be redesigned taking into account the new needs.

The first aspect to modify was the textile composition of the garment. Common VitalJacket® is made with a mixture of elastane (28%) and polyamide (62%), but since

(a) Adapted VitalJacket® shirt.

(b) Enhanced helmet, with a microelectronic module for the detection of CO level, temperature and barometric pressure, circled in white.

Figure 2.17: Evolution of VitalJacket® into the VitalResponder monitoring system. Retrieved from [4].

elastane is heat sensitive and can burn wearer's skin, textile composition had to be changed to follow international regulations on firefighters' garments. Textile composition was changed to a mixture of cotton (98%) and elastane (2%), with the external part of the shirt having only cotton. As the outer part heats more than the inner part of the shirt, having an elastane free composition in the outer part makes the shirt more protective and heat proof [4].

As electronics are embedded in the shirt and the shirt had its composition completely modified, it was also necessary to redesign the way micro-cabling and micro-electronic components were embedded in the shirt. Furthermore, since monitoring systems aimed at firefighters must monitor not only physiological signals but also acquire data from the surrounding environment, a microelectronic module that measures CO level, temperature and barometric pressure was inserted in firefighters' helmets [4]. The resulting monitoring system can be seen in Figure 2.17.

Parallel to the physiological and environmental data acquiring system previously de-

scribed, a wireless network based system was developed to monitor teams of first responders. This system clusters acquired data, including individual vital signs (e.g. ECG) and position (localization through GPS), and provides it to the team coordinator. This system does also have the ability to trigger alarms to the coordinator, supporting him in critical decision making by increasing his tactical awareness [4]. This system implements a three-tier WSN architecture. In tier 1, there is the vital signs collecting unit using the VitalJacket®. In tier 2, a Android smartphone (called DroidJacket) receives data from tier 1 and processes it, whilst also measuring data with its GPS, accelerometer and gyroscope sensors. DroidJacket is a key piece of the system as its data processing detects technical issues (e.g. loss of connectivity) and critical events in EGG (e.g. arrhythmias) or in activity patterns (e.g. fall or low activity patterns). Finally, data is sent to the mobile base station in tier 3 through Wi-Fi connection, where the team coordinator can control location and health status of each individual using the VitalJacket® and DroidJacket system [4].

Data acquired with VitalResponder systems is currently under study in order to analyse stress of firefighters while in action. These studies focus on detecting stress indicators that can be used for stress and fatigue management. This is of critical importance, as powerful methodologies remain yet to be defined for long term monitoring of first responders' stress and fatigue levels [4].

Chapter 3

VitalSensors - Towards a more intelligent, wearable monitoring system

This thesis aims to improve a wearable monitoring system's scalability, by working at firmware and software levels in order to make it more capable and intelligent. This work is inserted in the framework of different projects, namely VitalLogger (VL) and VitalResponder2.

3.1 Background

VitalLogger is a wearable monitoring device that seeks to expand VitalJacket®'s existing sensing capabilities. This device is directly connected to VitalJacket®'s main board, and it possesses sensors that enable the measurement of novel physiological signals and environmental parameters. VitalResponder2 is also an evolution of the VitalJacket® system, but that is specifically targeted at first responders. Among the various modules that VitalResponder2 has (adapted VitalJacket, helmet unit, etc), the system has various implemented sensors, namely sensors for various environmental parameters (gas sensors, positioning sensors, etc).

As referred previously in Chapter 1, work developed in this thesis is part of a greater project, where contributions from two other MSc students addressed specific areas of the project. A more extensive component diagram showing the framework that comprises this thesis' work is showed in Figure 3.1. The aim of this greater project is to aggregate data from diverse vital signs and environmental parameters, and while it is mostly based on VitalLogger and VitalResponder2, it also includes VitalX.

VitalX, which has its logo presented on the left part of the diagram, is an Android aggregator that receives, saves and displays information coming from connected devices. VitalX provides the user with the ability to easily control which sensors he wants to

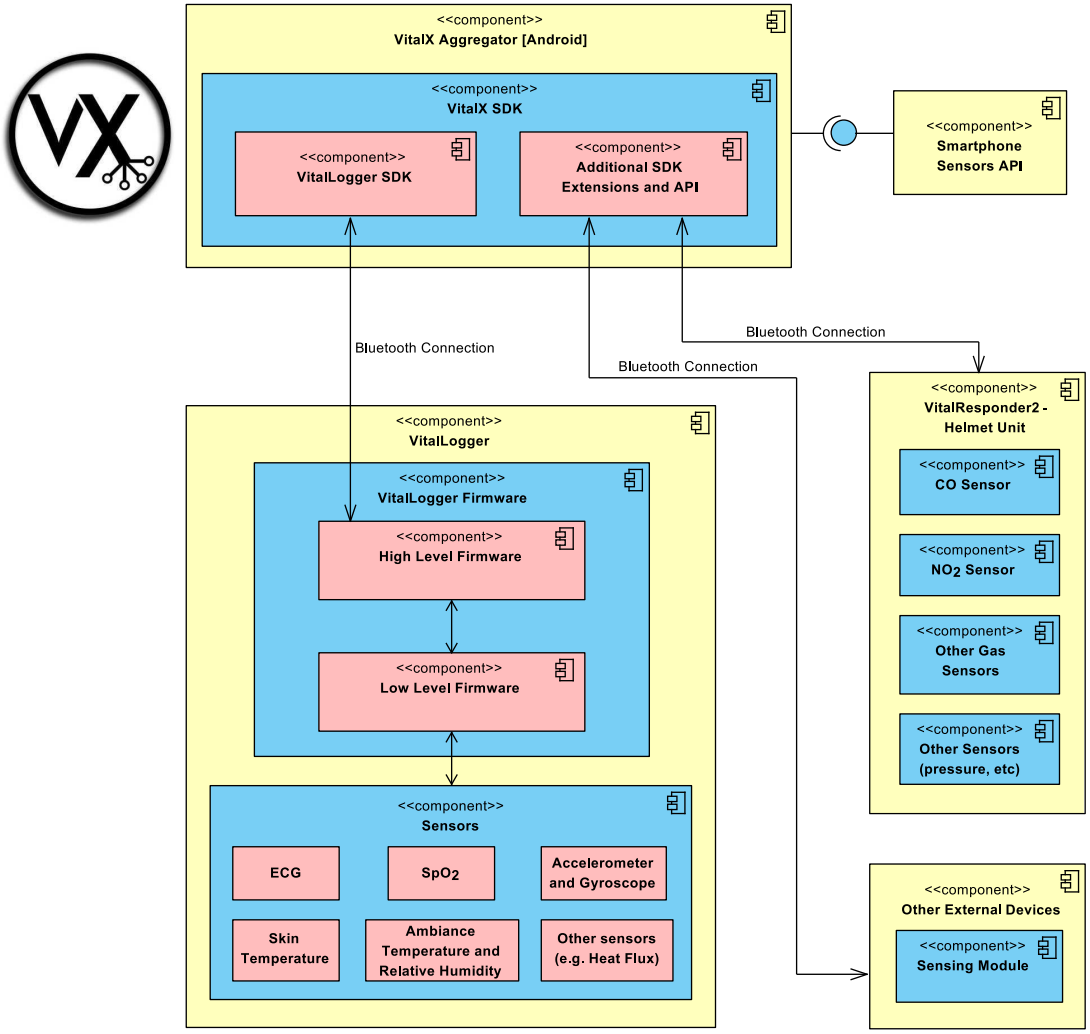

Figure 3.1: Component diagram of the framework which integrates this thesis' work.

gather data from, being it from the smartphone, VitalResponder2, VitalLogger or from other external devices connected to the device running VitalX. VitalX was developed by another MSc student in the scope of his Master Thesis.

VitalLogger is a system that aims to aggregate novel sets of sensors, increasing the range of physiological and environmental variables that can be measured. These sets of sensors can be configured for various purposes and scenarios, such as enabling better medical diagnosis or enhancing personal health monitoring, thus making the end system more versatile.

As it is possible to observe in Figure 3.1, VitalLogger comprises three main components, namely: sensors, which involves all the hardware of VitalLogger; firmware, which can be split in low and high level firmware; and the Software Development Kit (SDK). In what concerns the firmware component, low level firmware is responsible for the communication between VitalLogger's sensors, VitalLogger's circuit board and VitalJacket's board, whereas high level firmware is responsible for the communication between VitalJacket's

board and the devices to whom it is connected through Bluetooth connection.

The SDK is high level firmware's counterpart that runs at the connected device's end, being what enables, for instance, an Android application to receive and interpret data coming from the VitalLogger/VitalResponder, and also to send data back to the device. This thesis' work focused on the high level firmware and SDK components. Low level firmware and all the hardware for VitalLogger were addressed by another MSc student in his Master Thesis project.

Finally, VitalResponder, which has been explained in detail in the previous chapter, is a project targeted at First Responders that among its various interests, seeks to bring wearable monitoring systems to First Responders. While these systems currently provide physiological and environmental data, from deployed units, to the higher entities responsible for decision making and control of deployed units, they still lack important information such as physiological stress and fatigue levels of deployed units. Work developed in this thesis seeks to address this issue, by providing an index of physiological stress, PSI, which can give better insight on unit status, and hopefully help in the prediction of potential danger situations.

The joint contribution of the three Master Thesis encompassed in the framework presented in Figure 3.1, by acting both at the wearable sensing device end and at the more generic devices' end (e.g. smartphones), seeks to begin the foundations for a more scalable system, where the user gains a more active role by being presented with greater control over the system, and with more intuitive information.

Regarding the specific contribution of this thesis, a three-step workflow was followed, where each step addressed a different issue. This workflow is presented in Figure 3.2. The first step intends to increase the sensing capabilities of the wearable system, increasing the variety and amount of data that we can give to first responders.

The second step addresses the selection of acquired data, so that only the most relevant information is used and given to the Fire Chief, and it also involves providing this information to the Fire Chief through an intuitive interface.

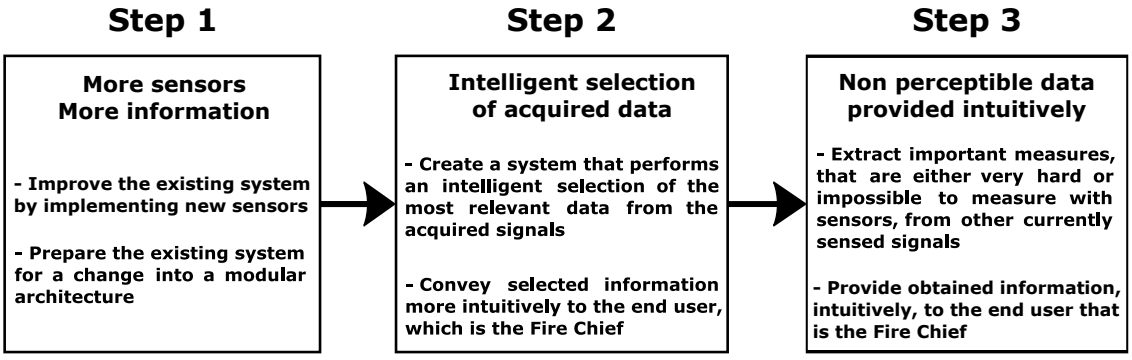

Figure 3.2: Detailed workflow of the work developed in this Master Thesis, in order to accomplish the objective of giving not only more, but better information to first responders.

Finally, there is important information for first responders that is hard to, or even cannot be acquired using sensors. The third step has the objective of implementing a system, based on a Kalman filter, that extracts this information from other currently sensed signals, information which should also be provided in an intuitive way to the Fire Chief.

Since the Kalman filter is a central part of the third step, it is important to understand how it works. The Kalman filter is one of the most important and commonly used data fusion algorithms - which are algorithms that fuse data from various different sensors in order to obtain more knowledge - being mostly used to smooth out noisy, measured data, and to predict values of variables of interest [69, 70, 71]. Great part of this filter's huge success resides in its small computational requirement, recursive properties, and status as the optimal estimator when dealing with one-dimensional linear systems that have Gaussian error statistics [69, 71]. Besides, the Kalman filter can explore correlations between phenomena that users would normally not think of exploiting [70].

This filter runs on the underlying assumption that the variables to be filtered are random and have a Gaussian distribution [70], and it can be seen as a Bayesian model where "the state space of the latent variables is continuous and where all latent and observed variables have a Gaussian distribution (often a multivariate Gaussian distribution)", being an algorithm that enables exact inference in linear dynamical systems [71]. The assumption that all variables follow a Gaussian distribution has immense impact on Kalman filter's recursive properties, as it enables the filter to explore a major property of the Gaussian function, which is that multiplying two Gaussian functions results in another Gaussian function. Hence, as we progress through time, the probability density function remains fully represented by a Gaussian function [71].

Correlation between variables is another important issue for the Kalman filter as, in the case of having correlated variables, the value of a given variable can provide us information on what the values of the other variables can be. Correlation is stored in a covariance matrix, $\sum_{ij}$, where each element holds the degree of correlation between the *ith* and *jth* variables [70].

In what concerns algorithm implementation, Kalman filter is basically a two-stage process consisting of a prediction step and an update step. In the prediction step, the following equations are used:

$$\begin{aligned} \hat{x}_{k|k-1} &= F_k\,\hat{x}_{k-1|k-1} + B_k\,\vec{u}_k \\ P_{k|k-1} &= F_k\,P_{k-1|k-1}\,F_k^T + Q_k \end{aligned} \tag{3.1}$$

Here, $\hat{x}_{k|k-1}$, which is the new best estimate for the state variable vector, is a prediction obtained from the previous best estimate, $\hat{x}_{k-1|k-1}$, plus a correction for known external influences, considered in the control input vector $\vec{u}_k$. F_k is the state transition matrix that applies the effect of the state variables at time $k-1$ on the system state at time k, and B_k is the control input matrix that applies the effect of all control input parameters, which

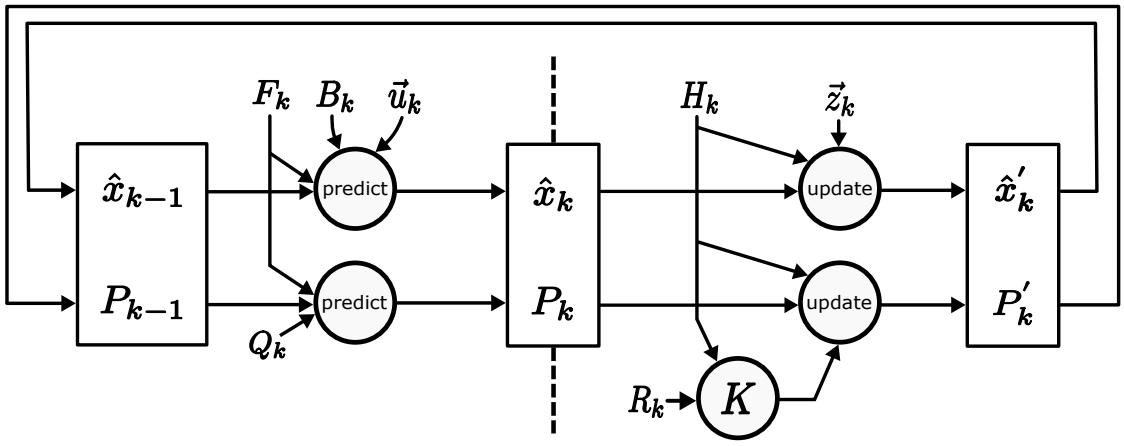

Figure 3.3: Schematic representation of the two-stage loop implementation of the Kalman filter. Adapted from [70].

are in $\vec{u}_k$, on the state vector. The new uncertainty, $P_{k|k-1}$, is predicted from the old uncertainty, $P_{k-1|k-1}$, taking into account additional uncertainty from the environment, Q_k. Both $P_{k|k-1}$ and $P_{k-1|k-1}$ are covariance matrices.

The following stage, which corresponds to the update step, consists of the following pair of equations:

$$\begin{aligned} \hat{x}_{k|k} &= \hat{x}_{k|k-1} + K(\vec{z}_k - H_k\,\hat{x}_{k|k-1}) \\ P_{k|k} &= P_{k|k-1} - K\,H_k\,P_{k|k-1} \end{aligned} \tag{3.2}$$

where K is the Kalman filter gain, which can be obtained using equation 3.3:

$$K = P_{k|k-1}\,H_k^T\,(H_k\,P_{k|k-1}\,H_k^T + R_k)^{-1} \tag{3.3}$$

Here, $\hat{x}_{k|k}$ is the new best estimate for the state vector obtained after the data fusion process. It is considered a data fusion process as, in the update step, data coming from the prediction step is fused with data obtained from measurements (which can be acquired with sensors). In this update process, the new best estimate obtained in the prediction step, $\hat{x}_{k|k-1}$, is corrected by adding a parcel which involves: the Kalman filter gain K, the vector of measurements $\vec{z}_k$, and $\hat{x}_{k|k-1}$ adjusted by a matrix H_k. The transformation matrix H_k maps the state prediction vector into the same domain of the measurements' vector, and is crucial as this mapping procedure enables the multiplication of the probability density functions together.

The uncertainty estimate obtained in the prediction step, $P_{k|k-1}$, is corrected during the update step, resulting in the uncertainty estimate after data fusion, $P_{k|k}$. This new estimate is computed by subtracting the predicted estimate $P_{k|k-1}$, adjusted with the Kalman filter gain K and transformation matrix H_k, from the predicted uncertainty itself. It should also be noted that the Kalman filter gain requires an additional variable R_k, which corresponds to the uncertainty matrix associated with the noisy set of measurements.

Figure 3.3 wraps up the iterative process in which the Kalman filter works. For the sake of simplicity, variables $\hat{x}_{k-1|k-1}$, $P_{k-1|k-1}$, $\hat{x}_{k|k-1}$, $P_{k|k-1}$, $\hat{x}_{k|k}$ and $P_{k|k}$ are displayed as $\hat{x}_{k-1}$, P_{k-1}, $\hat{x}_k$, P_k, $\hat{x}_k^{'}$ and $P_k^{'}$, respectively.

3.2 Methods

Before going through the explanation of the methods used to complete the proposed objectives, it is important to refer that the work herein described was developed in collaboration with Biodevices SA, and that all implemented systems were developed having hardware specifications and restrictions in mind, as these can be a limiting factor.

3.2.1 Novel Sensing Capabilities

The first step of the workflow regarded adding more sensors to the system, and thus making the system capable of gathering more information for first responders.

In order to address this issue, the first part of the work consisted in introducing new sensors, in the VitalLogger device, which extend VitalJacket®'s physiological and environmental sensing capabilities. Figure 3.4 shows a schematic representation of the migration from the old VitalJacket system, to the new VitalLogger one, where three new sensors were implemented.

Since this work was developed in collaboration with Biodevices SA, the choice of the new sensors to be integrated in the system was ultimately decided by Biodevices SA. The following set of sensors was selected to be integrated in VitalLogger: SpO_2 sensor, ambient temperature sensor and humidity sensor.

3.2.1.1 Firmware Development for VitalLogger

With the group of sensors defined, work began on VitalLogger's side, by dealing with the high level firmware component. Firmware development and implementation was done using C programming language, and using the following software: MPLAB® X IDE v3.00 with the necessary MPLAB® XC compiler (free edition) for the used microcontroller, MPLAB IPE v3.00 and PComm Terminal Emulator. MPLAB® X IDE was used to code and compile the .hex file (this is the firmware file) to run on the microchip. The circuit board was connected to the computer through a MPLAB ICD 3 In-Circuit Debugger, and MPLAB® X IPE was used to flash the .hex file into the microchip. Pcomm Terminal Emulator was used to connect the computer to VL's circuit board through Bluetooth connection, enabling the debugging of the coded firmware. An extension for MPLAB® X IDE v3.00, named MPLAB® Code Configurator, was also installed to facilitate control of the microcontroller's pins.

It was decided, in conjunction with Biodevices SA, to implement VL's firmware through the extension of VitalJacket's firmware, thus new firmware was coded directly on Vital-

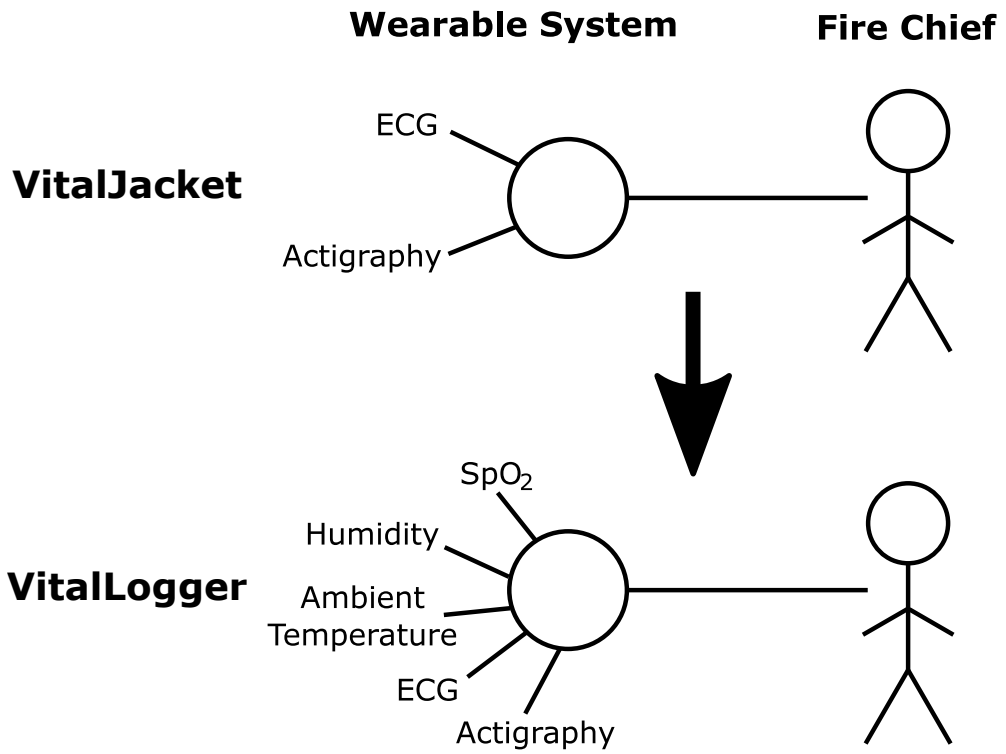

Figure 3.4: Schematic representation of the old system, and of the new system after implementing new sensors. On the top image, there is the old VitalJacket system which has only ECG and Actigraphy sensors. On the bottom, the VitalLogger system is represented, which has the new sensors for SpO_2, ambient temperature and humidity.

Jacket's existing firmware. This part of the work focused on implementing the interface between VL's hardware and connected devices (e.g. smartphones, PCs), on VL's side of the communication process. Data measured from VL's sensors is processed in the low level firmware, and when it gets to the high level firmware, it is arranged in a datagram before being sent to other devices, through Bluetooth connection. Due to the followed approach, transmitted datagrams contain data both from VitalJacket and VL's sensors. A schematic representation of a possible datagram sent by the device, through Bluetooth, is presented in Figure 3.5a. It is important to refer that priority was given to VitalJacket's sensors, hence these are always placed first in the datagram.

Data from each sensor must be identified in the datagram, so that the other end of the connection (e.g. smarthphone) is able to correctly interpret and manipulate received data. This is ensured by sending a tag value, that is unique for each sensor, immediately before each sensor's bytes of data, as it is possible to see in Figure 3.5b. For this purpose, a unique tag value was configured for each new sensor introduced in the hardware system, and the firmware was adapted to include the new sensors in the datagram.

The rate at which each sensor's data is sent by the device is defined by an independent variable, herein named as timestamp. Since each sensor has its own timestamp, it is possible to send data from different sensors at distinct rates. This means that the datagram

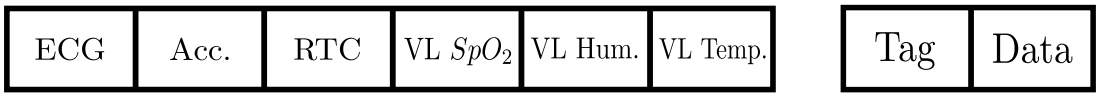

(a) Example of a datagram sent by the VL. Data from VL's sensors is always sent after data from VitalJacket's sensors. RTC means Real Time Clock.

(b) Composition of each sensor's section in the datagram.

Figure 3.5: Schematic representation of a possible datagram sent by VL through Bluetooth connectivity. For each sensor, a tag value must be sent previous to its data, in order to identify what data is present in each section of the datagram.

sent by the device can either be constant in terms of size - if all sensors have their data sent at the same rate - or change cyclically - if different sensors have different sending rates. While these timestamps are independent and can easily be manipulated, this 'property' will only be explored in another part of this thesis. Therefore, a fixed rate of 1 sample per second was defined for the SpO_2 sensor, whereas a rate of 1 sample each 5 seconds was defined for the ambient temperature and humidity sensors. Although a gyroscope sensor is comprised in VitalLogger's hardware, it was not implemented in the low level firmware at the time of this thesis. Nevertheless, a tag value and timestamp were allocated for this sensor in the high level firmware.

3.2.1.2 Implementation of the Extended SDK

After dealing with VitalLogger's side of the communication process, attention shifted to the other side, which comprises the devices that connect to VitalLogger, namely smartphones. In order to be able to correctly decrypt and interpret data contained in the received datagrams, VitalJacket's SDK had to be extended. Using a similar approach to that followed in the implementation of the extended firmware, SDK extension was achieved by implementing changes directly in VitalJacket's SDK. Code was implemented in Java programming language, with Android Studio 1.2 being the only software used for this part of the work.

Firstly, tag values for the new implemented sensors were configured in the SDK, in order to ensure proper reception and handling of the data contained in the datagrams sent by the VitalLogger. Since data sending rates were specified in the extended firmware, and sensors from the VL were configured to have different sending rates, an individual counter was implemented for each VL sensor, to control the amount of times data from each sensor was received in the device connected to the VitalLogger.

In order to test the functioning of the new SDK, a test Android application was adapted to run the new SDK and explore its new features, displaying data received from the new sensors, as well as the counters used to control data rates. Figure 3.6 shows the application running in a smartphone that is paired with the VitalLogger. It is important to refer that the images presented in Figure 3.6 were obtained from a test where a VitalJacket shirt connected to the VitalLogger, to ensure that the system worked fine with all sensors

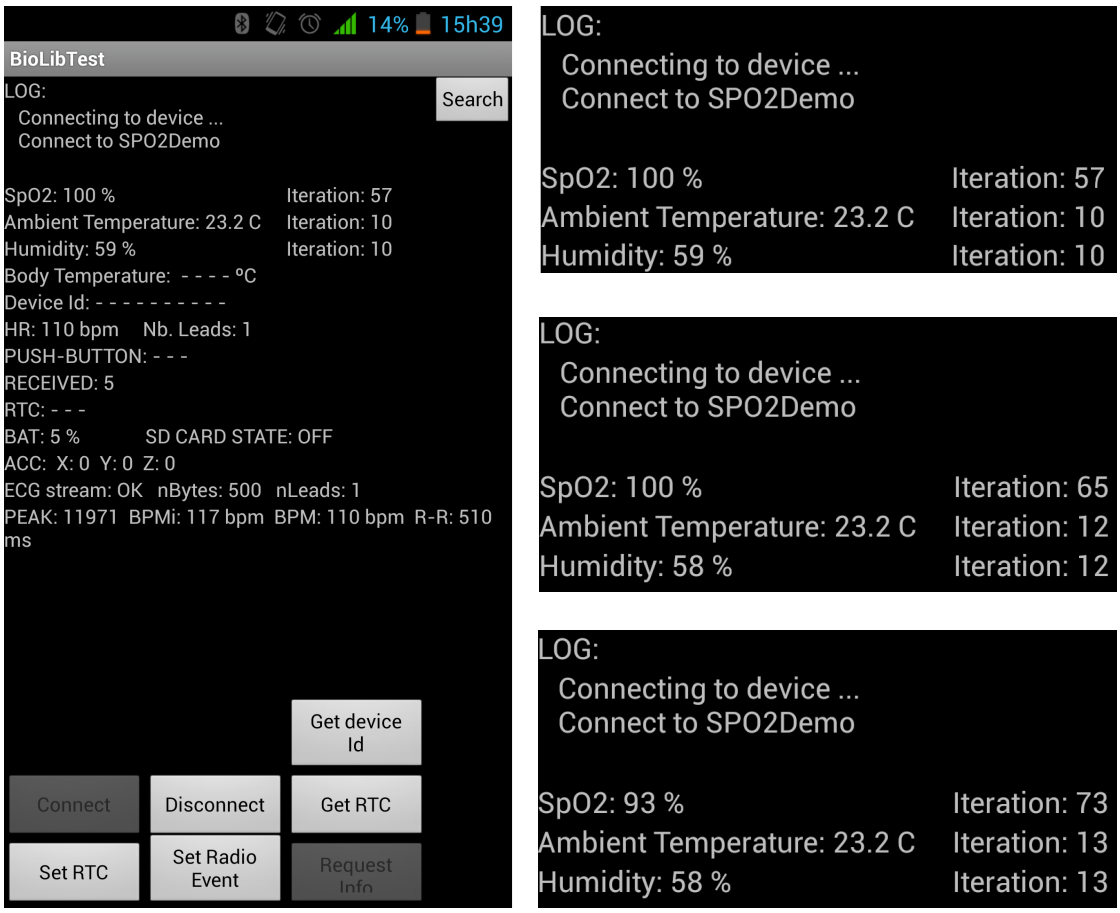

Figure 3.6: Test application displaying data and counters for the new implemented sensors. The images on the right show clearly that the SpO_2 sensor sends data at a rate around five times higher than the ambient temperature and humidity sensor, since the value in its counter is approximately five times the value in the other counters.

gathering data at the same time. On a side note, it is possible to see in Figure 3.6 that there is no data being received from the body temperature sensor, which was due to the fact that the VitalJacket shirt that was used in these tests was from an older version of VitalJacket, which did not possess the body temperature sensor.

As it is possible to observe in Figure 3.6, the counters provide us some information on the rates at which data from each sensor is being received, and, for instance, it is noticeable in Figure 3.6 that the counters for the ambient temperature and humidity sensors have the same value, whereas the counter for the SpO_2 sensor has a value that is approximately 5 times higher than that of the ambient temperature and humidity sensors. While the increase rates of these values go in agreement with the timestamps that were configured in VL's firmware, implemented counters do not present information in an intuitive way. Therefore, in order to present data sending rates in a more accurate and intuitive approach, an analysis based on timers was implemented for each sensor. These timers measure the time lapse between the reception of two consecutive samples of data for each sensor.

Figure 3.7: Test application displaying the data sending rates obtained with the timer implementation, the list of sensors being effectively used (placed below the timers), and the possible cases for the SpO_2 sensor. 1 - Full app interface; 2 - No finger is placed in the sensor; 3 - The finger is placed correctly; 4 - The finger is misplaced, hence incorrect SpO_2 measurements are acquired.

In what concerns code implementation, these timers were implemented recurring to the System.nanoTime() method.

Due to the influence of finger positioning in the SpO_2 sensor on the obtained SpO_2 measurements, the SDK was prepared to respond to two different flags that are sent by the sensor in specific situations. When there is no finger placed inside the sensor, the sensor obviously cannot detect a finger so it sends a flag with a value of 120, which is interpreted by the SDK by showing a text message in place of the measured sample saying "unplugged". The second situation occurs when the finger is badly placed inside the sensor. Here, SpO_2 is inaccurately measured, so the sensor sends a flag with a value of 110 in place of the SpO_2 measurement. The SDK interprets this flag by showing an empty sample in the application, displaying as "- - - %". When measurements occur correctly, the sensor just sends those SpO_2 measurements in the datagram.

Furthermore, while the VitalLogger possesses various sensors, namely those present in the VitalJacket added to those implemented in the VitalLogger hardware, the device can be configured to gather and send data only for some specific sensors. Hence, it is important to know which sensors are being used in a given configuration. For this purpose, a feature

was added to the SDK, where the sensors that are actually being used by the VitalLogger are placed in a list.

The test application was updated to run with the second version of the extended SDK and explore these new features. Figure 3.7 shows the new version of the test application running in a smartphone. Firstly, it is possible to see in Figure 3.7 that the presented data sending rates now match those configured in VL's firmware, being this information much more intuitive from the users' point of view. Then, it is possible to observe how the system handles the possible situations in SpO_2 measurements. In Figure 3.7, the images on the right show a succession where the sensor starts measuring with no finger inside it, then it measures a correct sample, and finally the finger is misplaced on purpose to produce an empty sample in the test application. Regarding the sensor list, it is possible to observe that the SDK is prepared to display sensors both from the VitalJacket and the VitalLogger, and that it only shows the sensors that are being used by the system.

Besides the Android version, the SDK was also adapted for Windows platform, using Microsoft Visual Studio 2010 for that purpose. The ECGTool from Biodevices SA used to test the SDK was adjusted to work with the new SDK, and thus to be able to acquire measurements from the SpO_2 sensor. In Figures 3.8 and 3.9, it is possible to observe the ECGTool acquiring data from VitalJacket's from VL's sensors. Figure 3.8 shows an acquisition being performed without a finger inserted in the SpO_2 sensor, which prompts the application to display "Sensor Unplugged". Figure 3.9 displays a normal acquisition, where the finger is inserted in the sensor and SpO_2 measurements are acquired.

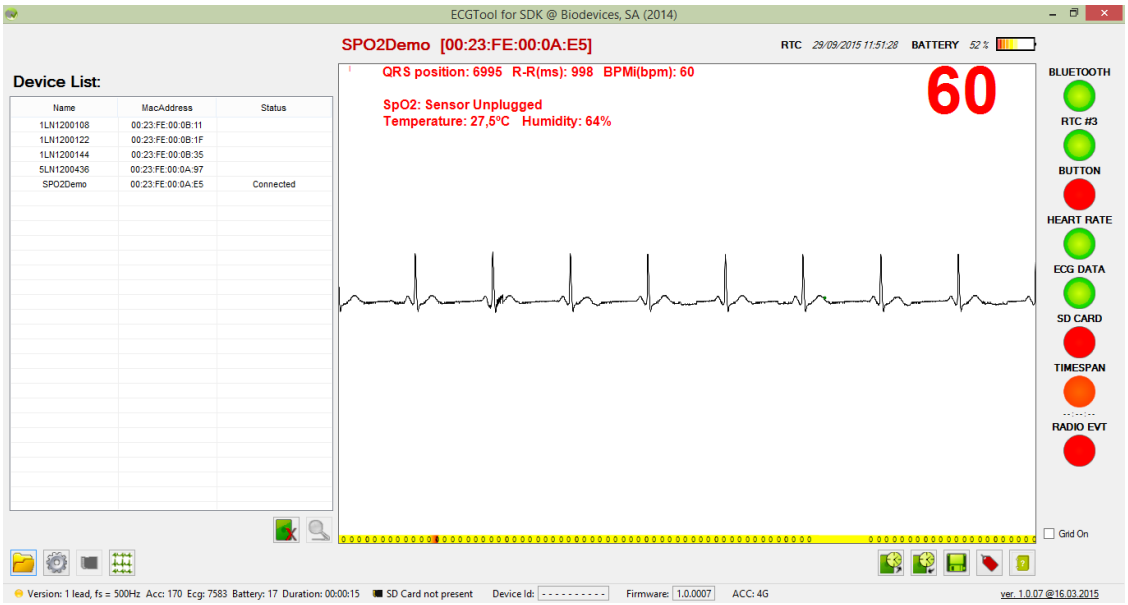

Figure 3.8: Acquisition from VitalLogger prototype, executed with the Windows SDK application from Biodevices SA, and performed without a finger inserted in the SpO_2 sensor.

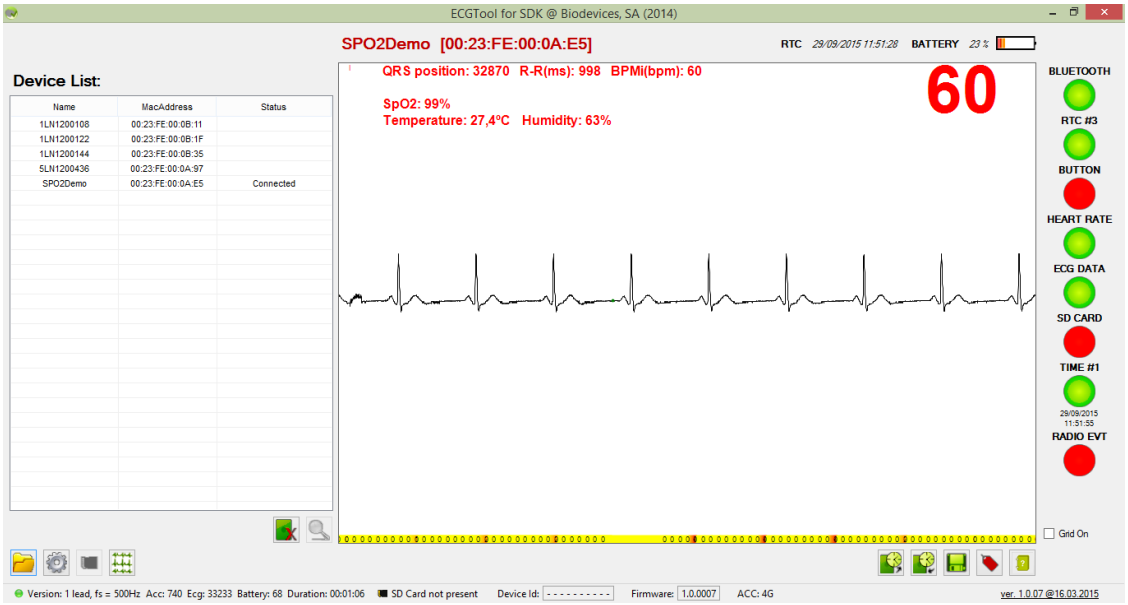

Figure 3.9: Acquisition from VitalLogger prototype, executed with the Windows SDK application from Biodevices SA, and performed with a finger inserted in the SpO_2 sensor.

3.2.1.3 Adapting Firmware For a Modular System

Still regarding step 1, which involves introducing new sensors that let us obtain more information, it is important to rethink the approach of having all sensors implemented in a single hardware board. While at the moment there is actually no specific issue with that, using a single hardware board for everything can be compromising as it limits the expansion of the system's sensing capabilities in the future, due to obvious physical limitations (e.g. the finite number of ports that the microcontroller has to use).

In order to make the system capable of complying with the sensing needs that might exist in the future, it is important to evolve the current system into a modular architecture system, such as the one depicted in Figure 3.10. This architecture implements a concept of master and slave, where the central unit (the master) controls all the slaves, and where slaves are responsible for having the sensors and acquiring data with them, data which is then sent to the master. This architecture lets novel sensors be added with less limitations, since they can be integrated in new modules (slaves) that must be connected to the master.

To address this issue, this part of the work consisted in the development of the firmware for a modular system architecture. At the time of this thesis there were no developed modules, with the wearable system having a hardware board with all sensors connected to the same microcontroller. Therefore, this part of the work was developed and tested with development boards simulating the modular system that can be used in the future.

All firmware was developed using MPLAB X® X IDE v3.00, and the MPLAB® XC16 compiler v1.25 (free edition), since 16-bit microcontrollers were used in this part of the work. The hardware set on which the firmware was tested consisted of two Explorer

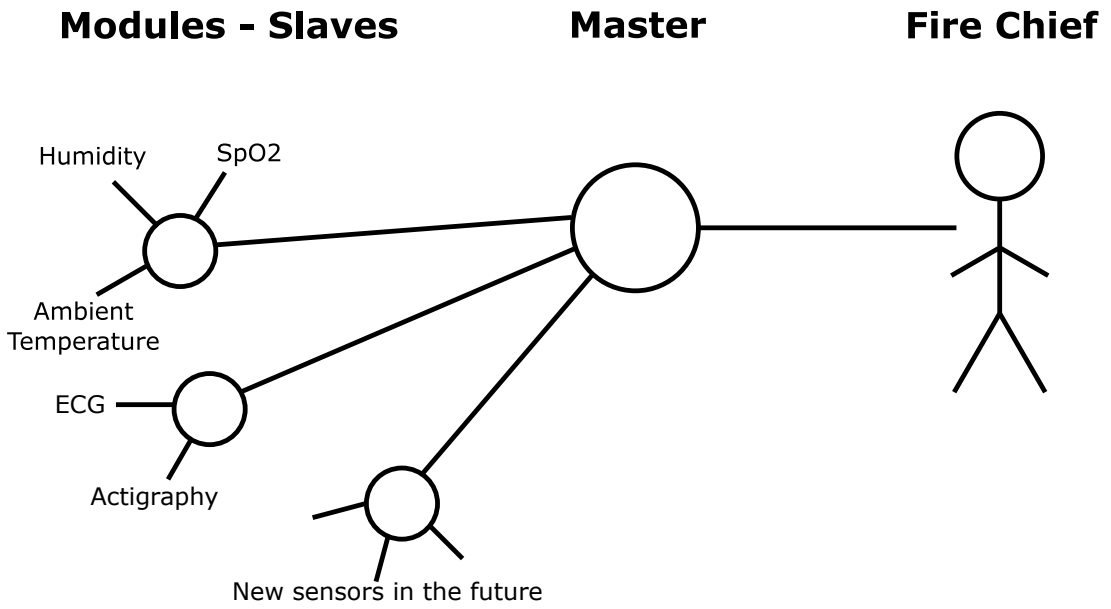

Figure 3.10: Schematic representation of the future system, with a modular architecture, that enables the expansion according to the sensing needs that might appear in the future. Here, a concept of master and slave is implemented, where all the sensing modules (slaves) are connected to the master. Data sent from the slaves to the master can be processed and sent to the end user, which is the Fire Chief.

16 Development Boards with 44-pin PIM, from Microchip, a MPLAB ICD 3 In-Circuit Debugger, and a Logic debugging hardware unit, from Saleae, coupled with its software Logic v1.1.1.15. The used hardware set in this part of the work can be seen in Figure 3.11.

Before going through this part of the work, it is necessary to understand the concept behind a modular approach. A modular system is essentially a system where components and tasks are more decentralized, splitting the workload across the different modules, and leaving the essential tasks to the central unit. This is important because it makes it possible to have more sensors in the system, enabling the expansion beyond the inherent hardware limitations of using a single hardware chip. The sensors can be connected to the modules, which are responsible for the signal acquisition and processing, and the resulting signals are sent to the central unit, which can further process the data and send it to external devices, for example, through Bluetooth connection.

In order to have this data flow between the modules and central unit working properly, it is necessary to have a robust way to communicate across hardware units. Since Biodevices SA currently uses Serial Peripheral Interface (SPI) protocol in its product, it was decided to use SPI in the new firmware implementation. Another possibility would be to use I^2C, which is another type of protocol, but it is known that there exist issues when using I^2C with components from Microchip. As the hardware set shown in Figure 3.11 is mostly composed of components from Microchip, it was decided to use SPI in the new firmware implementation.

SPI is a synchronous serial interface, which uses a bus (a collection of wires) to connect

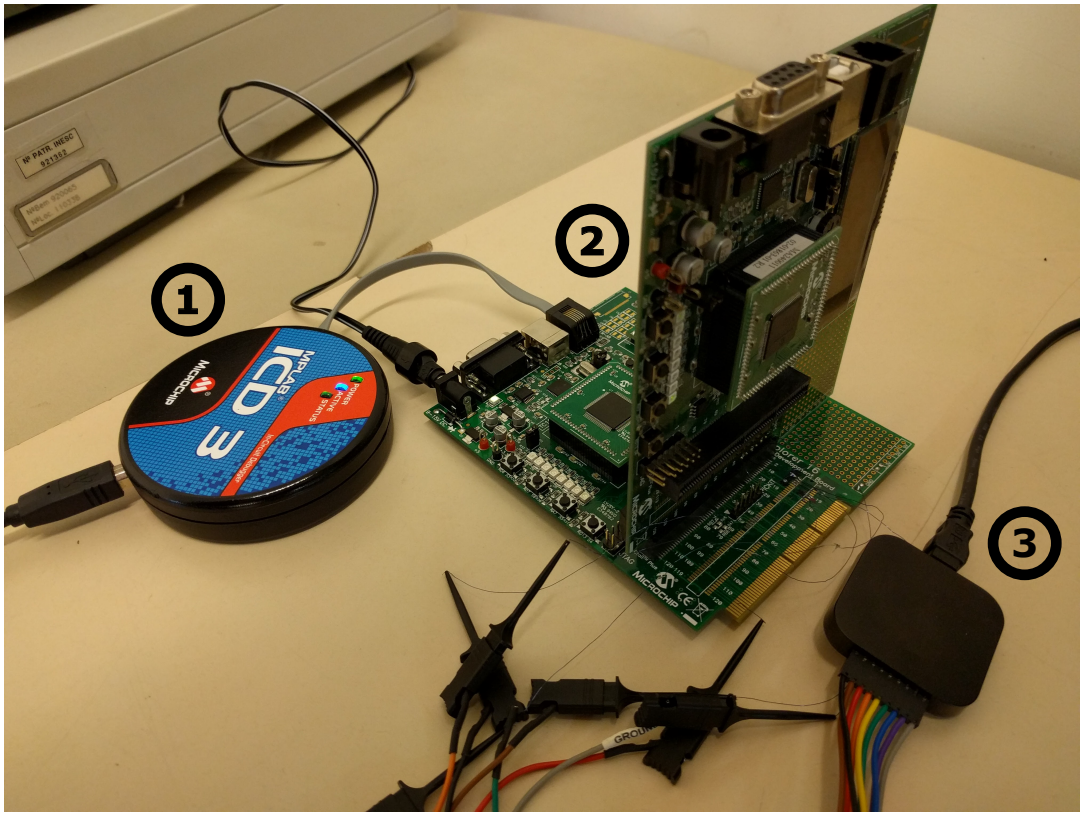

Figure 3.11: Hardware set used to simulate a system with modular architecture. 1 - MPLAB ICD 3 In-Circuit Debugger; 2 - Explorer 16 Development Boards, from Microchip; 3 - Logic debugging hardware unit.

all devices. While using a single bus to connect all devices naturally reduces the number of connections needed between the devices, it also has limitations, such as: only one device can "speak" at a time, and all devices must know when another device is already "talking" on the bus.

The SPI bus is implemented in a way that overcomes the problems of using a bus. Firstly, if defines that one device must be the master, commanding all remaining devices, which are called slaves. The master can communicate with all slaves, and the slaves cannot communicate between each other, ensuring that each slave can only report to the master. An enable line is used by the master to inform a slave if it is active at a given time, being active when the line is low (0) and inactive when the line is high (1). This line can be referred to as either Enable, Slave Select, or Chip Select, and each slave has its own enable line connecting it to the master.

The master also has a clock (CLK), which is sent to the slaves through the CLK line in the bus. This clock is responsible for the synchronicity of this communication protocol (remember that SPI is a synchronous serial interface). Finally, there are two lines where data is sent to and by the master. The master transmits data to slaves through MOSI (Master out, Slave in) and receives data from the slaves through MISO (Master in, Slave

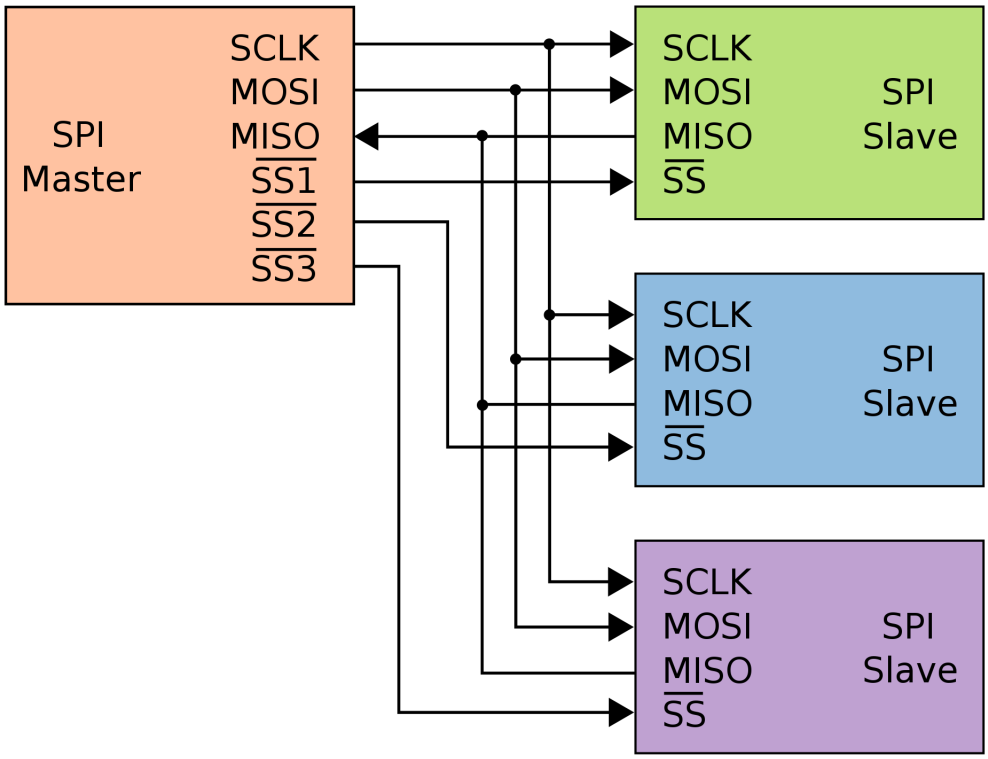

Figure 3.12: Schematic representation of a master connected to three slaves through the SPI bus. The bus has the SCLK (or CLK), MISO and MOSI lines, which are shared by all slaves with the master, and the SS (or CS) lanes that are specific to each slave. Retrieved from [72].

out). Only one slave can send data through MISO at a time, and the Most Significant Bit is mostly sent first.

Communication between master and slave occurs in a way that when the master sends data to a slave, the slave must send some information back to the master, and when the slave sends data to the master, the master must also send data back in exchange. This is because in SPI data is *exchanged* between master and slave. A schematic overview of this typical SPI protocol can be seen in Figure 3.12.

Furthermore, some devices require an extra flow control signal from slave to master, defined as Data Ready, which is used by the slave to inform the master when it has information ready to be sent. The Data Ready signal is active when low (0), and it must be enabled between words, which are the pieces of information sent by the slaves to the master on the MISO line [73].

To implement a modular architecture, a SPI protocol to be used between the master and the slaves was firstly defined. This protocol is used by the slaves to send data from its sensors to the master, and its structure is based on the file structure described in [74], but having a much simpler structure. The basis of this protocol is composed of 5 different units. The first byte contains a command tag which signals that data from the sensors

Command tag	Number of bytes	Module ID	Data	Data	CRC

Figure 3.13: SPI protocol defined to use in the communication between the slaves and the master in the modular system.

is going to be sent to the master. The second byte contains the number of bytes that the master must read from that point until the end of the data sent by the slave. The third byte has the unique identifier that identifies each different module. The following bytes contain the data from the sensors on the module, and can vary according to the module sending the data (modules with different unique identifiers have different sensors and, consequently, different data). This section extends until the penultimate byte in the datagram. The last byte holds the Cyclic Redundancy Check (CRC) value, which is used to confirm the validity of the data received by the master. This protocol is displayed in Figure 3.13.

This protocol was implemented in a state machine where each state is responsible for reading one of the 5 units in the protocol that were described previously. When the master first receives the data from the slave, it calculates the CRC value of the received data and compares it with the CRC value sent by the slave. If both values are equal, data received by the master is valid and can be used.

In order to check if the boards emulating a slave and a master were communicating correctly with the defined SPI protocol, the slave board was firstly set to send fixed values for each unit in the "datagram", and the master board was set to send the same byte in each SPI data exchange with the slave. The probes from the Logic debugging hardware were connected to the SPI ports (MISO, MOSI, CLK, CS and Data Ready). This unit was connected to a computer running Logic v1.1.1.15 software, where the communication

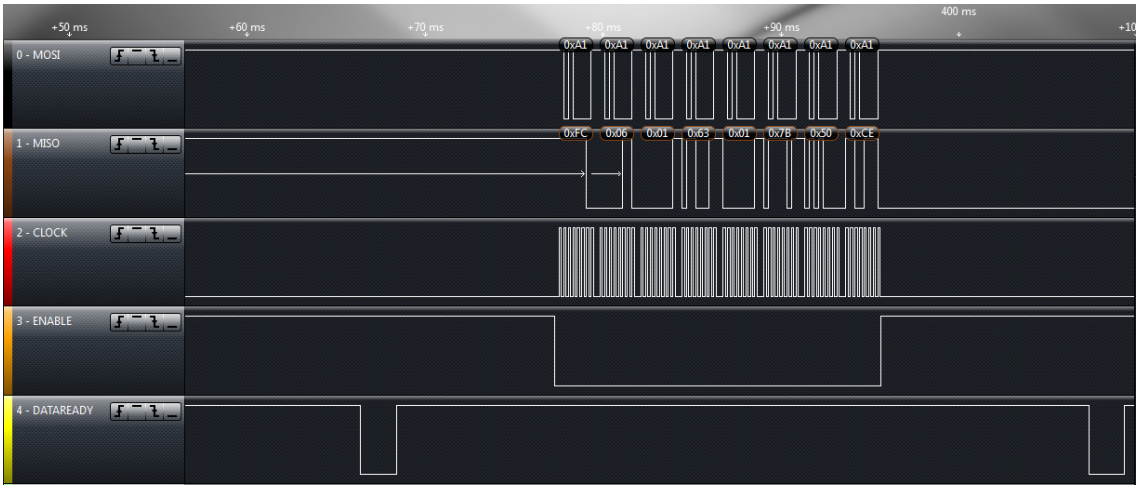

Figure 3.14: A single section of the SPI communication between the master and the slave, with the MOSI, MISO, CLK, CS and DataReady lines observed in Logic v1.1.1.15.

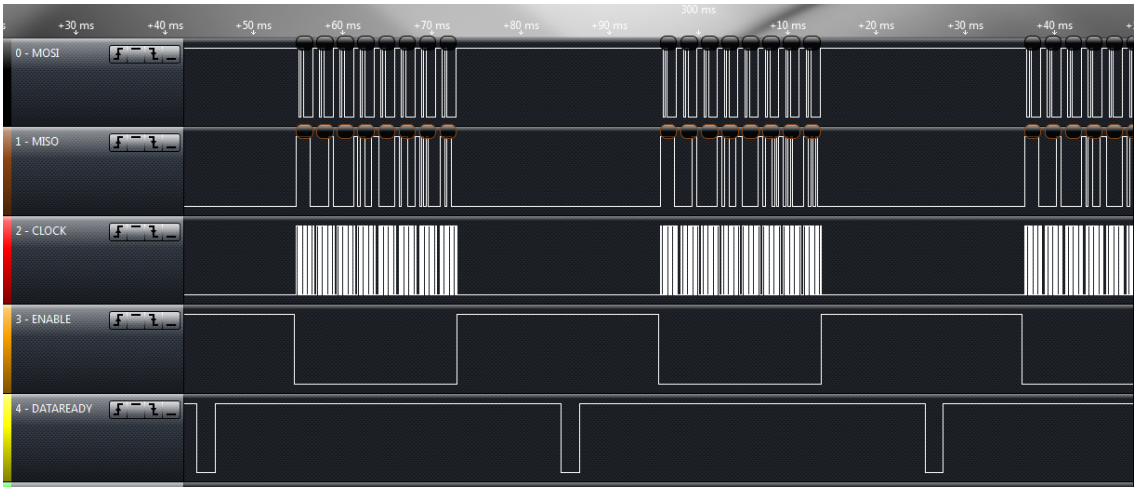

Figure 3.15: View of the SPI communication between the master and the slave with three different segments, with the MOSI, MISO, CLK, CS and DataReady lines observed in Logic v1.1.1.15.

between the boards can be seen. The resulting image can be seen in Figure 3.14. Here, it is possible to see that the process starts with the slave signaling that it has data ready to be sent, by activating the Data Ready line (putting the line in low, and setting it back to high after some time). Then, the master activates the CS line for the slave, making it low as well, which signals that the slave can start sending its data. Shortly after, the slave sends its data (MISO line), and the master exchanges a byte that is constant for each exchange (MOSI line). This sending "procedure" is synchronized by the master's clock.

With the SPI protocol running correctly, a configuration with a different group of bytes to be sent (different module ID and data) was tested. The final test consisted in running a VitalLogger emulating board, with one byte for the SpO_2 value, two bytes for ambient temperature (the first byte has the most significant byte), and one byte for the humidity value. Figure 3.15 displays the SPI communication for this case, running correctly synchronized. Moreover, since data from the ambient temperature sensor will be important further in the work, the slave was configured to send temperature data from a vector with a temperature signal. This signal is iterated through, in the slave, to have the slave sending one sample from the vector each time data is sent to the master.

Once having the SPI communication working correctly for the VL board emulation, with a temperature signal being sent by the slave, the second state machine was implemented, which is basically a parser where data received by the master is run through. This state machine must first check the identifier of the module. As this parser is configured to know how to handle data from datagrams with different identifiers, after checking the identifier the machine knows the procedure to follow in order to extract data correctly.

In the case of the VitalLogger module, the machine must firstly extract the byte with the SpO_2, then the two bytes that contain the ambient temperature (the first byte has the most significant byte), and finally the byte with the value for humidity. It is important

to refer once again that configurations for future modules must be implemented in this state machine, so that it knows how to properly handle data received from different slaves. After running the data through the parser, extracted data is ready for being used by the master in other tasks.

3.2.2 Intelligent Data Reduction

With large amounts of data being gathered by the wearable system, for instance from VitalLogger and VitalResponder, it is important to select the data that is given to the Fire Chief, in order to reduce data redundancy and to make it easier for the users, namely the First Responders who have to carefully control gathered data and analyze it to detect risk situations. Moreover, this information should be conveyed intuitively, so that the Fire Chief can interpret it more easily and quickly.

To reduce the amount of data passed from the wearable system to the user, a control system was developed to intelligently select the data to be sent to the interface that shows the data to the user (for instance, an android application running on a smartphone), thus reducing data redundancy. The algorithm for this control system was projected and developed so that it complies with data from the different sensors that are implemented. Then, it was decided to implement the system with a specific sensor. The ambient temperature sensor was selected as it possesses important information for the First Responders, who frequently operate on hazardous conditions.

Figure 3.16 is important to explain how this system works. This figure exemplifies, with an ambient temperature signal, two possible scenarios that the selecting system can be presented with. In both signals ambient temperature starts within acceptable levels. Two thresholds are visible in the figure, but since this work is aimed at first responders, namely firefighters, only the higher one is relevant. When temperatures stay within this "safe region", data is sent to the Fire Chief at a slower rate, as changes within this region are less important for the Fire Chief to keep track of.

As temperature increases beyond the upper threshold, the system should notify the Fire Chief with more information, by providing him temperature measurements at a faster rate. When temperature rises above the upper threshold, two situations can occur. The first one is shown by Signal 1 in Figure 3.16, where temperature rises sharply above the threshold. When temperature change is steep, the system should automatically select a faster rate for sending temperature measurements to the Fire Chief. The second possible situation is depicted by Signal 2, where temperature rises above the threshold but far less sharply. Here, the system should adapt itself to send temperature measurements to the Fire Chief at a faster rate than that used inside the "safe region", yet slower when compared to the rates used in the situation presented in Signal 1. When temperatures get back below the upper threshold, the system should automatically start sending temperatures at a slower rate.

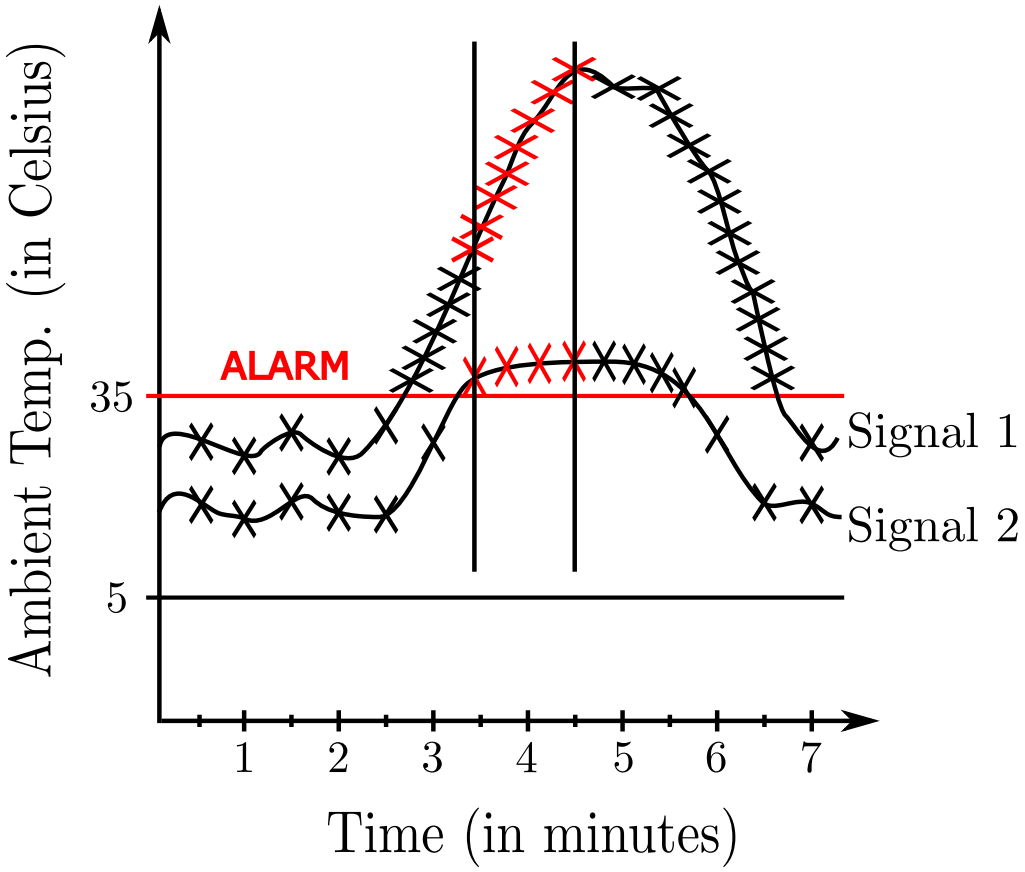

Figure 3.16: Two different scenarios, exemplified with an ambient temperature signal, where the algorithm for data selection can work, and where different responses are obtained. For temperatures above the higher threshold, an alarm is triggered, and an algorithm starts working, which selects more or less samples of data depending if the signal is varying significantly (Signal 1), or if it is relatively stabilized (Signal 2).

Moreover, the higher threshold can be used to trigger an alarm for hazardous situations, which defines when firefighters are being subjected to dangerous environmental conditions. Therefore, when temperature rises above the threshold, the Fire Chief should be notified that a dangerous situation exists, so that he can control his units and means on the field based on that knowledge. According to the Occupational Safety & Health Administration from the United States Department of Labor, when air temperature exceeds 35 degrees Celsius, heat load on the body increases [75], therefore the threshold was set with this limit to notify Fire Chiefs when ambient temperature starts being considered a risk factor.

The control system responsible for this data selection procedure can be decomposed in two components: one that works when temperatures are inside within the thresholds, and another one that works as soon as temperatures step outside the thresholds. The first component is pretty straightforward, with the system sending data at a slower, fixed rate. On the other hand, the basis of the second component lies on an algorithm that checks whether data sensed by a given sensor is changing significantly or not, using the obtained

response to decide on speeding up, maintaining or lowering the rate at which data is sent.

As it was stated previously, the rate at which data from a given sensor is sent is configured through a variable, herein referred as timestamp, which is independent, in the sense that each sensor possesses its very own timestamp, and manipulable, as they can have their value easily changed. A key aspect to take into account is that, actually, not every sensor can have its timestamp changed. The way existing firmware is implemented determines that some sensors must have their timestamps fixed at a constant, immutable value, in order for the system to work properly. The sensors implemented in the VitalLogger can have its timestamp changed, therefore the ambient temperature sensor was selected to test the developed system, as this variable presents great interest for the First Responders, more specifically for firefighters who operate in hot environments.

The system responsible for selecting data, when the signal is outside the "safe region" defined by the thresholds, can be split in the algorithm and in the state machine, where the algorithm is implemented in the firmware. These will now be explained in detail in what concerns their implementation.

3.2.2.1 Algorithm development

While the data reduction system was implemented for VitalLogger's ambient temperature sensor, the algorithm described in this section was developed considering the premise that it should be compliant with various types of sensors, namely the SpO_2, ambient temperature and humidity sensors from VitalLogger, enabling easy implementation so that this control system can work with any sensor out of the box.

Regarding algorithm development, MATLAB was the software used to develop it and to do the first tests. Then, using Codeblocks, the algorithm was migrated into C programming language, tested and updated until a stable version of the algorithm was obtained. Finally, the full system was implemented in the firmware using MPLAB X.

The basic workflow of the algorithm responsible for detecting significant changes in the signal is presented in Figure 3.17. The algorithm uses a buffer to keep track of the sensed signal. These samples that are stored in the buffer are the only knowledge on the signal that the algorithm possesses for the analysis procedure. The algorithm starts by filling the buffer with samples from the signal. When the buffer is finally full, the algorithm starts analysing the signal contained in the buffer and checking for significant changes in the signal, classifying the variation in the signal as significant or non-significant. Also, after the buffer is full, when a new sample acquisition is performed, the oldest sample in the buffer is erased and the new sample takes its place.

In order to test and tune the algorithm's configurations, the algorithm had to be applied firstly on reliable test signals. Thus, before developing the algorithm itself, the signal issue had to be addressed, using a three-step approach for that purpose, which can be seen in Figure 3.18.

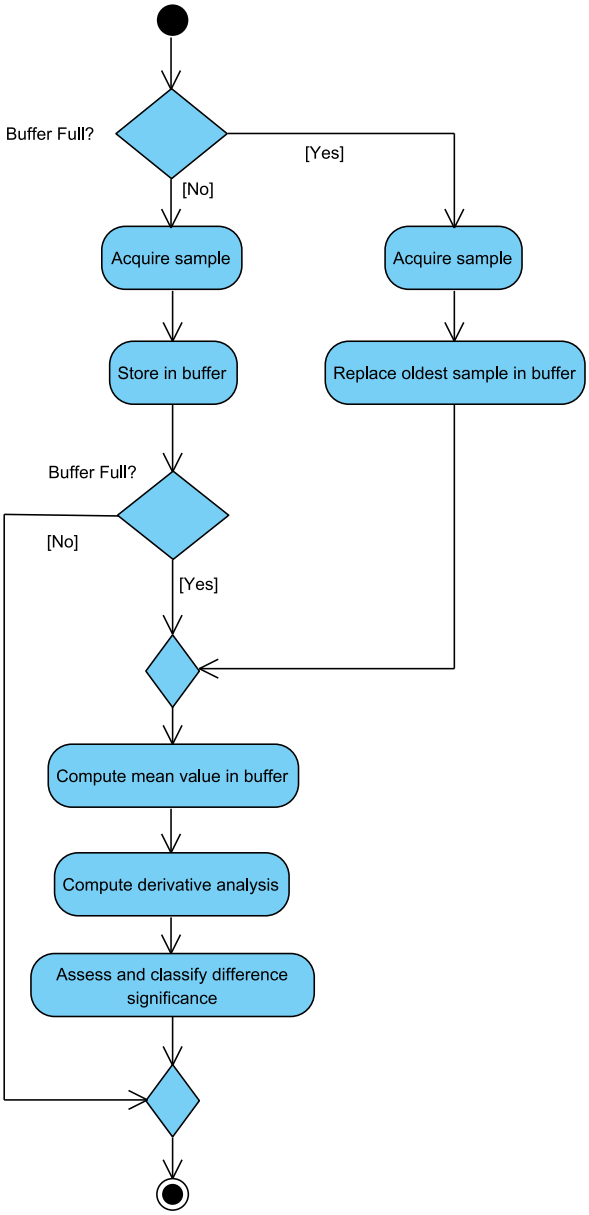

Figure 3.17: Basic workflow of the algorithm developed to detect significant changes in sensed signals.

The three-step process is a simple, yet necessary process to evaluate the algorithm in a reliable, validated way. In this process, an expected binary classification, where 1 represents a significant variation and 0 a non-significant one, is firstly created. This expected classification is the ground truth that will be used for comparison later on. From the expected binary response, a signal is created that, when analysed with the developed algorithm, should result in the expected binary response. The algorithm is applied to the signal and a binary classification is obtained. This classification can differ from the one used as the ground truth. By comparing the obtained classification with the ground truth one, it is possible to extract metrics that enable the evaluation of the algorithm's

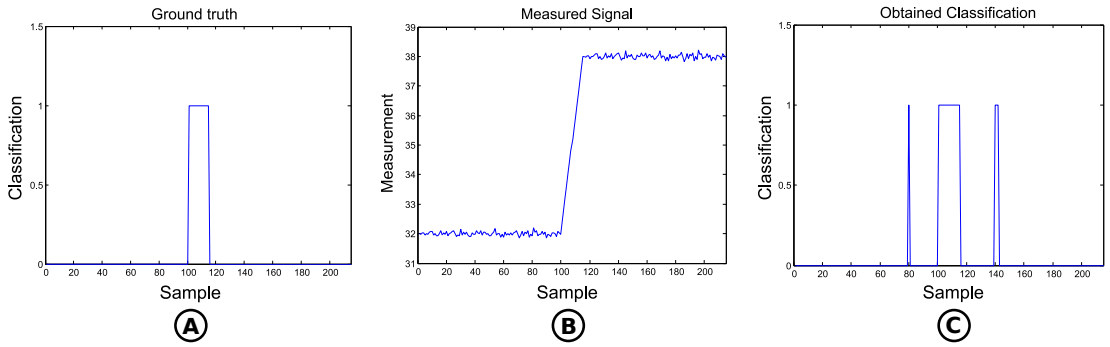

Figure 3.18: Three-step process used to test and evaluate the algorithm with known signals. A - classification's ground truth, B - original signal, C - classification obtained with the algorithm.

performance.

To use this three-step process, a signal generator with different binary responses and resulting signals was created. For each binary response, different possible signals were created, with each binary response representing a possible trend in the signal. The final version of the generator has 14 different signals, which were used to evaluate and tune the algorithm. An example of a signal contained in the generator is the one presented in Figure 3.18, where the binary classification on the left and the signal in the middle are both contained in the generator. This specific example represents a situation where a sudden, significant change in a noisy signal occurs. Due to the presence of noise in the signal, there is the possibility of detecting false significant changes in the signal.

With the signal generator fully functional, it was time to work on the algorithm itself. The development phase had to take into account the existing limitations at the hardware level (e.g. free memory available to use), which directly affects some aspects such as used buffer size. Consequently, buffer size limits the maximum possible delay to use in the derivative analysis, which is buffer size minus 1, since 1 of the samples in the buffer holds the value for the current measurement.

The threshold selected for the classification of signal variation as significant or non-significant is based on the mean value of the signal contained in the buffer. This is in fact an adaptative threshold since it works as a sliding mean which changes according to the knowledge on the signal we have from past samples present in the buffer. This threshold criteria enables the implementation of the algorithm for various types of signal, as the criteria only depends on the measured signal. It should be noted that since this threshold depends on the magnitude of the signal, some baseline bias might occur.

The effective threshold criteria used in the algorithm consists in a percentage of the above mentioned mean value of the signal saved in the buffer, hence the higher the signal's magnitude, the bigger the signal changes must be in order to be labeled as significant.

While developing and testing the algorithm, three different parameters were varied: buffer size, which directly affects the threshold and the maximum possible delay; sample

delay to use in the derivative analysis; and the percentage of the mean value of the signal in the buffer to use as threshold. In order to get a good understanding of the algorithm, these three parameters were varied as follows, keeping in mind the hardware restrictions:

- Buffer size: 5, 10 and 20 samples;
- Sample delay: varied from 1 to 19, in integer values;
- Percentage of the mean value: varied from 0.0001% to 10%.

Buffer size was kept small in order to comply with hardware issues such as available memory. Delay was varied to the maximum value that the buffer size enables, which is buffer size minus 1. Threshold was varied from very low to very high values to assess how the algorithm behaves throughout the threshold span.

All variables are important in the system as each of them affects how the algorithm responds to noise. For instance, higher buffer sizes and sample delays should increase signal smoothing and noise filtering, whereas higher thresholds should result in the algorithm picking up less noise, since noise is frequently associated with smaller, non-significant changes, that are wrongly detected by the system. The optimal combination of these three variables is a crucial aspect to achieve a system that can perform well when given either clean or noisy signals.

The algorithm was firstly implemented in MATLAB, varying the parameters as previously referred. Since signals generated by the developed signal simulator contained random noise, the algorithm was run for a high number of iterations (1500), for each combination of the three parameters, in order to reduce the influence of the random nature of noise in the results obtained for the different parameter sets.

To evaluate the performance of the algorithm, accuracy, precision, sensitivity, specificity and F_1 score were computed using equations 3.4 through 3.8, where TP, TN, FP and FN mean, respectively, True Positives, True Negatives, False Positives, and False Negatives.

$$Accuracy = \frac{TP+TN}{TP+TN+FN+FP} \tag{3.4}$$

$$Precision = \frac{TP}{TP+FP} \tag{3.5}$$

$$Sensitivity = \frac{TP}{TP+FN} \tag{3.6}$$

$$Specificity = \frac{TN}{TN+FP} \tag{3.7}$$

$$F_1 = \frac{Precision \cdot Sensitivity}{Precision + Sensitivity} \tag{3.8}$$

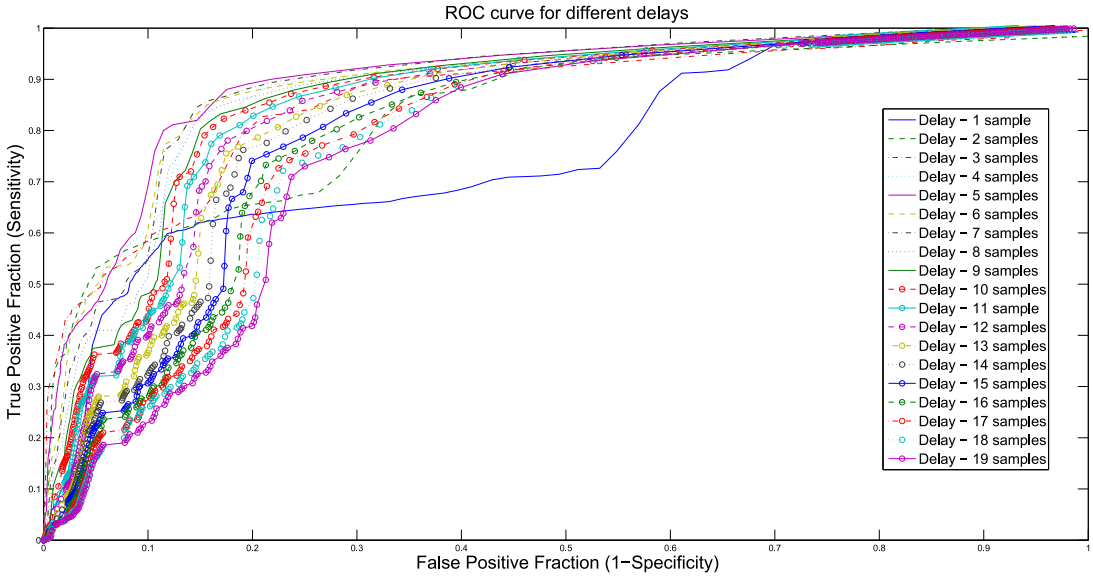

Figure 3.19: ROC curves obtained with the algorithm using a buffer with 20 samples, sample delays from 1 to 19 samples, and thresholds from 0.0001 to 10%. Sample delays over 10 samples have a notoriously prejudicial effect in the ROC curve of the algorithm, and are displayed with circular markers to show that behavior more intuitively.

After calculating sensitivity and specificity, it was possible to plot the Receiver Operating Characteristic, also known as ROC curve, for the algorithm. The size of the buffer directly influences the maximum delay, hence the bigger the buffer that is utilized, the more ROC curves it is possible to plot.

The ROC curves obtained from running the algorithm with a buffer size of 20 samples, and with nineteen different delays, are presented in Figure 3.19.

While it is noticeable that when using very low delays, increasing used delay has a major impact on the ROC curve, it is also noticeable that this improvement starts big but ends up stagnating around the ROC curve obtained for a delay of 5 samples. Not only that, but increasing used delay to further, higher values, can produce a counter-effect that is in fact prejudicial to the algorithm's response. For delays up to 8 samples, the ROC curve seems to keep converging to the optimal corner where TPF=1 and FPF=0. However, increasing the delay from 9 up to 19 samples results in ROC curves that are progressively pulled away from the optimal point, which shows that higher delays do not necessarily mean better performance for the binary classifier.

A peculiar phenomenon is observable in Figure 3.19 for lower delays, where a plateau appears between the phase where TPF ramps up and where FPF ramps up. This plateau is attenuated as used delay increases, and stops appearing in ROC curves obtained with delays above 3 samples. The reason why this plateau is only observable for lower delays is owed to the presence of noise in the signals used to test the algorithm, and to how the algorithm reacts to the presence of noise when analysing the signal with low delays.

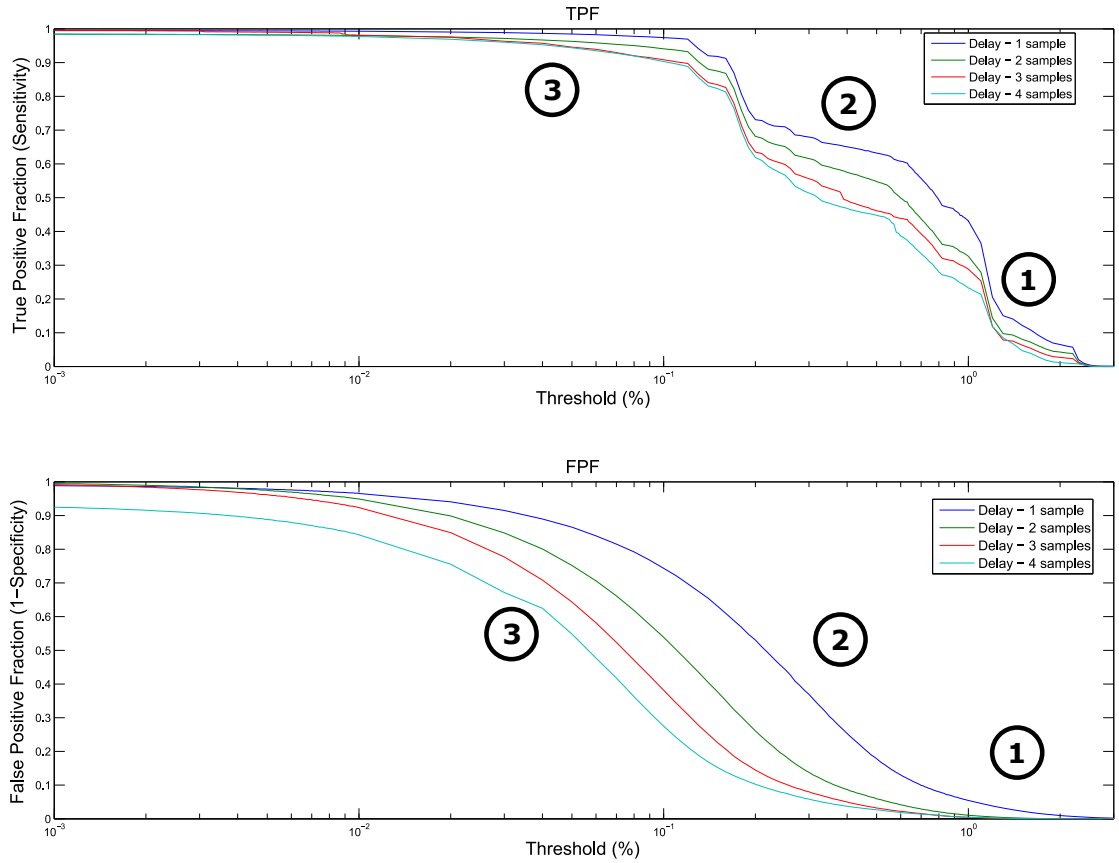

Figure 3.20: True Positive Fraction (TPF) and False Positive Fraction (FPF) obtained using a buffer with a size of 5 samples, delays varied from 1 to 4 samples, and a threshold varied between 0.001 and 3% of the mean value of the signal contained in the buffer. 1 - TPF increasing faster than FPF; 2 - FPF increasing faster than TPF; 3 - TPF increases faster than FPF, followed by the stabilization of both.

When the algorithm computes the difference between samples of the signal that are too close, particularly when a delay of 1 sample is used which makes the algorithm compute the sample to sample difference, the algorithm is more prone to the influence of noise, and ends up picking a lot more point to point differences as significant differences, resulting in a higher number of false positives, and reducing the ratio TP to FP. As delay is increased, the algorithm detects less false positives since the computation of signal difference uses a more weighted "knowledge" of the past of the signal. Therefore, selected sample delay acts as a filter that helps filtering out the influence of noise in the analysis of the signal, which is why the plateau appears for low delays but disappears as delay is increased.

The plateau phenomenon can also be analysed recurring to the TPF and FPF curves obtained for low delays, which are presented in Figure 3.20. When the threshold is too high, both curves stay at a null value, since no TP or FP are detected. As the threshold starts decreasing, TPF increases rapidly, whereas FPF increases at a slower pace (section

numbered with 1 in Figure 3.20), which leads to the initial vertical evolution observed on the ROC curves (Figure 3.19). After a given threshold is reached, TPF starts increasing at a slower pace whereas FPF keeps increasing at a steady pace, therefore catching up with TPF (section numbered with 2 in Figure 3.20). This originates the horizontal shift (the plateau region) observed in Figure 3.19). Lastly, after another specific threshold is reached, TPF has a rapid increase while FPF continues increasing at a slower rhythm, with both stabilizing later on (section numbered with 3 in Figure 3.20). This last phase is responsible for the inflection point where the ROC curves enter the second vertical shift, which marks the end of the plateau. From there, FPF keeps increasing, with the ROC

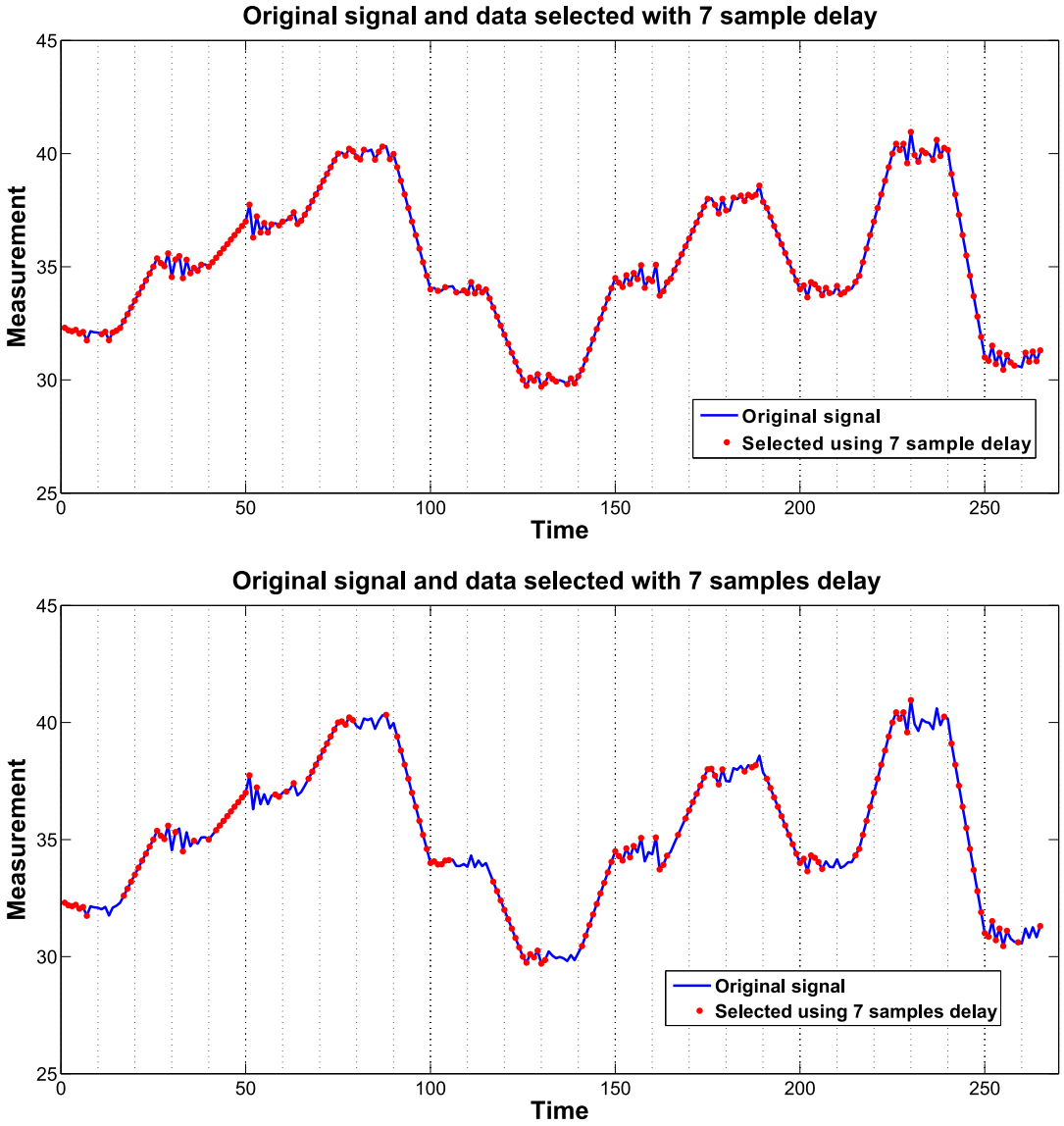

Figure 3.21: Example of signal from the signal generator, analysed with the algorithm using a threshold of 0.2% (threshold inside the plateau zone), and a delay of 1 and 7 samples. Selected data, for each delay, is presented in red.

curves moving to the corner where both TPF and FPF have a unitary value.

The influence of used delay in noise filtering and in the resulting signal classification obtained with the algorithm is demonstrated in Figure 3.21. Here, a signal from the signal generator is analysed with the algorithm using a threshold which lies on the plateau zone observed in Figure 3.19, more specifically a threshold of 0.2% of the mean value of the signal contained in the buffer. As it is possible to observe, for a delay of 1 sample, the signal obtained after running the algorithm shows weak filtering of the noisy sections where the signal stays relatively constant. This means that noisy sections, where the signal does not change significantly, are detected as having significant signal changes, leading to a high number of false positives.

When we move to a higher delay, namely a delay of 7 samples, selected data contains less data from the noisy sections (with some false positives still being detected), so the resulting segmented signal is mostly constituted by the sections where the signal effectively changes at a significant rate. This simple, yet practical example shows that used delay plays a crucial role in the performance of this algorithm, and it also demonstrates that the plateau effect observed in Figure 3.19 has its existence explained by the influence of noise and by how badly the system manages to filter it out when using low delays. It is then possible to conclude that for high enough thresholds, selected delay does not make a huge difference, whereas for lower thresholds, delay can have a major impact, with bigger delays presenting better results, specially in the situations where we deal with noisy signals such as those generated by the signal simulator herein used.

Before moving to the finer tuning of the algorithm, the influence of using bigger buffer sizes than needed for a given delay was assessed. Since delays over 8 samples showed worse

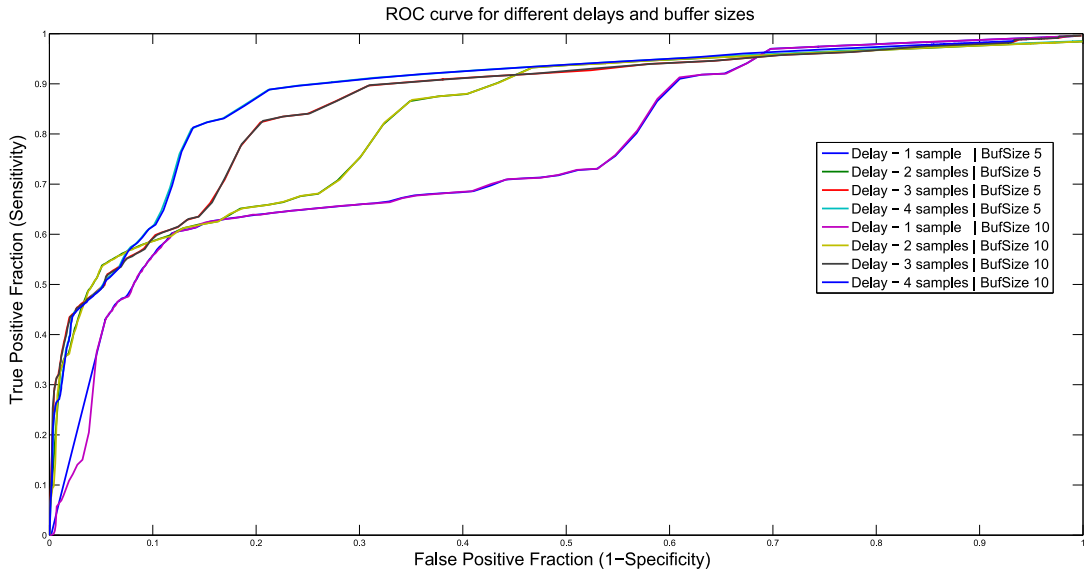

Figure 3.22: ROC curves obtained with the algorithm using a buffer with 5 and 10 samples, sample delays from 1 to 4 samples.

ROC curves, and smaller buffer sizes are preferable considering the hardware limitations of the current system, it was decided to assess this influence just with buffer sizes of 5 and 10 samples. For each buffer size, the algorithm was tested with delays varied from 1 to 4 samples. This selection of delays is explained by the fact that, for a buffer size of 5 samples, the maximum delay possible of using is 4 samples, since one of the slots in the buffer is used to store the most recent sample of the signal. The resulting ROC curves are presented in Figure 3.22.

As can be clearly seen, using a buffer size bigger than what is needed for a given delay does not bring improvements in terms of ROC curve response, since the ROC curves for each delay pretty much overlap themselves. This is specially relevant considering the existing hardware limitations that must be taken into account during the implementation of the controlling system described in this section. Thus, when using a given delay in the algorithm's configuration, a buffer size of delay+1 shall be used in the implementation.

In order to find which combination of threshold and delay optimized the algorithm, the F_1 score for each ROC curve was computed. The combination which led to the best performance was selected and used in the final algorithm implementation.

3.2.2.2 Finite State Machine

After developing the algorithm, it was necessary to have a framework running it and exploring its potentialities, hence the next step was to design and implement a Finite State Machine. It is important to refer that the state machine was the selected approach due to its simplicity and ease of implementation, which makes it a great option for a control system that must be easily reproduced for various distinct sensors. This assumes special relevance considering that the VitalLogger and VitalResponder system have various sensors in their hardware, hence an implementation approach that was easily extensible for various sensors contained in the framework presented in Figure 3.1, and for other sensors to implement in the future, was considered the natural option to follow.

Regarding state machine functioning, this machine must control the timestamp for a given sensor by analysing data gathered from that sensor, which is where the analysing algorithm comes into play. The algorithm is responsible for assessing if the signal coming from the sensor is varying significantly or not, providing this information to the state machine. The state machine then uses this information to decide whether the timestamp shall be reduced, increased or maintained.

Moreover, since each sensor has its own independent timestamp, it is possible to implement various state machines in a parallel approach, where each state machine is responsible for controlling a different signal, enabling the control of various sensors simultaneously. This does, however, bring some implications, namely those related with hardware limitations. Since each machine has an associated computational cost and needs resources from the microcontroller, for example in terms of memory, one must be wary when implementing various state machines in the firmware.

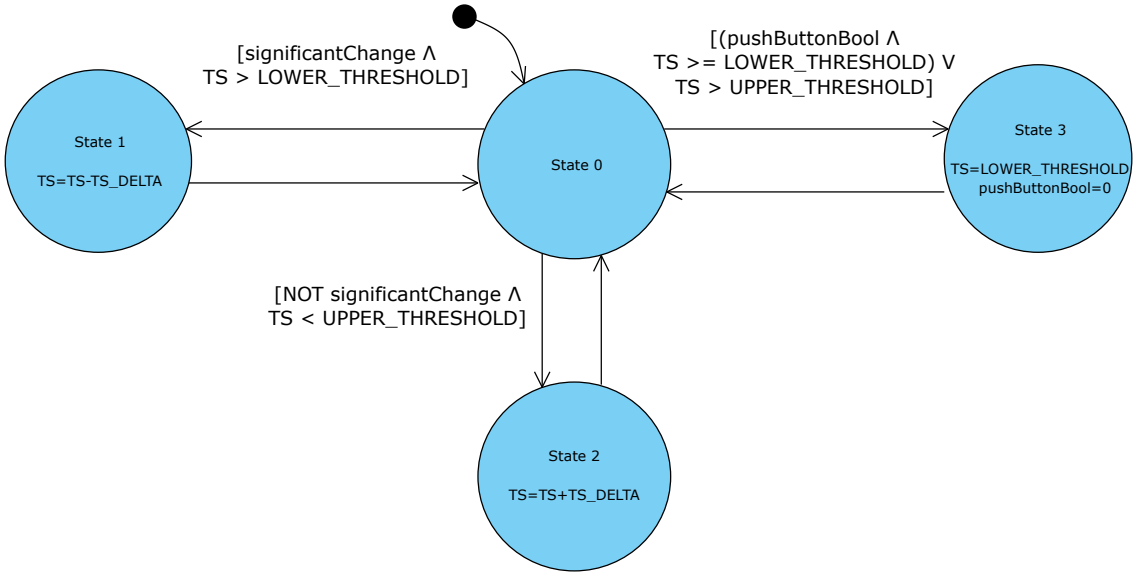

Figure 3.23: Schematic representation of the state machine developed to control the sensors. States 0 to 3 are generic states that every finite state machine must have in order to control a sensor's timestamp. Other extra states might need to be added for some specific sensors.

The finite state machine must be integrated in the firmware, gathering samples from the sensor and using them to detect if sensed data is varying significantly or not. Thus, in what concerns implementation, the state machine was firstly implemented and tested using Code::Blocks 13.12 IDE [76] for that purpose. It is important to refer that while developing the algorithm for sensed data analysis, a C friendly approach was used since the beginning to ensure easy migration into the finite state machine, which must be programmed in C programming language. When a stable version of the control system was achieved, the system was integrated in the firmware using MPLAB X, and tested with the hardware system.

A generic state machine was designed to work with all types of sensors. Since it was defined that the ambient temperature sensor would be the one used to test and validate the control system, no additional states had to be create since this sensor does not have any special needs that must be addressed in the state machine. This machine can be seen in Figure 3.23. This framework is transverse to all sensors, and is composed of four states: State 0, 1, 2 and 3. Since this machine is based on the concept of a Moore machine, only the transitions between different states are represented in Figure 3.23, in spite of the existence of some additional checking clauses in State 0. Nevertheless, all conditions are herein explained in detail.

State 0 is a control state where the system is checking for triggers to transition to one of the other states, hence being the central state in Figure 3.23. From here, it is possible to move to three different states, which actuate on the sensor's timestamp, leading to the manipulation of the data sending rate. It is here, in State 0, that the algorithm for sensed

data analysis is run, having to be fed with incoming samples measured by the sensor. The arrow above State 0, that can be seen in Figure 3.23, means that this is the state where the state machine is initialized.

State 1 is the state responsible for lowering the timestamp controllably, which lets more data be sent. In order to transition to this state, the algorithm on State 0 must detect that the signal measured by the sensor is varying significantly. Moreover, the timestamp has a lower threshold which defines the minimum possible timestamp for the sensor. It must only be possible to get to State 1 if the timestamp is higher than this threshold, so that the timestamp is not lowered beyond what the system can comply with.

State 2 is exactly the opposite of State 1, in the sense that it is the state responsible for increasing the timestamp in controlled increments, which results in fewer data being sent (data is more spaced in time). Here, instead of looking for significant changes in the measured signal, the system is actually looking for situations where the signal is not changing significantly, as is the case when the signal is quasi-constant. Similarly to State 1, there is a threshold restricting the change of the timestamp, except that now it is an upper threshold, that defines the maximum possible timestamp for the sensor. This threshold limits how slow the "data sending rate" can be, so that sensed data sent in the datagram is not overly spaced in time.

State 3 was implemented so that in the presence of a specific event, such as the detection of a dangerous situation, the user can force the system to send sensed data at the "fastest rate" possible. This was implemented by taking advantage of the button that exists in VitalJacket's box. For this purpose, a boolean variable that controls button presses was created outside the state machine. When the button is pressed by the user, the button handler function in the firmware sets the boolean variable to true, signaling that there is an existing button press to be handled. The state machine checks this variable, so that when it is true, the machine transitions to Stage 3 and forces timestamp's value to that of the lower threshold. After having the timestamp changed, the boolean variable that controls button presses is reset to false. Since the machine can only actuate on the timestamp if its current value is higher than the lower threshold, the check condition was defined so that when the button is pressed and the timestamp is already at the lowest possible value, the system resets the boolean variable to false and maintains the timestamp unchanged.

As it was referred previously, aside from the states and transitions presented in Figure 3.23, two other checking conditions had to be introduced in Stage 0 to ensure proper functioning of the system. The first condition was created to ensure that the system does not increment past the upper threshold. This condition checks if measured signal change is not significant and if the timestamp is already at the maximum value. If this situation is detected, this condition stops the system from incrementing the timestamp beyond the upper threshold's value. On the other hand, the second condition is responsible for controlling the other extreme of timestamp values, ensuring that the system does not decrement the timestamp past the lower threshold. Here, the condition checks if the signal is chang-

ing significantly and if the timestamp is already at the lower threshold's value, and, if that situation is verified, this checking condition stops the system from further decrementing the timestamp.

Regarding practical implementation details, it was decided to set timestamp's upper threshold with a value that corresponds to a data sending rate of a sample per 5 seconds, and the lower threshold with a value for a rate of one sample per second, which is the current rate at which the VitalJacket sends all its data. Since data from the VitalLogger must be sent in the same datagrams as data from the VitalJacket, the modified timestamps must be spaced in multiples of 1 second, therefore, $\Delta timestamp$ was defined as 1 second. This means that, with the selected threshold, the system can send data at a rate in the 1-5 second band, with the possibility of having the rate changed inside that band as the state machine is analyzing the sensed signal. Moreover, and considering that when the VitalLogger is started all sensors are far from being stabilized, the initial timestamp was set with the fastest possible rate (1 sample per second).

Still concerning compilation issues, the transition from state 0 to state 3 had to be implemented in the firmware in a way that this was the first condition to be checked every time the system is in state 0. This is because if transitions from state 0 to states 1 or 2 appeared first in the code, the system would almost always go for one of these two states, even in situations where the button had been pressed, which would render state 3 close to useless.

The final issue to address in this control system was related with the timestamps. In order to know when to send data, the system must keep track of how much time has passed since the last sample was sent. When the timer controlling it reaches the value in the timestamp, data is sent in the datagram.

However, since the control system monitors the signal and actuates on the timestamps

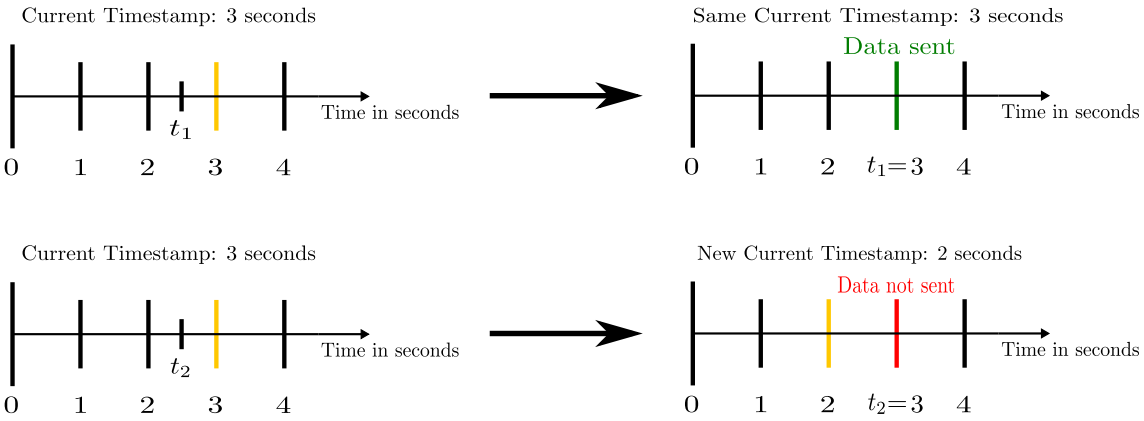

Figure 3.24: Possible scenarios that can appear when using the control system. Timestamps are marked in the timeline in yellow. On the first scenario, when the timer t_1 reaches the timestamp, the timestamp remains the same so data is sent. On the second one, when the timer t_2 reaches the old timestamp, the timestamp has already changed to a smaller value so data is not sent.

at a faster rate than data is sent by the system, before the timer gets to the time point in the timestamp, that timestamp might have changed to different values various times. If the new timestamp has its value maintained or if its value corresponds to a time higher than the time contained in the timer, the system just keeps working until that timestamp is reached, sending data when it hits that time. This is the first case represented in Figure 3.24.

On the other hand, if by the time the timer reaches the old timestamp, the timestamp has changed to a value that corresponds to a time in the past (which the timer has already passed), the system will not send the data because it is not prepared to do so. This second case is also depicted in Figure 3.24. To overcome this issue, the existing system's firmware had to be changed so that when the second case occurs, data is sent by the system on the next datagram to be sent with data from other sensors.

After developing the state machine in Code::Blocks IDE, tests were performed on the command line, in order to debug the state machine before implementing it in the firmware. In order to simulate the press of the button, a specific value of 20 was set to simulate the act of pressing the button in the physical system. Figure 3.25 demonstrates the state machine running with measurements that are given to the machine manually by the user. The graphical interface showed in Figure 3.25 firstly prompts the user to insert the new measurement. After introducing the measurement, the interface shows the classification result (1 for a significant change, 0 for a non-significant one), the newly

```
Introduce data measurement: 97
Significant: 0 | New Sample: 97 | Change: 0 | Buffer: [97 99 98 97 98 98 98 97]

Current State: 0 -> Next State: 2 | Current Timestamp:10
Current State: 2 -> Next State: 0 | Current Timestamp:20

Introduce data measurement: 98
Significant: 1 | New Sample: 98 | Change: -0.142857 | Buffer: [99 98 97 98 98 98 97 98]

Current State: 0 -> Next State: 1 | Current Timestamp:20
Current State: 1 -> Next State: 0 | Current Timestamp:10
```

```
Introduce data measurement: 97
Significant: 0 | New Sample: 97 | Change: 0 | Buffer: [97 99 97 98 97 97 98 97]

Current State: 0 -> Next State: 2 | Current Timestamp:40
Current State: 2 -> Next State: 0 | Current Timestamp:50

Introduce data measurement: 20
Significant: 1 | New Sample: 20 | Change: -11.2857 | Buffer: [99 97 98 97 97 98 97 20]

Current State: 0 -> Next State: 3 | Current Timestamp:50
Current State: 3 -> Next State: 0 | Current Timestamp:10
```

Figure 3.25: Demonstration of the implemented state machine, before implementing in the firmware. The transition to State 3, which is triggered by pressing VJ's button, was simulated by configuring a specific SpO_2 value (20 in this case) to work as the button in the real system.

introduced measurement, the calculated change in the signal, and the buffer with the samples contained in it.

The first box shows a case where the signal starts by changing not significantly, which leads to a transition to state 2 and an increase in the timestamp, followed by a significant change, which leads to a transition to state 1 and a decrease in the timestamp.

The second box presents a case where the signal is also changing not significantly, with the timestamp reaching its maximum possible value. Then, a value of 20 is introduced to simulate the act of pressing the button in VJ's box, which triggers a transition to state 3, and a decrease in the timestamp directly to the lowest possible value.

While Figure 3.25 presents just a relatively small demonstration of how the state machine works, it portraits the workflow where the state machine can transition from state 0 to one of the 3 other states, or just stay in state 0 in case none of the state transitions is triggered.

The final system, responsible for the intelligent data reduction, was implemented specifically for the ambient temperature signal. For that purpose, the designed state machine was implemented with the threshold verification condition (which checks if the signal is within the safe limits). With this system, when ambient temperature steps out the safe range of values, the machine uses the developed algorithm to analyse if the signal is changing significantly or not, and adjusts the amount of data to select accordingly.

3.2.3 Non Perceptible Physiological Indicators

The final step of this thesis consisted in obtaining relevant information for first responders, that is either hard or impossible to measure using sensors, and that can be provided in an intuitive way to give better knowledge on the first responders using the wearable system.

Stress and fatigue are important physiological measures for the first responders that cannot be acquired using sensors, thus being hard to obtain. However, there are indicators, such as the Physiological Strain Index (PSI) that is used to evaluate heat stress, which can be obtained from other vital signs. In fact, PSI has already been implemented in some systems, mostly for military uses, as presented in literature [77].

PSI can be obtained using heart rate and core temperature measurements. The problem with estimating PSI is that there is currently no completely non-invasive way to sense core temperature. The gold standard for measuring core temperature consists in using a rectal probe, which is not practical and comfortable for first responders to use while working, thus not being a viable option to be implemented in a wearable system like VitalResponder.

Moreover, core temperature, on its own, can be used as a good indicator of physiological status to prevent/minimize physiological strain [78], with literature referring that workers should not be permitted to work when their core temperature exceeds 38°C [75]. Therefore, it is important to extract core temperature and PSI from sensed data, as this is relevant

information that can be implemented on alarm systems, which are known to be more useful than the measurements themselves for the Fire Chief.

In what concerns the extraction of core temperature from currently sensed data, there are two main novel non-invasive approaches described in literature, which exploit the fact that when thermoregulation mechanisms begin to fail, variables like heart rate and skin temperature correlate more directly with core temperature. First responders are frequently subject to harsh conditions and heavy physical exertion, and are thus a great target population for these approaches.

The first approach is more sensor dependent, and estimates core temperature using data acquired from various sensors such as skin temperature, heat flux and ambient temperature sensors. Despite showing promising results, it is complex and requires specific equipment to be developed for this purpose [61, 54, 79].

The second approach is based on a Kalman filter that estimates core temperature from heart rate measurements, and was developed with the aim of creating a simpler and practical system that only requires a single input, and that can easily be deployed in ambulatory field settings. This method showed good results and also holds great promise for the near future [55, 56]. In fact, it has already been implemented by Zephyr^{TM} in a commercialized solution for First Responders, the BioHarness^{TM} [24, 22], and there exists literature supporting that core temperature estimates from BioHarness^{TM} can be used as a reliable surrogate measurement of core temperature in the field setting [78].

Since PSI can be easily obtained using heart rate and core temperature measurements, the challenging part of this step of the work is to develop a robust core temperature predictor. In this step of the thesis, it was decided to implement a Kalman filter predictor, using MATLAB software, to obtain core temperature estimations from heart rate measurements. The Kalman filter was the selected approach because of its relative simplicity and inherent properties that make it a great tool for prediction systems.

Core temperature estimations obtained from the implemented predictor were used to compute the Physiological Strain Index. In order to develop the predicting system, it was firstly necessary to have access to a database with the needed information, and to process that data before using it. All these aspects will now be discussed in detail.

3.2.3.1 Assembling a Dataset

The first issue of this part of the work to be addressed, was to have access to a database with information from various vital signs, namely from heart rate and rectal temperature. The reason why rectal temperature, obtained with a rectal probe, is a must have when developing a system with the purpose of predicting core temperature, is because it is considered the gold standard for assessing core temperature. Therefore, in order to be able to evaluate the performance of the implemented system, it is crucial to have this ground truth for comparison.

Access to data for this step of the work was granted by Aitor Coca, from NIOSH/CDC, Pittsburgh, Pennsylvania. This data was acquired in a study which had the intent of assessing the viability of a core temperature estimating system, in this specific case the BioHarness^{TM} that estimates core temperature from heart rate, under several heat stress conditions [78].

This data was obtained in thermoneutral and in heat stress conditions (high temperature and relative humidity), simulating the hazardous environmental conditions that first responders often face when working. 12 healthy men were used in these experiment sets, and four different conditions were simulated: control, active, passive and with personal protective equipment. In these experimental sets, heat stress and exercise conditions to which individuals were subjected were varied, and the termination criteria was a rise in rectal temperature of 1.5°C. Access was only given to data from control, passive and active conditions.

In order to acquire the physiological signals, subjects were instrumented with the following sensors: a rectal probe to measure rectal temperature, skin temperature sensors and heat flux sensors. These last two types of sensors were placed in five different body sites (forehead, chest, shoulder, thigh and calf). Finally, a BioHarness^{TM} was used to measure heart rate and to provide core temperature estimates. For the sake of simplicity, the system with the rectal probe, skin temperature and heat flux sensors will be referred to as system A, and the BioHarness system will be referred to as system B. Both systems were used simultaneously during the tests. System A was operated at a sampling rate of 0.5Hz, whereas system B was operated at a sampling rate of 0.4Hz.

After having access to the files with data from these experiments, the first step was to extract data to MATLAB, and process it so that it could be used for the implementation of the Kalman filter predicting system. In order to be able to compare measurements from both sensing systems, it was necessary to adjust the sampling rate of the data from one of the systems, so that it matched the sampling rate of the other system. In this thesis, it was opted to downsample the longer signals, which were those obtained with the rectal probe, skin temperature and heat flux sensors. This was performed using the resample function from MATLAB.

Figure 3.26 presents a resampled rectal temperature signal, which is from the system with higher sampling rate, and an original estimated core temperature signal, which is from the system with lower sampling rate. It can be noticed that both signals match relatively well in terms of time, which enables direct comparison of signals from both systems, namely between estimated core temperature and rectal and/or skin temperature.

Despite the good signal matching that can be seen in Figure 3.26, using MATLAB's resample function to downsample the longer signal generated another issue, related with artifact creation. This phenomenon is shown in Figure 3.27. In order to solve this issue, all signals had a fixed number of samples trimmed off both at the beginning and end sections of the signal. The number of samples to be trimmed off was set at 10 samples at both

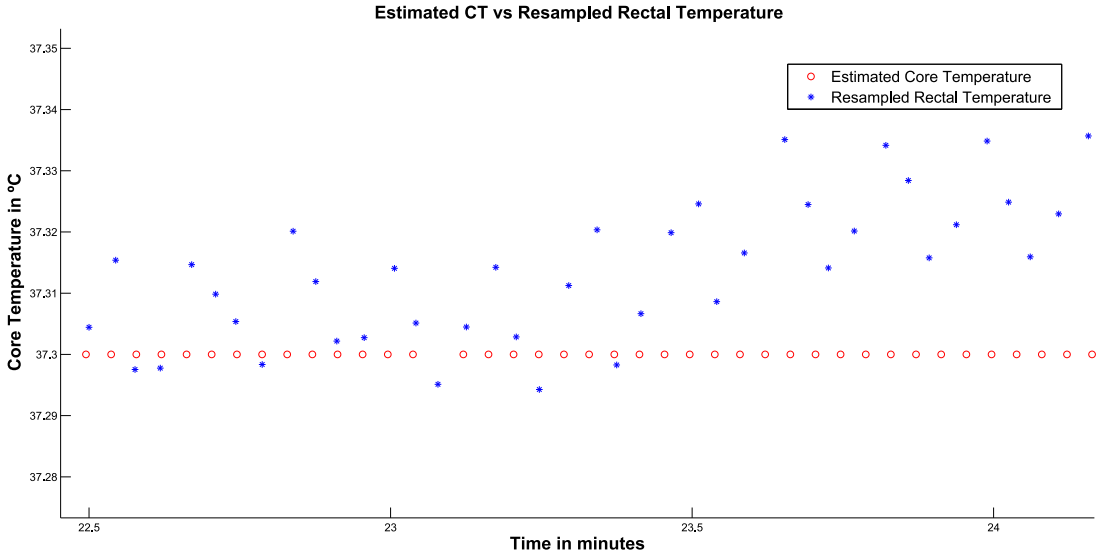

Figure 3.26: Resampled rectal temperature signal and original estimated core temperature signal, displayed in function of time. It is possible to observe that the resampled signal matches the original signal relatively closely, in terms of its disposition in the time scale.

ends of the signal.

After processing the signals for all subjects, in every experimental condition, obtained data was organized in a dataset, being grouped by experimental condition. Since for some subjects, in certain experimental conditions, there were hardware failures that rendered the acquired data useless, the resulting dataset is composed of data from 11 subjects for active and control conditions, and 10 subjects for the passive condition. Each acquisition

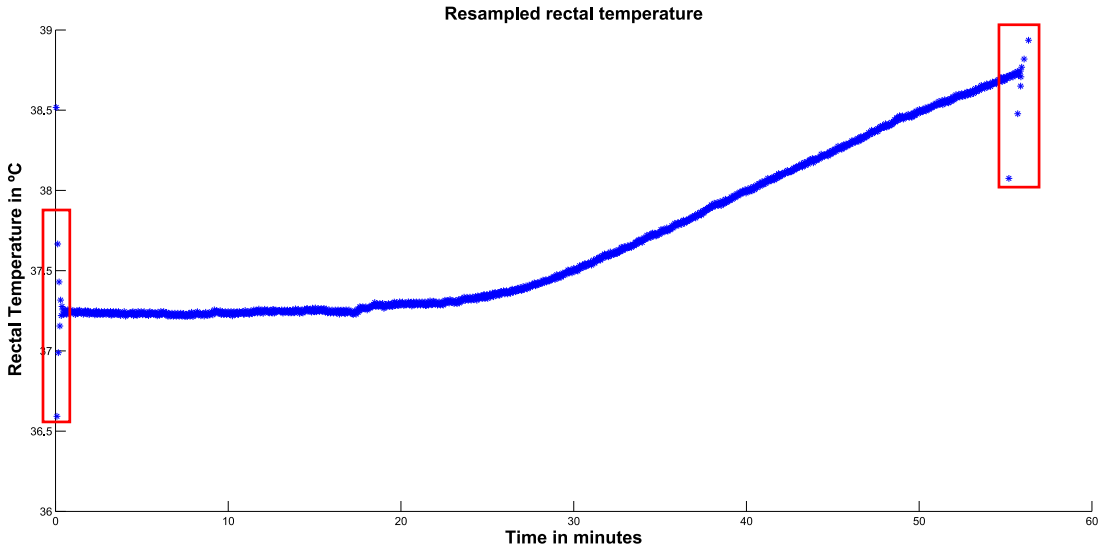

Figure 3.27: Artifact creation at the beginning and end sections of the resampled signals, resulting from the usage of the resample function from MATLAB.

is composed of the following data: time from system A, skin temperature on the forehead, chest, shoulder, thigh and calf, heat flux on the forehead, chest, shoulder, thigh and calf, time from system B, estimated core temperature and heart rate. Since the termination criteria was stipulated as an increase of 1.5°C in rectal temperature, the duration for each acquisition differs.

3.2.3.2 Core Temperature and PSI Estimating System

As it has been referred previously, there are two main approaches described in literature for core temperature estimating systems, with the first one being more sensor dependent, in the sense that the garment must acquire data from more sensors [54, 61, 79], and the second one, based on a Kalman filter predictor, being more simple as it only needs data from heart rate measurements [55, 56].

Since the Kalman filter approach has already been implemented in commercialized solutions (namely in BioHarness™ from Zephyr™ [22, 24]), and core temperature estimations resultant from these solutions can be used as a reliable surrogate measurement of core temperature in the field setting [78], it was decided to implement a core temperature predictor based on the Kalman filter approach.

After having the dataset assembled, and before implementing the Kalman Filter predictor, data had to be visually analysed to inspect the relationships between the various acquired physiological signals.

It is known from physiology that when heart rate increases, core temperature should increase too [57]. However, the conditions that subjects are exposed to, influence this relationship between heart rate and core temperature. Therefore these were the first variables to be analysed. Rectal temperature was analyzed in function of heart rate for the three experimental conditions: active, passive and control. Figure 3.28 presents those variables, for all subjects in the active setting, Figure 3.29 for the control setting, and Figure 3.30 for the passive setting.

It is possible to observe that as heart rate increases, core temperature increases too, as expected. However, the evolution of core temperature with heart rate varies along the three experimental settings. In the active setting, core temperature seems to present a linear correlation above a certain values of heart rate (around 140 bpm). In the control setting, core temperature also rises with heart rate, but the correlation between both variables at higher heart rates is more weakly defined when compared to what is observable for the active setting. Finally, in the passive setting, core temperature also increases with heart rate, but its measurements seems to be more dispersed, and only present a linear correlation for high heart rates in some specific subjects.

These three figures also display the existing intravariability in each experimental setting, which in turn occurs due to the existence of intervariablity between subjects. This explains why, for equal experimental conditions, there is such disparity in terms of mea-

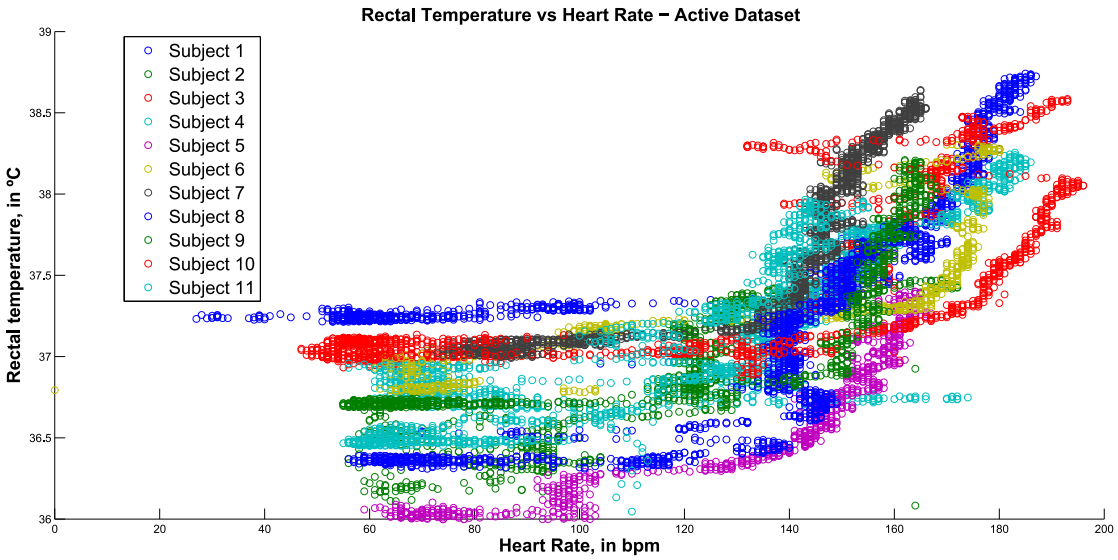

Figure 3.28: Rectal temperature in function of heart rate, for the Active condition dataset.

sured heart rate and core temperature, which is specially notorious in the "plateau" zone that exists for low heart rates in the three experimental settings.

Since firefighters frequently operate on hazardous environmental settings, and are subject to strenuous physical exertion, their heart rate is most frequently situated in the range of higher heart rate values. As expected, this matches what is observable in Figure 3.28, which corresponds to the active setting.

Furthermore, it is only in this range of higher heart rate values, situated approximately

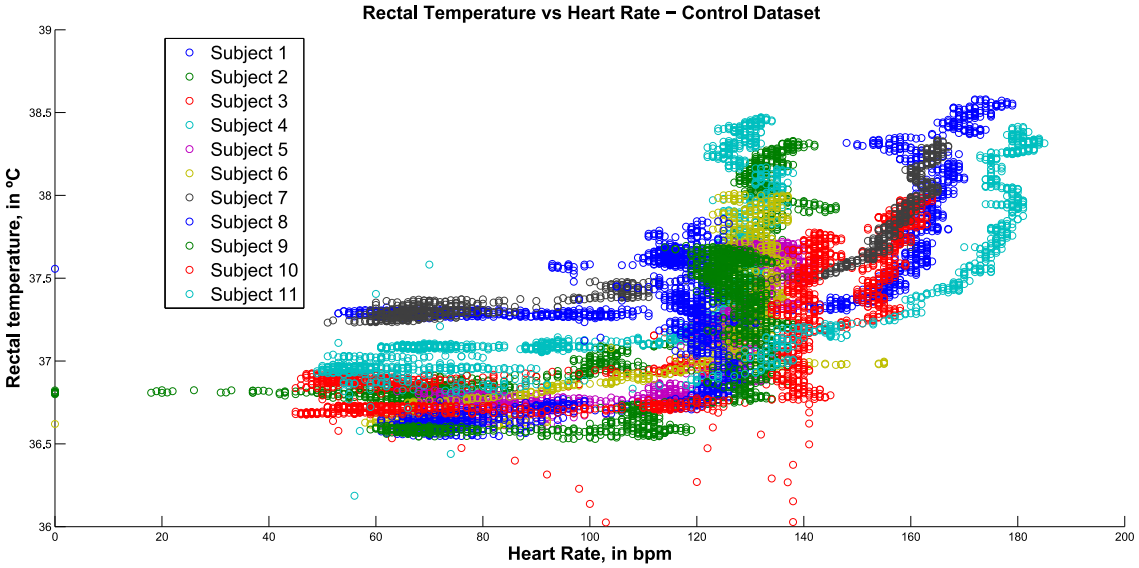

Figure 3.29: Rectal temperature in function of heart rate, for the Control condition dataset.

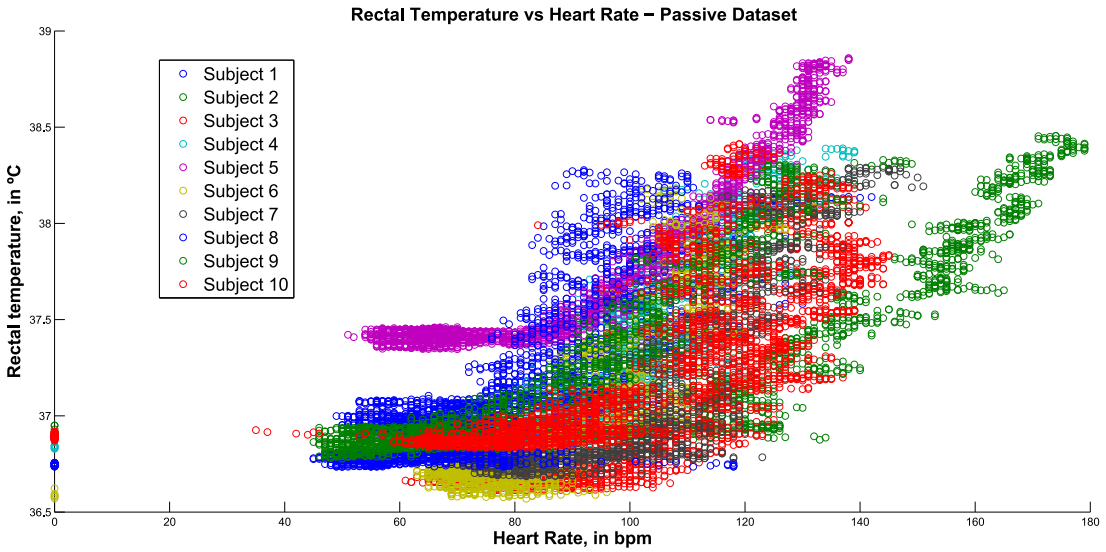

Figure 3.30: Rectal temperature in function of heart rate, for the Passive condition dataset.

above 120/130 bpm, that core temperature starts presenting a linear correlation with heart rate, which means that heart rate can be used as proxy for core temperature in this region. As firefighters mostly operate in this range of values, and the core temperature estimating system to be developed in this thesis is projected for firefighters, it was decided to use only the active dataset in the development of the estimating system based on a Kalman filter.

Skin temperature is also physiologically related to core temperature, thus this relationship was also analysed. According to human physiology, an increase in skin temperature can lead to an increase in core temperature if skin temperature increases above a certain level. In case skin temperature oscillates below that level, thermoregulatory mechanisms compensate the change in skin temperature, so that core temperature stays regulated.

In spite of being referred in literature that core and skin temperature correlate with an offset around 0.25°C to 0.75°C when skin temperature is above 36°C [54], experimental data presented in Figure 3.31 shows that this correlation can start appearing for skin temperatures above 35°C. Nonetheless, it is noticeable that this correlation is more notorious after the stabilization phase, some time after the subject starts exercising. After 30 minutes of acquisition, skin temperatures stabilize at around 35°C and start increasing at a steady rate, along with core temperature, with values between skin and core temperature having an offset around 1°C, thus going in agreement with what is mentioned in the literature.

This means that, as supported by [54], when temperatures are near the range that is considered dangerous, which happens with various first responders, skin temperature can also be used to predict core temperature. However, as it is referred in [61], sensor placement can significantly influence measurements, being the sternum one of the most

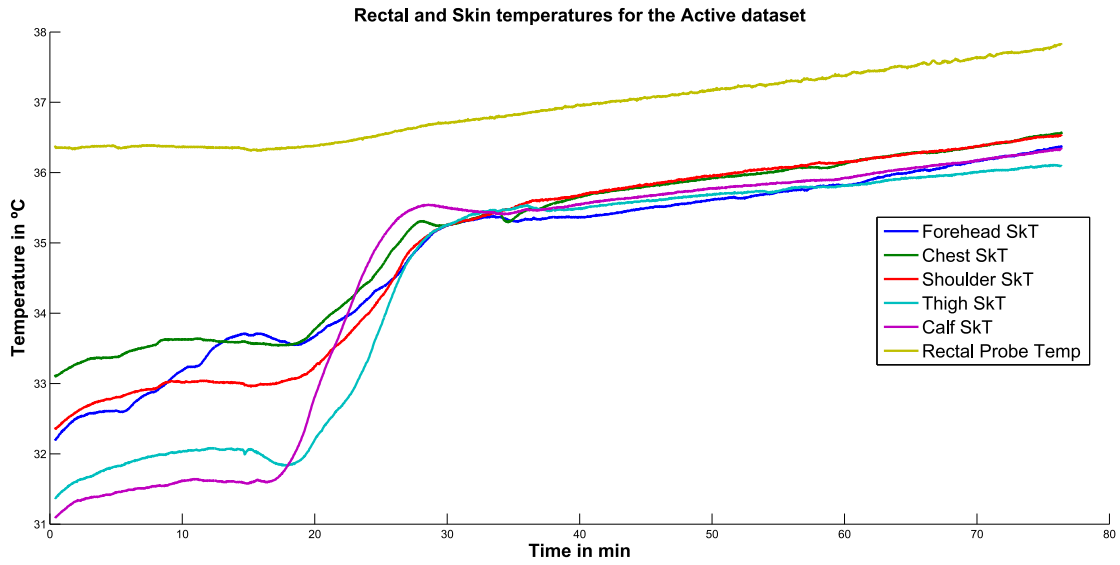

Figure 3.31: Rectal temperature and skin temperature measurements for the five different body sites, from one subject. While skin temperatures show a linear evolution with core temperature, their values remain below core temperature during the whole experiment, for all subjects.

promising locations for systems using these sensors.

The acquisition system used in [78] also had heat flux sensors, which are presented by literature as a promising solution for core temperature estimation, due to the fact that these sensors are less influenced by environment and attachment method when compared to skin temperature sensors [79].

Nevertheless, heat flux sensors also present several issues. Firstly they are more noisy and bulky. Secondly, they demand the integration of a datalogger in the system, which must receive thermocouple or thermistor type sensors. Finally, these sensors are very expensive, with prices of 250 Dollars per sensor in [80], and of at least 225 Euros per sensor in [81]. As the objective is to integrate the core temperature estimating system in VitalResponder, and these factors greatly limit the integration of heat flux sensors, in the near future, in the wearable system, it was decided to leave heat flux out from this analysis.

Finally, core temperature estimates obtained with BioHarness were analysed, to inspect how it works. In Figure 3.32, estimated core temperature and heart rate are plotted in function of time, with presented data belonging to a subject in the active dataset. When heart rate is at low/medium levels (approximately up to 100 bpm) core temperature should change just slightly, which is in fact visible in the stabilization phase (until around 15 minutes of acquisition). When the subject starts exercising, heart rate increases, which is visible in the rapid increase that occurs at the 17th/18th minute of the acquisition.

As the subject continues exercising, heart rate keeps increasing, staying in the range above 130 bpm. As previously referred, this is the range where the correlation between core

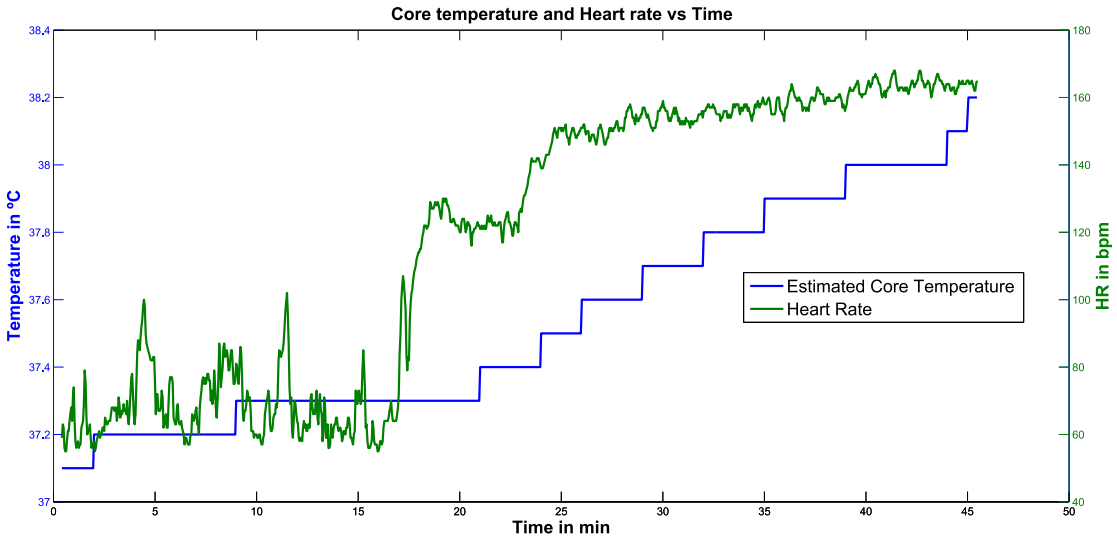

Figure 3.32: Core Temperature estimation and Heart Rate in function of time. This data was obtained with a BioHarness^{TM}, and shows the tendency that core temperature increases with heart rate.

temperature and heart rate is more significant, thus an increase in heart rate inside this range should result in an increase in core temperature. This can be observed in Figure 3.32 from the 20th minute until the end of the acquisition, therefore results from the existing solution from Zephyr^{TM} match what was expected. It is also important to notice that the BioHarness only seems to update the output value, of estimated core temperature, if the temperature change since the last output value reaches a threshold value of 0.1°C, which generates the observable step-like signal.

After analysing the data in the dataset, the next step consisted in implementing the Kalman filter estimator. In this thesis, it was decided to implement a system similar to that described in [55, 56], with the integration of data from skin temperature sensors being projected to occur once a robust version of the basic system was achieved.

Both systems described in [55, 56] are based on a Kalman filter estimator, with the system in [56] being an evolution of the one presented in [55]. The most recent system implements a variation of the Kalman filter, which is the Extended Kalman filter. This type of Kalman filter is applied when the process to be estimated and/or the measurement relationship of the process is non-linear, as it linearizes about the current mean and covariance. The major flaw of this approach is that using nonlinear transformations leads to distributions of the random variables that are no longer normal [82].

The Kalman filter was implemented based on the implementation presented in [56], which has its parameters drawn from a larger dataset, that comprehends various laboratory and field studies on the military. Regarding implementation details, the F_k matrix, that is used during the prediction step (Equations 3.1) to predict the new value of the state variable from the previous one, was defined as an identity matrix based on the assumption

that there exists thermal inertia, as referred in [56].

As the mapping matrix H_k - which maps the predicted state variable into the same dimension of the measured variable (Equations 3.2) - referred in [56] was working very poorly on the dataset used in this thesis, this matrix was computed for the existing dataset using k-fold cross-validation (with k=11), thus being estimated with data from 10 subjects and tested on one subject every time. To estimate H_k, the polyfit function from MATLAB was used to fit a polynomial function to the dataset.

Finally, as the Kalman filter uses state and measured variables, core temperature was implemented as the state variable, and heart rate as the measured variable. Moreover, since the used dataset only contained data from 11 subjects, k-fold cross-validation (with k=11) was used, with 11 different implementations being obtained.

In order to compare the performance of the implemented estimator with that of BioHarness, root mean square error (RMSE) was used to evaluate the performance of the implemented models, and the mean RMSE of all implementations was computed. RMSE is a good measure of accuracy that aggregates the magnitudes of the errors in predictions along various times, but which can only be used to compare models that compute their predictions based on the same variable. RMSE can easily be computed with the following equation:

$$RMSE = \sqrt{\frac{\sum_{t=1}^{n}(\hat{y}_t - y)^2}{n}} \tag{3.9}$$

where $\hat{y}_t$ is the predicted value of the variable of interest, y is the measured variable (in this case the rectal temperature) and n the total number of samples.

Stress and fatigue are important physiological indicators for the first responders, but they cannot be measured with sensors. However, indicators like PSI can be obtained using other acquired signals, thus, PSI was obtained using core temperature estimations and the acquired heart rate measurements.

PSI was computed with the rectal temperature, to serve as the ground truth for comparison, and with core temperatures estimates obtained from BioHarness and from the implemented core temperature predictor. To compare the performance of the PSI estimators, RMSE was the selected metric.

3.3 Results and Discussion

3.3.1 Novel Sensing Capabilities

With the extended firmware and SDK implemented, the system is capable of receiving data from the three newly implemented sensors. In Figure 3.33, a test application running with the extended version of the SDK is shown. Here, it is possible to observe that the

new sensors are working correctly, with its data being shown in the applications' interface (numbered with 1 in the figure).

However, and even more importantly, the system is capable of detecting the sensors that it has available to gather data from, presenting them in a list in the interface, which is marked in red. Since this list only displays the sensors that are available, if a VitalJacket is connected to the smartphone running the application, only the sensors showed in 2 are presented in the interface.

If a VitalLogger, which has the two sensors from from the VitalJacket as well as the three newly implemented sensors, is connected to the smartphone, the list in 1 will contain all the sensors presented in 2, 3 and 4.

Regarding future necessities in terms of adding new sensors in the wearable system, which was addressed by preparing the system for a migration into a modular architecture, a SPI protocol was defined for the communication between slaves (modules) and master. The new firmware was designed so that it is easier to expand the system by adding new modules.

With this approach, when a new module is created, there is only the need to add a new configuration to the firmware. Since each type of module is unique, having its unique identifier, by adding the configuration for a new module to the firmware, the master is able to parse correctly the data received from that new module.

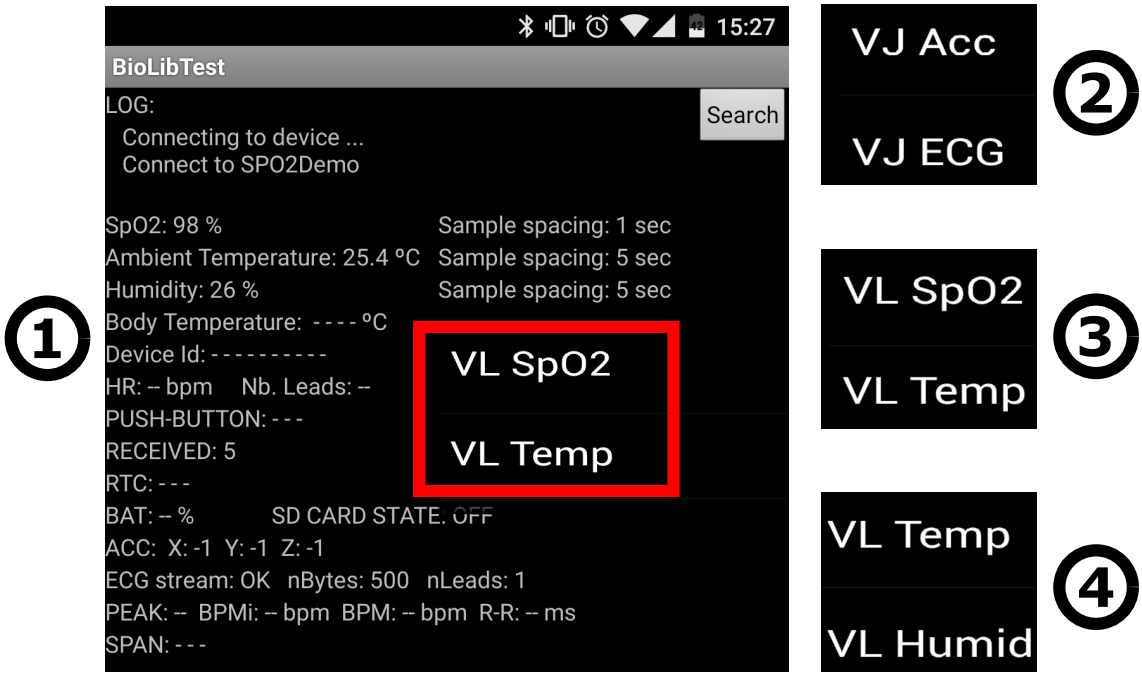

Figure 3.33: Test application running with the extended SDK, which is adapted to the new sensors (SpO_2, ambient temperature and relative humidity. The system is capable of detecting the existing sensors, displaying them in a list (marked in red). If the smartphone is connected to a VitalJacket, the sensors in 2 are shown, whereas if it is connected to a VitalLogger, the sensors in 2, 3 and 4 are shown to the list.

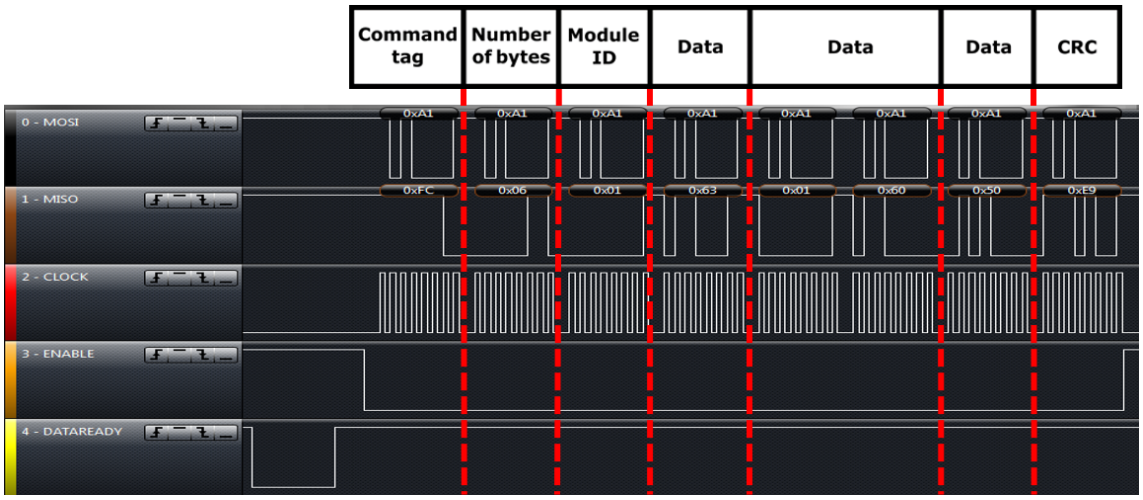

Figure 3.34: SPI communication between a fictitious VitalLogger module (slave) and a master. The sections of the datagram are aligned with the respective bytes in the MISO channel. The second "data" segment corresponds to the ambient temperature data, which is contained in two bytes of information.

During this work, the SPI protocol was implemented with a configuration for a VitalLogger module, which might be created in the near future, that contains data from the SpO_2, ambient temperature and relative humidity sensors.

The datagram for the SPI communication between this module and the master comprises three data segments, which correspond to the data from the three sensors that the fictitious VitalLogger module possesses. Both the datagram and the SPI communication itself, captured using Logic, are presented in Figure 3.34, with the datagram being aligned with the respective bytes seen in MISO channel. The identifier for this module was set with the number 1, as can be seen in Figure 3.34.

Also, while this module possesses three sensors, information for ambient temperature has to be represented using two bytes of information. This is because ambient temperature must be sent as an integer value. When the master receives the ambient temperature from the slave, its parser divides the value by 10, hence obtaining the temperature with an integer and a float part. Therefore, the first byte after module ID contains SpO_2 data, the second and third ones contain ambient temperature data, and the fourth byte contains the measurement for relative humidity.

3.3.2 Intelligent Data Reduction

In order to select the best configuration (buffer size, delay and threshold) to implement in the generic data reduction algorithm, the F_1 score was computed for each delay.

Table 3.1 summarizes the highest F_1 score obtained for each delay (from 1 to 9 samples, since delays higher that 9 showed worse performance in the ROC curve analysis), and it also has the threshold used to obtain the given F_1 score. Moreover, Table 3.1 also contains

Table 3.1: Summary of the best F_1 score for each delay, with its respective threshold, and of the algorithms' mean Accuracy obtained at the same delay and threshold.

Delay (num. of samples)	**Threshold (%)**	**F_1 Score**	**Mean Accuracy (%)**
1	0.67	0.694	69.9
2	0.16	0.712	76.6
3	0.16	0.742	82.1
4	0.16	0.768	84.3
5	0.15	0.836	84.7
6	0.14	0.823	84.3
7	***0.12***	***0.845***	***87.4***
8	0.11	0.834	87.1
9	0.11	0.823	86.2

the algorithm's mean Accuracy obtained when using the same delay and threshold as those used to obtain the F_1 scores presented in the table.

The F_1 score, which is a measure that basically consists in a weighted average of sensitivity and precision, had its highest value in 0.845, observed for a delay of 7 samples with a threshold of 0.12%. This specific pair of delay and threshold also presented the highest mean Accuracy, with a value of 87.4%. The second and third highest F_1 scores had a value close to 0.835, which is roughly 1% lower than the highest F_1 score. Regarding accuracy, it can be seen that higher delays are associated with higher accuracies, hence the next best combination to consider is a delay of 8 samples with a threshold of 0.11%. After analysing the obtained results, it was decided to implement the analysing algorithm with the following specifications:

- Buffer Size: 8 samples | Delay: 7 samples | Threshold: 0.12%

Since the algorithm was developed with the intent of working with various different signals, the algorithm was validated on two different signals: ambient temperature and SpO_2. After acquiring the data using the VitalX Android application, data had to be manually labeled in order to enable the computation of metrics used to evaluate algorithm performance.

During this labeling procedure, the following considerations were taken into account: regarding the ambient temperature signal, only the transition zones, where the signal increases or decreases sharply, should be marked as significantly changing; concerning the SpO_2 signal, it is usually stabilized in a saturation value around 98-99% and variations are detected in multiples of 1%, so, every existing variation should be labeled as significantly changing.

An example of acquired ambient temperature and SpO_2 signals, as well as the resulting signal after applying the algorithm on the original signals, is presented in Figure 3.35. The original signals are shown in blue, whereas selected data is presented in red.

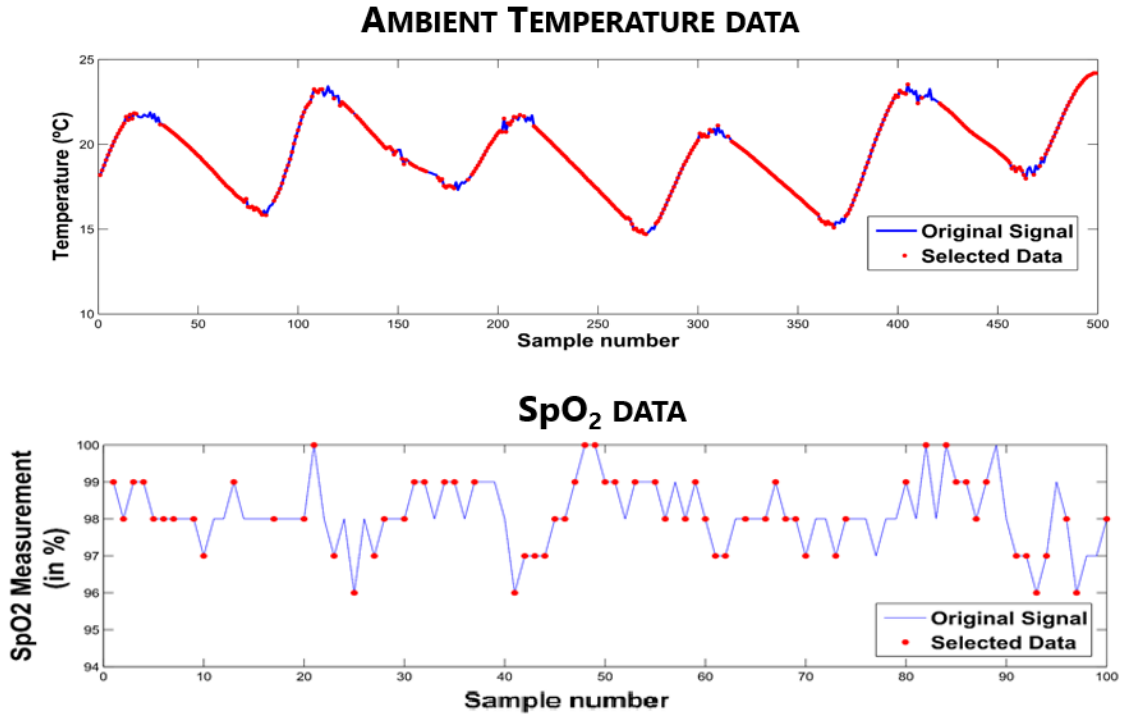

Figure 3.35: Ambient temperature and SpO_2 signals analysed with the developed algorithm. The original signal is presented in blue, and data that is considered relevant by the algorithm is presented in red.

It is possible to observe that for the ambient temperature signal, the algorithm selects the data in the transition zones (where it varies significantly), and drops out samples in the sections where the signal stabilizes, as expected. However, for the SpO_2 signal, the algorithm seems to be less consistent, leaving data in the transitions zones unselected, and selecting data in stabilized sections where the signal is not varying.

After running the algorithm on various acquired ambient temperature and SpO_2 signals, algorithm performance was evaluated based on the computation of the following metrics: Accuracy and F_1 Score. Mean accuracy and mean F_1 score resulting from the analysis of all signals is presented in Table 3.2.

Concerning ambient temperature, mean accuracy is lower than that obtained with the algorithm for the signals generated by the signal simulator but F_1 is higher (85.5% vs 87.4% and 0.905 vs 0.845, for accuracy and F_1 score, respectively). Regarding the SpO_2 signal, both values are clearly lower when compared to those obtained with the signals

Table 3.2: Mean Accuracy and F_1 Score for ambient temperature and SpO_2 signals obtained with the VitalLogger.

	Mean Accuracy	**Mean F_1 Score**
Ambient Temperature	85.5%	0.905
SpO_2	59.7%	0.678

generated by the signal simulator (59.7% vs 87.4% and 0.678 vs 0.845, for accuracy and F_1 score, respectively). These results show that the algorithm works well with ambient temperature signals, but performs less well when used in SpO_2 signals.

However, it must not be forgotten that the algorithm was designed to be generic (i.e. work with dat from various types of sensors), and implemented having its specifications configured according to algorithm response for 14 different types of signals, in order to have an algorithm capable of generalizing instead of overfitting to data. The possibility of having worse response for certain signals is a reality and an inherent trade-off resulting from the chosen implementation for the data selection system, since the algorithm was projected and developed with the aim of being capable of analysing various different signals, in order to enable fast and easy out of the box implementation of the controlling system for different sensors in the VitalLogger and VitalResponder.

To sum up, while in this thesis the algorithm was only validated on ambient temperature and SpO_2 signals, it was possible to observe that the system works better with some specific signals. In cases where it is absolutely crucial that the algorithm performs very well for a specific type of signal, the set of parameters (buffer size, sample delay and threshold) that optimizes algorithm response for that signal should be computed, and implemented in the algorithm's configurations.

With the algorithm implemented with the selected configuration, it was integrated in the designed finite state machine. While the control system was developed with the aim of having a generic control system, which means that it can work with signals from various different sensors, in this thesis it was specifically implemented for the ambient temperature sensor that was introduced with the VitalLogger.

The developed algorithm and state machine were integrated with the system responsible for selecting data when the signal is within the thresholds displayed in Figure 3.16. The final system was implemented so that the buffer used in the state machine starts being filled when the system starts working. This means that the state machine can only start working when that buffer is filled.

If a measured sample is within the safe temperature thresholds, samples from the signal are sent in fixed intervals of for example a sample each 30 seconds. When the signal leaves the "safe region", the first sample to be sensed is sent to the Fire Chief. When temperatures are outside the threshold limited area, the state machine autonomously selects which data should be sent or not.

This system was implemented in the firmware, for the ambient temperature sensor, and Figure 3.36 shows an original temperature signal, the upper temperature threshold that was defined as 35 degrees Celsius, and the resulting signal after it went through the control system. It is possible to observe that below the threshold, few samples are selected by the sensor. In this demonstration, it was defined that samples selected below the threshold should be spaced at a fixed distance of 6 samples.

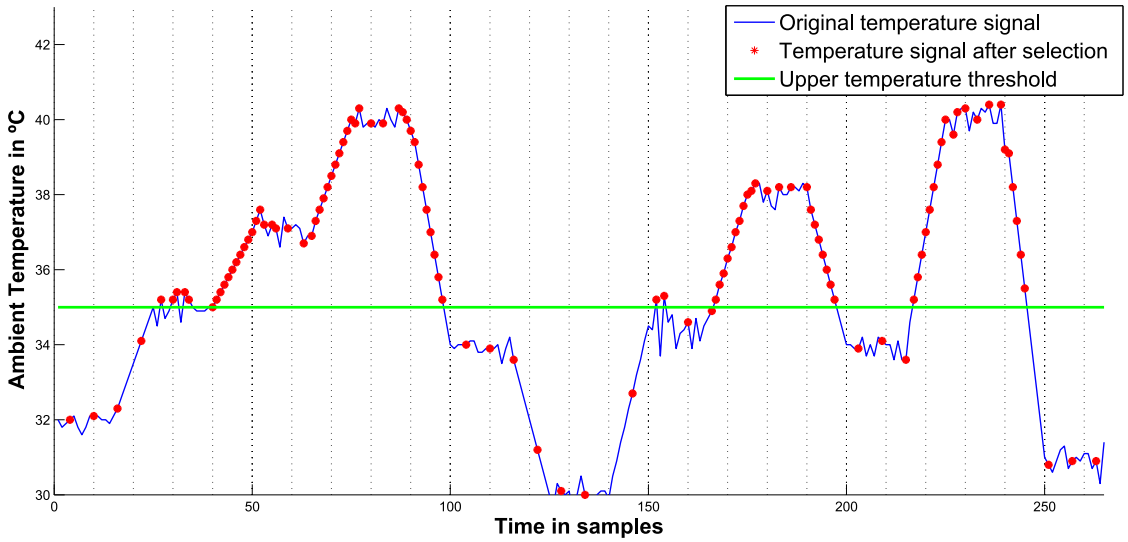

Figure 3.36: Demonstration of the control system that selects data, running on ambient temperature signal. Below the threshold few samples are selected. Above the threshold the number of selected samples increases, with the number of selected samples depending on whether the signal is changing significantly or not.

When the signal rises above the threshold, it is possible to see that the first sample that appears is selected. Then, depending on whether the signal has a sharp change or if it stabilizes around a specific value, the system selects more or less data according to the sensed signal change. It can be clearly seen that in steep changes, more data is selected than in sections where the signal remains close to constant. Nevertheless, it can be noticed that when the signal presents small changes but the signal value is above the threshold, more data is selected compared to when small changes exist but the signal is below the presented temperature threshold, which matches what is expected from the system. While the system was only tested with the ambient temperature sensor, it should work exactly the same way with other sensors that may exist in the wearable platform.

By actuating on the amount of data that is sent to device being used by the Fire Chief, which is sent using Bluetooth protocol, some energy savings might occur. However, these are negligible considering the remaining amount of data that is sent from other sensors, such as data from the ECG sensors, to the connected device (e.g. smartphone).

More than having potential energy savings from using this system, the objective of this thesis is to improve the current wearable system so that it fulfills more of the firefighters' needs. Since firefighters frequently operate on hazardous conditions, where ambient temperature can reach high levels, it is important to notify them of dangerous situations when these appear.

From what was obtained by inquiring firefighters, Fire Chiefs, who are responsible for managing not only firefighters on the field but also the supporting units (e.g. vehicles), are frequently busy with dealing with all the resources they have to manage, so they cannot

pay close attention to the monitoring device and see if the value for a given signal changed or not.

In order to meet their needs, aside from providing them the temperature values, the end result must be something intuitive, such as firing an alarm in the application running in their mobile device if the ambient temperature rises above the upper threshold. Therefore, the mobile application was adapted to receive the selected data, show temperature status according to the measured temperature, and fire an alarm system when temperature leaves the "safe zone".

In normal conditions, where temperature is below the threshold, temperature status is displayed as OK and no measurement is shown. If temperature rises above the upper threshold (of 35 degrees Celsius), an alarm situation is triggered so temperature status changes to a warning "stance". When showing the alarm, the application also shows the

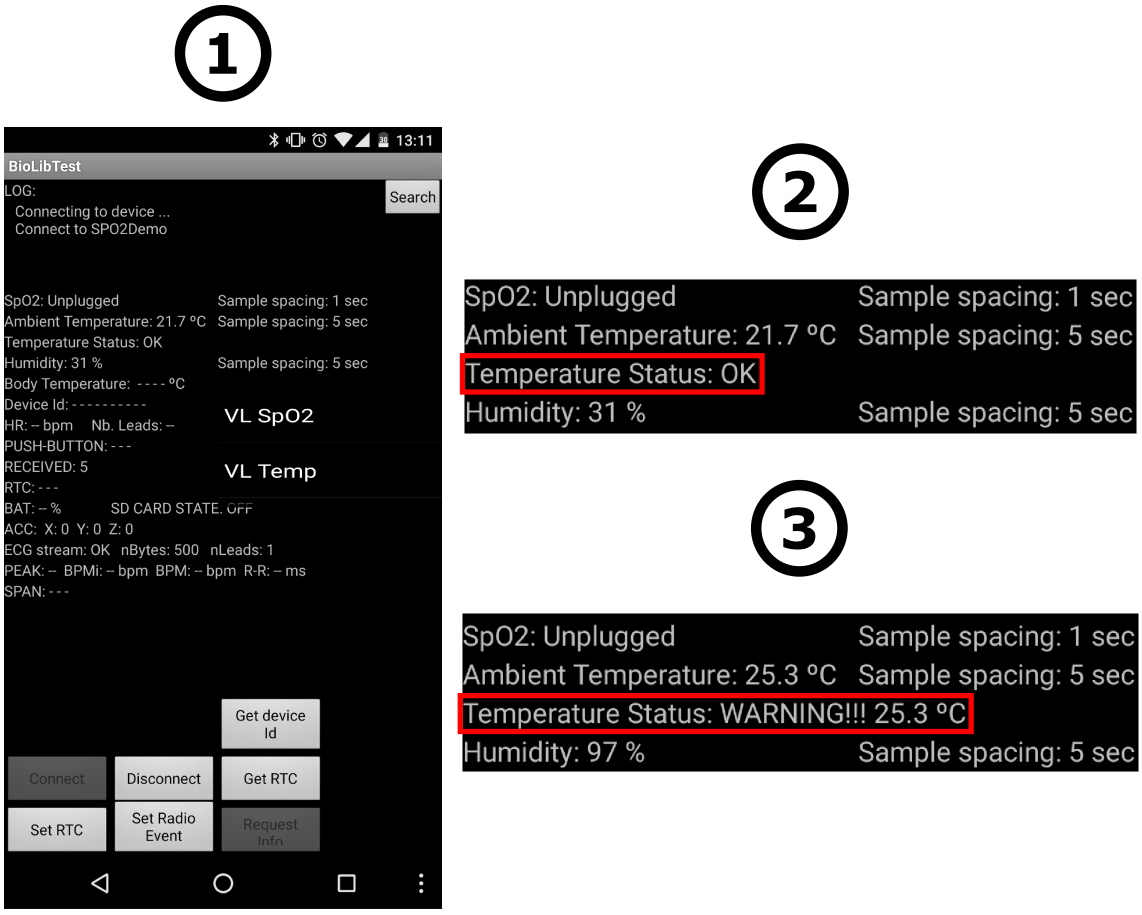

Figure 3.37: Demonstration of the mobile application with an alarm system implemented, that is triggered by ambient temperature. In this demonstration, the application was configured to trigger the alarm when ambient temperature rose above 25 degrees Celsius. 1 - Overall interface of the application; 2 - Temperature status showed when temperature is below the threshold; 3 - Temperature status showed when temperature is above the threshold.

temperature measurement that is triggering it, so that the Fire Chief can have an idea of how high ambient temperature is in fact.

For testing purposes, the application was implemented with a threshold of 25 degrees Celsius, to make it easier to trigger the alarm and test the application. The VitalLogger, without the SpO_2 sensor connected, was connected to the smartphone through Bluetooth. Hot air was blown to the ambient temperature sensor to make sensed temperature change. Figure 3.37 shows the resulting temperature status shown by the application when temperature is below and above the defined threshold. Figure 3.37 also displays the full graphical user interface of the application.

The resulting system reduces the data redundancy which Fire Chiefs are subjected to, and also notifies Fire Chiefs of the existence of a potential risk situation more intuitively, making it easier for the end user to interpret information gathered with the system. In order to make the alarm system more effective, it should be improved to provide sensory feedback to the Fire Chiefs, by making the device produce a loud noise, vibrate or flash the screen.

3.3.3 Non Perceptible Physiological Indicators

The core temperature estimating system, based on a Kalman filter, was implemented using k-fold cross-validation, with k=11 since the dataset used in this implementation contains data from 11 different subjects. This means that the system was trained in 10 subjects and tested in 1, in a total of 11 different combinations.

In order to assess the performance of the implemented system, and compare it with the performance of the BioHarness, RMSE was the selected metric, and rectal temperature was used as the ground truth. Due to the fact that 11 different implementations were obtained from the k-fold cross-validation approach, in order to assess the general performance of the implemented system, mean RMSE from all 11 different implementations was computed.

The mean RMSE of the implemented estimator was 1.06, but since each model was tested only in a single subject, there is the possibility of existing inaccurate RMSE values (that can either be very low or very high), which introduce bias in mean RMSE, leading to a less accurate assessment of the performance of the system. Thus, it cannot be assured that a model developed with this data will work well with all signals.

In order to verify the reliability of an implemented model, a larger dataset should be used, so that it can be tested on more data, enabling the calculation of a more reliable and representative RMSE. Another possibility is to select only the better performing models, since subject inter variability is known to exist, and it impacts on the performance of the system. As all 11 implementations were considered in the computation of the mean RMSE, the cases where the implemented model performed less well led biased the mean RMSE to a higher value. This means that by selecting only the better performing models, it is possible to have an implemented core temperature estimating system with better RMSE.

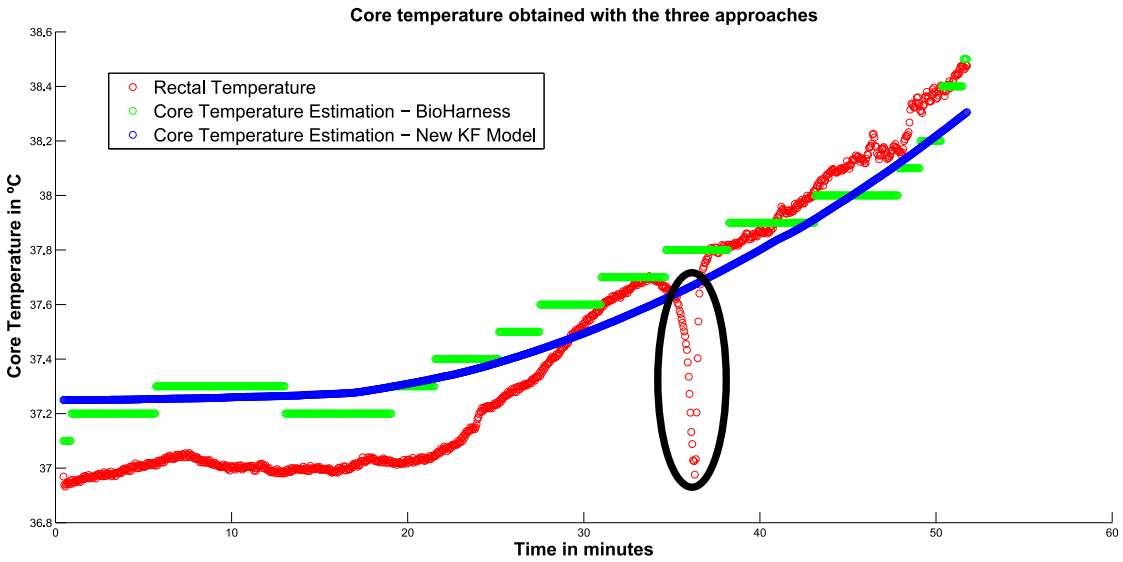

Figure 3.38: Comparison of core temperature obtained with the three different approaches: using a rectal probe (in red), using BioHarness (in green), and using the implemented system (in blue). In this case, the implemented system works quite well, following the trend of the rectal temperature. The drop in rectal temperature around the 37th minute, marked with a black ellipse, was due to problems with the probe, which had to be repositioned.

Two examples of obtained Kalman filter estimators being tested with data from the dataset are shown in Figures 3.38 and 3.39, to illustrate how significantly the performance

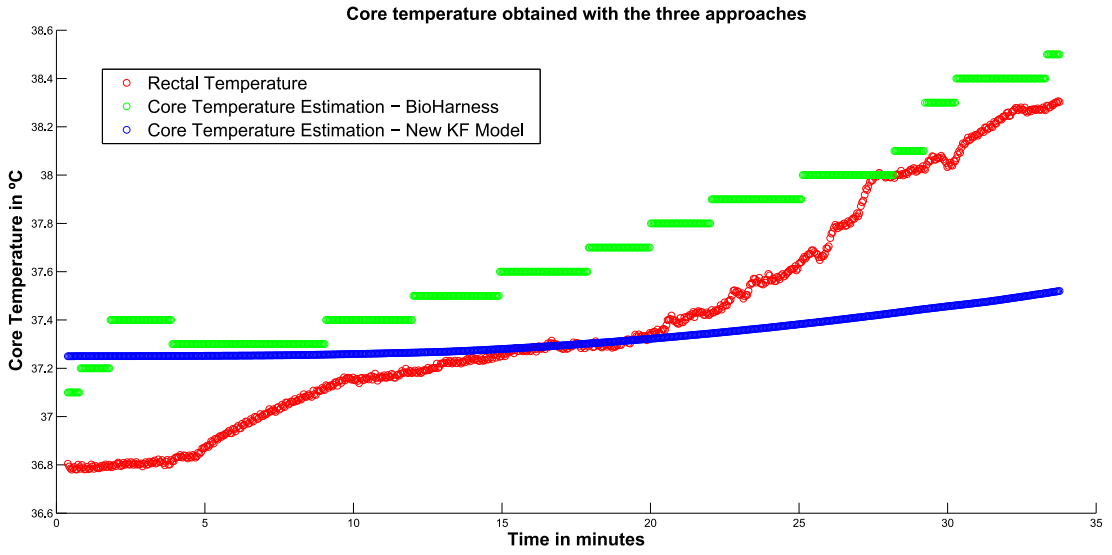

Figure 3.39: Comparison of core temperature obtained with the three different approaches: using a rectal probe (in red), using BioHarness (in green), and using the implemented system (in blue). In this case, the implemented system works very badly, producing slight changes in the estimated core temperature throughout the signal.

of the models can vary. In Figure 3.38, a relatively good estimator was obtained, with its estimations following those of BioHarness closely, and accompanying the trend of the rectal temperature signal. Similarly to BioHarness estimations, the implemented system seems to struggle in the stabilization phase of the signal, where rectal temperature is 0.2°C lower than the estimated core temperature. Nonetheless, when in exercise conditions, the system seems to perform well. The drop in rectal temperature around the 37th minute was due to problems with the probe, which had to be repositioned during the acquisition.

On the other hand, in Figure 3.39, it is easily observable that the implemented model is performing very poorly, with obtained estimations of core temperature being just slightly changed throughout the whole signal. This serves to demonstrate that the Kalman filter can perform both very well and very badly, thus, in order to have a more reliable implemented system, that performs better, a larger dataset with data from the active setting should be used, or only the better performing models should be selected.

Moreover, the performance of the implemented Kalman filter estimator was compared against that of the system implemented in BioHarness, also using RMSE as the selected metric. This is possible as both BioHarness and the implemented estimator have core temperature as the predicted variable. BioHarness' RMSE was computed for all subjects in the active setting dataset, with the mean RMSE being computed in the end.

As expected, Zephyr^{TM}'s system performs better, having a mean RMSE of 0.70, compared to the mean RMSE of 1.06 obtained with the implemented system. However, it has been shown in practical cases of Figure 3.38 and 3.39 that the implemented estimator can greatly vary depending on the data it is developed and tested on.

Therefore, while the mean RMSE from the implemented system is lower than that obtained by BioHarness, if only the better performing models (from the implemented system) are taken into account, it possible to have an implemented system with a lower RMSE that is comparable to that of BioHarness, with its value standing around 0.8.

With the heart rate measurements from BioHarness, and with the core temperature estimations from BioHarness and from the implemented predictor, PSI was then computed and compared for both systems, using RMSE as the evaluation metric.

In Figure 3.40, PSI was computed for a case where core temperature estimates were close to the real core temperature (rectal temperature). It is visible that PSI values remain close together throughout most of the signal, with PSI computed using CT estimates from the implemented core temperature estimator being overestimated in the upper range of PSI values, having a maximum PSI value of 7. It can also be seen that PSI values computed with core temperatures from the rectal probe and from BioHarness are very close to each other (with a maximum PSI of 6.2), which shows that BioHarness is a reliable core temperature estimator, as demonstrated in [78].

In Figure 3.41, PSI was computed for a case where core temperature estimates were less accurate. Here, PSI was overestimated for temperatures from both core temperature estimators. However, BioHarness' PSI is overestimated with a relatively constant offset

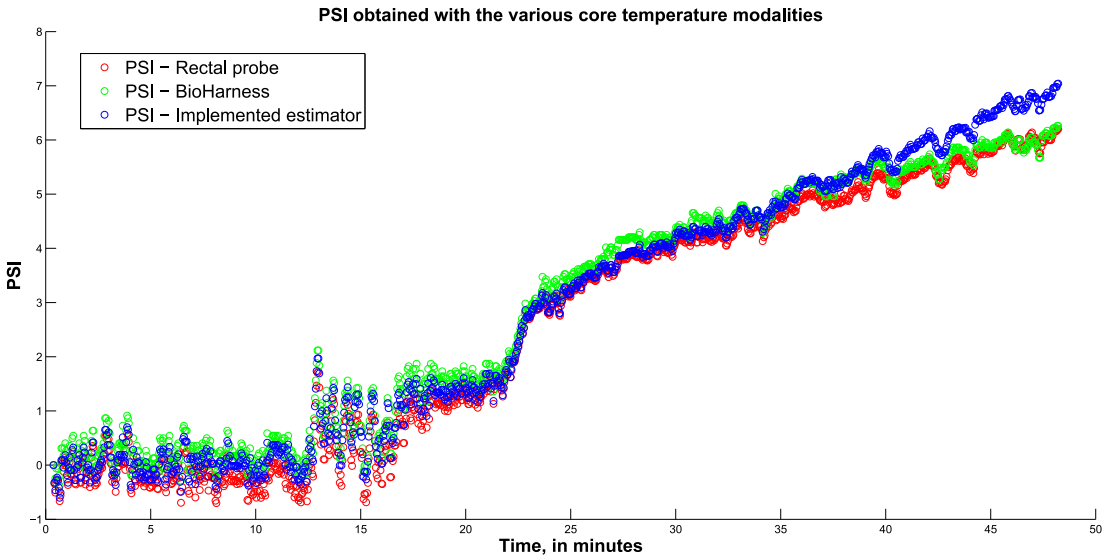

Figure 3.40: Comparison of PSI computed with core temperature from three different sources: rectal probe (in red), BioHarness (in green), and implemented system (in blue). In this case, PSI estimations remain close for core temperature from all sources, with PSI obtained using core temperature estimates from the implemented CT estimator being overestimated in the upper range of PSI values.

during the exercising period, whereas PSI obtained with core temperatures from the implemented Kalman estimator increases in a non controlled way few time after the start of the exercising period. The maximum PSI values were of 6.3, 7 and 10.6 for PSI computed with core temperatures from the rectal probe, BioHarness, and implemented core temperature estimator, respectively.

In practical terms, this means that for the situation presented in Figure 3.41, the implemented system would lead to a classification of a risk situation (because its PSI goes over 7.5) when in fact it was a controlled situation (ground truth PSI was 6.3). However, this type of situation is only verified when the core temperature estimator also performs badly, as PSI depends directly on the core temperature estimates. As explained previously, if only the better performing models are selected for the implemented core temperature estimator, the PSI estimator will also have better performance, hence this type of situations will be minimized.

It is also important to refer that, by analysing PSI for core temperatures obtained with the rectal probe, it is possible to see that the maximum PSI value registered during the experiment was of 6.3. Considering that the risk threshold for PSI is at 7.5, this shows that the experiments where data was acquired stayed within the safe range of physiological stress. Other studies have reported that PSI begins to increase noticeably when skin temperature is above 36°C [54], and, in fact, it can be seen in Figures 3.40 and 3.41 that PSI starts increasing more noticeably some time after the subjects starts exercising, which when matched with data from core temperature estimation, and from

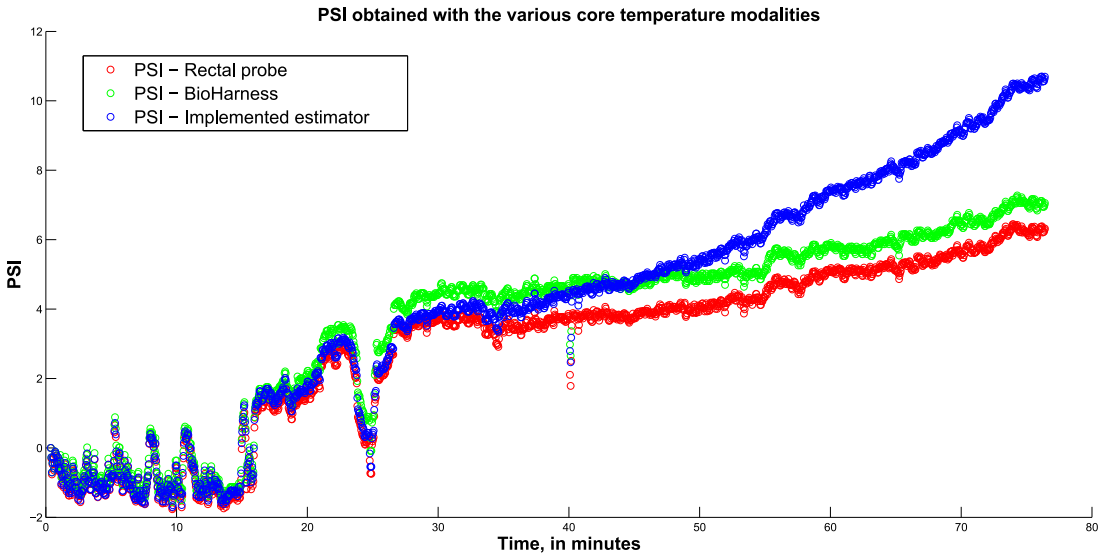

Figure 3.41: Comparison of PSI computed with core temperature from three different sources: rectal probe (in red), BioHarness (in green), and implemented system (in blue). In this case, PSI estimations are worse for both CT estimating systems, but while with CT estimations from BioHarness, PSI is constantly overestimated with an almost fixed offset, for the implemented CT estimator PSI overshoots in temperatures obtained during the exercise phase.

the comparison of rectal temperature with skin temperatures, corresponds to when skin temperature is above around 36°C, thus corroborating what is described in the literature.

To compare PSI estimations from both sources of estimated core temperature, it was necessary to compute the RMSE of PSI estimations for all 11 developed core temperature estimators, and the RMSE of PSI estimations for BioHarness applied in all 11 subjects' data. PSI obtained with rectal temperature was used as the ground truth.

Zephyr's BioHarness presented a RMSE of 0.64 whereas the implemented estimator presented a RMSE of 1.94. This shows that core temperature estimations from BioHarness can be used to estimate PSI more reliably than core temperature estimations obtained with the implemented CT predictor. This is expected since PSI only needs HR and CT to be computed, and the average implemented CT predictor currently performs worse than BioHarness' CT estimator.

Nonetheless, and as it was referred previously, if the implemented core temperature estimator is based only on the better performing models, it is possible to have an implemented system that has a performance more comparable to that of BioHarness, which means that it is possible to have a good core temperature estimator implemented in VitalResponder, that can be further used as a good PSI estimator.

With these two new physiological indicators - core temperature and PSI - which better represent the physiological state of firefighters, an alarm system can be implemented in the Android application that interfaces the wearable system and the Fire Chief, so that

this relevant physiological information can be provided in an intuitive and practical way to the Fire Chiefs, hopefully contributing to make firefighters' job more secure.

Chapter 4

Conclusions and Future Work

While wearable health systems are a promising and attractive market, most of its applications are focused on medical applications, and more recently on sports and fitness. Nevertheless, the versatility of wearable health systems enables their adaptation to different target markets. This Master thesis focused on improving an existing wearable health system that is centered on first responders, by providing not only more but better information to first responders. In order to accomplish this objective, a workflow of three different steps was elaborated to address different issues of the system. While it was managed to complete some of the projected objectives, others were only partially fulfilled. In the following lines the status of the objectives of each step will be summed up, and some indications for future work will be provided.

The first step regarded providing more information to first responders, by increasing the number of sensors available in the wearable system. This objective was successfully completed with the adaptation of existing high-level firmware and SDK from VitalJacket to VitalLogger, a prototype wearable health system that expands the sensing capabilities of VitalJacket by adding a SpO_2, ambient temperature and humidity sensor. This system can be integrated in VitalResponder, increasing the amount of data it can provide to first responders.

However, since there might be other sensing needs in the future that require the addition of more sensors, VitalLogger's firmware was prepared for a migration into a modular architecture. Here, a SPI protocol was successfully designed and implemented for the communication between master and slaves, but since there are currently no modules available, the protocol was tested in a simulated hardware set using development boards. The system is prepared so that configurations for new modules to be developed only need to be introduced in the master's parsing state machine, in order for the master to know how to correctly handle data received from each slave. In order to further improve the system, the capability of turning sensors from the modules on and off when needed is an interesting new feature to add.

Regarding the second step, which addressed the issue of selecting only relevant in-

formation from acquired data, and conveying it in an intuitive way to the Fire Chief, the projected objectives were also completed by creating a system that is capable of autonomously selecting the relevant data in a sensed signal, and also through the creation of an alarm system that informs that Fire Chief about the safety status of ambient temperature. However, there are several improvements that can be made to the system. Firstly, new parameter specifications for the data selection algorithm can be obtained by developing the algorithm on a more complete signal simulator. Not only that, but specific configurations can be developed for different types of signal (SpO_2, ambient temperature, etc) and added to the system as presets that can be easily selected during implementation in the firmware. This will ensure that the data selecting system performs well for the various different types of signals.

Another interesting aspect for future work is to develop the data selecting system with other metrics, such as signal variance, which might be more effective in the selecting process. These new metrics must be analysed along with the available hardware resources, as a metric like signal variance might require a larger buffer size in order to work properly.

Lastly, and regarding the communication of selected information in an intuitive way to the Fire Chiefs, the alarm system for signals such as ambient temperature can be improved to provide sensory feedback (vibrate, produce a loud noise, flash) to the Fire Chiefs when in the presence of a dangerous situation. This feature is very important as with all the chaos that exists in the field, sensory feedback has the potential to alert the Fire Chief more effectively.

Finally, in what regards the third step, which addressed the issue of providing relevant physiological information from first responders that cannot be measured directly with sensors, the defined objectives were only partially completed. The first part, which comprised getting access to a database with different sensing modalities (rectal and skin temperature, heat flux and heart rate), and assembling a dataset with that information was successfully completed. Since the assembled dataset contains various sensing modalities for different experimental conditions, it can be useful, in the future, for other works that are not directly related to the core temperature estimator.

The second part involved developing a core temperature estimator with a performance similar to that of an existing system in the market, which is the BioHarness. This objective was partially completed as the obtained estimator must still be improved before implementing in the VitalResponder. Future work to improve the first version of the estimator can involve improving the estimation of certain parameters of the Kalman filter, namely the mapping matrix H_k.

With a robust estimator that uses only heart rate measurements to estimate core temperature, it is possible to compute PSI values, which can be implemented in an alarm system. Similarly to what was suggested in the second step, this alarm system should provide sensory feedback (e.g. producing a loud sound) in case of an existing risk situation. Finally, the estimator can be improved even further, by adding data from skin

temperature sensors to increase the accuracy of the core temperature estimations, which will consequently improve the accuracy of computed PSI values, while reducing the bias in PSI resultant from heart rate measurements.

Work developed during this thesis had the objective of moving towards a more complete wearable sensing system. The improvements made with this work were projected with the intent of matching the specific needs of first responders. Nevertheless, since the wearable solution and technology from Biodevices SA is versatile, the newly implemented features can be exploited for different uses and target markets. Moreover, it is hoped that after implementing the suggested improvements, specially regarding the core temperature estimator, the resulting work from this thesis can help Biodevices SA expanding its solutions.

References

[1] D. Curone, E. L. Secco, A. Tognetti, G. Loriga, G. Dudnik, M. Risatti, R. Whyte, A. Bonfiglio, and G. Magenes, "Smart garments for emergency operators: the proeTEX project," *IEEE Trans Inf Technol Biomed*, vol. 14, no. 3, pp. 694–701, 2010. [Online]. Available: http://www.ncbi.nlm.nih.gov/pubmed/20371413

[2] "Know thyself: Tracking every facet of life, from sleep to mood to pain, 24/7/365," June 2009 2009. [Online]. Available: http://archive.wired.com/medtech/health/magazine/17-07/lbnp_knowthyself?currentPage=all

[3] A. Lymberis and L. Gatzoulis, "Wearable health systems: from smart technologies to real applications," *Conf Proc IEEE Eng Med Biol Soc*, vol. Suppl, pp. 6789–92, 2006. [Online]. Available: http://www.ncbi.nlm.nih.gov/pubmed/17959513

[4] J. P. Cunha, "pHealth and wearable technologies: a permanent challenge," *Stud Health Technol Inform*, vol. 177, pp. 185–95, 2012. [Online]. Available: http://www.ncbi.nlm.nih.gov/pubmed/22942053

[5] P. Lukowicz, T. Kirstein, and G. Troster, "Wearable systems for health care applications," *Methods Inf Med*, vol. 43, no. 3, pp. 232–8, 2004. [Online]. Available: http://www.ncbi.nlm.nih.gov/pubmed/15227552

[6] C. C. Poon and Y. T. Zhang, "Perspectives on high technologies for low-cost healthcare," *IEEE Eng Med Biol Mag*, vol. 27, no. 5, pp. 42–7, 2008. [Online]. Available: http://www.ncbi.nlm.nih.gov/pubmed/18799389

[7] R. Paradiso, G. Loriga, and N. Taccini, "A wearable health care system based on knitted integrated sensors," *IEEE Transactions on Information Technology in Biomedicine*, vol. 9, no. 3, pp. 337–344, 2009.

[8] S. Tennina, M. Di Renzo, E. Kartsakli, F. Graziosi, A. S. Lalos, A. Antonopoulos, P. V. Mekikis, and L. Alonso, "WSN4QoL: A WSN-oriented healthcare system architecture," *International Journal of Distributed Sensor Networks*, 2014. [Online]. Available: <GotoISI>://WOS:000336172300001

[9] A. Asensio, A. Marco, R. Blasco, and R. Casas, "Protocol and architecture to bring things into internet of things," *International Journal of Distributed Sensor Networks*, 2014. [Online]. Available: <GotoISI>://WOS:000335325200001

[10] X. F. Teng, Y. T. Zhang, C. C. Poon, and P. Bonato, "Wearable medical systems for p-Health," *IEEE Rev Biomed Eng*, vol. 1, pp. 62–74, 2008. [Online]. Available: http://www.ncbi.nlm.nih.gov/pubmed/22274900

[11] Z. A. Khan, S. Sivakumar, W. Phillips, and B. Robertson, "ZEQoS: A new energy and QoS-aware routing protocol for communication of sensor devices in healthcare system," *International Journal of Distributed Sensor Networks*, 2014. [Online]. Available: <GotoISI>://WOS:000337435500001

[12] H. B. Lim, D. Ma, B. Wang, Z. Kalbarczyk, R. Iyer, and K. Watkin, "A soldier health monitoring system for military applications," in *Body Sensor Networks (BSN), 2010 International Conference on*, June 2010, pp. 246–249.

[13] H. Y. Xu, L. Y. Wang, and H. Xie, "Design and experiment analysis of a hadoop-based video transcoding system for next-generation wireless sensor networks," *International Journal of Distributed Sensor Networks*, 2014. [Online]. Available: <GotoISI>://WOS:000333838200001

[14] "Cooperative communication." [Online]. Available: http://wcomm.ulsan.ac.kr/research/research.htm

[15] "ZigBee® wireless standard." [Online]. Available: http://www.digi.com/technology/rf-articles/wireless-zigbee

[16] "Wireless connectivity - overview for ZigBee® (IEEE 802.15.4)." [Online]. Available: http://www.ti.com/lsds/ti/wireless_connectivity/zigbee/overview.page?DCMP=hpa_rf_general&HQS=NotApplicable+OT+zigbee

[17] "What is ZigBee?" [Online]. Available: http://zigbee.org/what-is-zigbee/

[18] G. Appelboom, E. Camacho, M. E. Abraham, S. S. Bruce, E. L. Dumont, B. E. Zacharia, R. D'Amico, J. Slomian, J. Y. Reginster, O. Bruyere, and J. Connolly, E. S., "Smart wearable body sensors for patient self-assessment and monitoring," *Arch Public Health*, vol. 72, no. 1, p. 28, 2014. [Online]. Available: http://www.ncbi.nlm.nih.gov/pubmed/25232478

[19] F. Seoane, I. Mohino-Herranz, J. Ferreira, L. Alvarez, R. Buendia, D. Ayllon, C. Llerena, and R. Gil-Pita, "Wearable biomedical measurement systems for assessment of mental stress of combatants in real time," *Sensors (Basel)*, vol. 14, no. 4, pp. 7120–41, 2014. [Online]. Available: http://www.ncbi.nlm.nih.gov/pubmed/24759113

[20] A. B. Farjadian, M. L. Sivak, and C. Mavroidis, "SQUID: sensorized shirt with smartphone interface for exercise monitoring and home rehabilitation," *IEEE Int Conf Rehabil Robot*, vol. 2013, p. 6650451, 2013. [Online]. Available: http://www.ncbi.nlm.nih.gov/pubmed/24187268

[21] "EQ02 LifeMonitor - sensor electronics module (SEM)." [Online]. Available: http://www.equivital.co.uk/assets/common/SEM_Data_Sheet_General_HIDA3330-DSG-02.2_.2_.pdf

[22] "BioHarness 3 - wireless professional heart rate monitor & physiological monitor with bluetooth." [Online]. Available: http://zephyranywhere.com/products/bioharness-3/

[23] "BioPatch™ wireless device." [Online]. Available: http://zephyranywhere.com/products/biopatch/

[24] "First Responders - Zephyr Technology Corporation." [Online]. Available: http://www.zephyranywhere.com/training-systems/first-responders

[25] "WASP: Wearable Advanced Sensor Platform." [Online]. Available: http://www.globeturnoutgear.com/innovations/wasp

[26] "WASP^{TM} - Wearable Advanced Sensor Platform - brochure." [Online]. Available: http://www.globeturnoutgear.com/uploads/PDFs/Globe_Catalog_WASP_System.pdf

[27] "ProeTEX partners." [Online]. Available: http://www.proetex.org/partners.htm

[28] E. L. Secco, D. Curone, A. Tognetti, A. Bonfiglio, and G. Magenes, "Validation of smart garments for physiological and activity-related monitoring of humans in harsh environment," *AMERICAN JOURNAL OF BIOMEDICAL ENGINEERING*, vol. 2, 2012. [Online]. Available: http://dx.medra.org/10.5923/j.ajbe.20120204.07

[29] C. Hertleer, S. Odhiambo, and L. Van Langenhove, *12 - Protective clothing for firefighters and rescue workers.* Woodhead Publishing, 2013, pp. 338–363. [Online]. Available: http://www.sciencedirect.com/science/article/pii/B9780857090560500121

[30] M. R. Roberts, "Watch and wear - globe turnout gear," January 2013 2013. [Online]. Available: http://goo.gl/gcnZcJ

[31] "What is P25 technology?" [Online]. Available: http://www.project25.org/technology

[32] Tehrani, Kiana, and A. Michael, "Wearable technology and wearable devices: Everything you need to know," March 26, 2014. [Online]. Available: http://www.wearabledevices.com/what-is-a-wearable-device/

[33] "Wearable device market value from 2010 to 2018 (in million u.s. dollars)," May 2013. [Online]. Available: http://www.statista.com/statistics/259372/wearable-device-market-value/

[34] M. Boustany and J. Bouchaud, "MEMS & sensors for wearables report - 2014," September 30, 2014. [Online]. Available: https://technology.ihs.com/496122/mems-sensors-for-wearables-2014

[35] V. Yussuff, "Apple watch spurs rapid growth of market for wireless charging in wearable technology in 2015," January 15, 2015. [Online]. Available: http://goo.gl/l65t08

[36] A. Michael, "Morgan stanley: Wearable devices a potential $1.6 trillion business," November 20, 2014. [Online]. Available: http://www.wearabledevices.com/2014/11/20/morgan-stanley-wearable-devices/

[37] J. Bouchaud, "Wearable sensor market to expand sevenfold in five years," October 16, 2014. [Online]. Available: https://technology.ihs.com/513647/wearable-sensor-market-to-expand-sevenfold-in-five-years

[38] "Wearable technology application chart." [Online]. Available: http://www.beechamresearch.com/article.aspx?id=20

[39] V. Yussuff, "Wireless charging in wearable technology report - 2015," December 19, 2014. [Online]. Available: https://technology.ihs.com/518744/wireless-charging-in-wearable-technology-2015

[40] E. Markowitz, "How the department of homeland security is tapping silicon valley for futuristic first-responder gear," November 2015. [Online]. Available: http://www.ibtimes.com/how-department-homeland-security-tapping-silicon-valley-futuristic-first-responder-2111288

[41] M. Elliott and A. Coventry, "Critical care: the eight vital signs of patient monitoring," *Br J Nurs*, vol. 21, no. 10, pp. 621–5, 2012. [Online]. Available: http://www.ncbi.nlm.nih.gov/pubmed/22875303

[42] A. J. Bandodkar and J. Wang, "Non-invasive wearable electrochemical sensors: a review," *Trends Biotechnol*, vol. 32, no. 7, pp. 363–71, 2014. [Online]. Available: http://www.ncbi.nlm.nih.gov/pubmed/24853270

[43] G. Tröster, "The Agenda of Wearable Healthcare," *IMIA Yearbook of Medical Informatics 2005: Ubiquitous Health Care Systems*, pp. 125–38, 2005.

[44] Y. M. Chi, J. Tzyy-Ping, and G. Cauwenberghs, "Dry-contact and noncontact biopotential electrodes: Methodological review," *Biomedical Engineering, IEEE Reviews in*, vol. 3, pp. 106–119, 2010.

[45] J. A. G. Gnecchi, A. D. V. Herrejon, A. D. T. Anguiano, A. M. Patino, and D. L. Espinoza, "Advances in the construction of ECG wearable sensor technology: The ECG-ITM-05 eHealth data acquisition system," *2012 Ieee Ninth Electronics, Robotics and Automotive Mechanics Conference (Cerma 2012)*, pp. 338–342, 2012. [Online]. Available: <GotoISI>://WOS:000324574000057

[46] A. D. Droitcour, O. Boric-Lubecke, V. M. Lubecke, J. S. Lin, and G. T. A. Kovacs, "Range correlation and I/Q performance benefits in single-chip silicon doppler radars for noncontact cardiopulmonary monitoring," *Ieee Transactions on Microwave Theory and Techniques*, vol. 52, no. 3, pp. 838–848, 2004. [Online]. Available: <GotoISI>://WOS:000220177500013http://ieeexplore.ieee.org/xpl/articleDetails.jsp?arnumber=1273725

[47] A. Sa-ngasoongsong, J. Kunthong, V. Sarangan, X. Cai, and S. T. S. Bukkapatnam, "A low-cost, portable, high-throughput wireless sensor system for phonocardiography applications," *Sensors*, vol. 12, no. 8, pp. 10 851–10 870, 2012. [Online]. Available: http://www.mdpi.com/1424-8220/12/8/10851

[48] Y. P. Hsu and D. J. Young, "Skin-coupled personal wearable ambulatory pulse wave velocity monitoring system using microelectromechanical sensors," *Ieee Sensors Journal*, vol. 14, no. 10, pp. 3490–3497, 2014. [Online]. Available: <GotoISI>://WOS:000341629100004

[49] J. Franco, J. Aedo, and F. Rivera, "Continuous, non-invasive and cuff-free blood pressure monitoring system," *2012 Andean Region International Conference*, pp. 31–34, 2012.

[50] S. Fuke, T. Suzuki, K. Nakayama, H. Tanaka, and S. Minami, "Blood pressure estimation from pulse wave velocity measured on the chest," *Conf Proc IEEE Eng Med Biol Soc*, vol. 2013, pp. 6107–10, 2013. [Online]. Available: http://www.ncbi.nlm.nih.gov/pubmed/24111133

[51] L. Guo, L. Berglin, U. Wiklund, and H. Mattila, "Design of a garment-based sensing system for breathing monitoring," *Textile Research Journal*, vol. 83, no. 5, pp. 499–509, 2012.

[52] J. Sola, S. Castoldi, O. Chetelat, M. Correvon, S. Dasen, S. Droz, N. Jacob, R. Kormann, V. Neumann, A. Perrenoud, P. Pilloud, C. Verjus, and G. Viardot, "SpO2 sensor embedded in a finger ring: design and implementation," *Conf Proc IEEE Eng Med Biol Soc*, vol. 1, pp. 4295–8, 2006. [Online]. Available: http://www.ncbi.nlm.nih.gov/pubmed/17946619

[53] C. Zysset, N. Nasseri, L. Buthe, N. Munzenrieder, T. Kinkeldei, L. Petti, S. Kleiser, G. A. Salvatore, M. Wolf, and G. Troster, "Textile integrated sensors and actuators for near-infrared spectroscopy," *Opt Express*, vol. 21, no. 3, pp. 3213–24, 2013. [Online]. Available: http://www.ncbi.nlm.nih.gov/pubmed/23481780

[54] E. Gaura, J. Kemp, and J. Brusey, "Leveraging knowledge from physiological data: On-body heat stress risk prediction with sensor networks," *Biomedical Circuits and Systems, IEEE Transactions on*, vol. 7, no. 6, pp. 861–870, Dec 2013.

[55] M. J. Buller, W. J. Tharion, R. W. Hoyt, and O. C. Jenkins, "Estimation of human internal temperature from wearable physiological sensors." in *Innovative Applications of Artificial Intelligence Conference*, 2010, Conference Proceedings.

[56] M. J. Buller, W. J. Tharion, S. N. Cheuvront, S. J. Montain, R. W. Kenefick, J. Castellani, W. A. Latzka, W. S. Roberts, M. Richter, O. C. Jenkins, and R. W. Hoyt, "Estimation of human core temperature from sequential heart rate observations," *Physiological Measurement*, vol. 34, no. 7, p. 781, 2013. [Online]. Available: http://stacks.iop.org/0967-3334/34/i=7/a=781

[57] M. N. Sawka and A. J. Young, *Chapter 23 - Physiological Systems and Their Responses to Conditions of Heat and Cold*. Lippincott Williams & Wilkins, 2006.

[58] Z. Popovic, P. Momenroodaki, and R. Scheeler, "Toward wearable wireless thermometers for internal body temperature measurements," *Ieee Communications Magazine*, vol. 52, no. 10, pp. 118–125, 2014. [Online]. Available: <GotoISI>://WOS:000346036300018

[59] C. Boano, M. Lasagni, K. Romer, and T. Lange, "Accurate temperature measurements for medical research using body sensor networks," in *Object/Component/Service-Oriented Real-Time Distributed Computing Workshops (ISORCW), 2011 14th IEEE International Symposium on*, March 2011, pp. 189–198.

[60] R. C. Webb, A. P. Bonifas, A. Behnaz, Y. Zhang, K. J. Yu, H. Cheng, M. Shi, Z. Bian, Z. Liu, Y. S. Kim, W. H. Yeo, J. S. Park, J. Song, Y. Li, Y. Huang, A. M. Gorbach, and J. A. Rogers, "Ultrathin conformal devices for precise and continuous thermal characterization of human skin," *Nat Mater*, vol. 12, no. 10, pp. 938–44, 2013. [Online]. Available: http://www.ncbi.nlm.nih.gov/pubmed/24037122

[61] X. Xu, A. J. Karis, M. J. Buller, and W. R. Santee, "Relationship between core temperature, skin temperature, and heat flux during exercise in heat," *European Journal of Applied Physiology*, vol. 113, no. 9, pp. 2381–2389, 2013. [Online]. Available: http://dx.doi.org/10.1007/s00421-013-2674-z

[62] D. S. Moran, A. Shitzer, and K. B. Pandolf, "A physiological strain index to evaluate heat stress," *American Journal of Physiology - Regulatory, Integrative and Comparative Physiology*, vol. 275, no. 1, pp. R129–R134, 1998.

[63] M. J. Buller, W. A. Latzka, M. Yokota, W. J. Tharion, and D. S. Moran, "A real-time heat strain risk classifier using heart rate and skin temperature," *Physiological Measurement*, vol. 29, no. 12, p. N79, 2008. [Online]. Available: http://stacks.iop.org/0967-3334/29/i=12/a=N01

[64] J. P. S. Cunha, B. Cunha, A. S. Pereira, W. Xavier, N. Ferreira, and L. Meireles, "Vital-Jacket®: A wearable wireless vital signs monitor for patients' mobility in cardiology and sports," in *Pervasive Computing Technologies for Healthcare (PervasiveHealth), 2010 4th International Conference on-NO PERMISSIONS*, 2010, Conference Proceedings, pp. 1–2.

[65] "VitalJacket® - real ECG to monitor real life," 2013. [Online]. Available: http://www.vitaljacket.com/wp-content/uploads/2013/07/VJ_2013_en.pdf

[66] "VitalJacket®." [Online]. Available: http://www.vitaljacket.com/?page_id=153

[67] "VitalResponder Project." [Online]. Available: http://www.vitalresponder.pt/

[68] "VitalResponder 2.0 | Vital Responder 2.0 Project: Intelligent management of critical events of stress, fatigue and smoke intoxication in forest firefighting." 2015. [Online]. Available: http://vitalresponder.web.ua.pt/

[69] X. Lai, Q. Liu, X. Wei, W. Wang, G. Zhou, and G. Han, "A survey of body sensor networks," *Sensors*, vol. 13, no. 5, p. 5406, 2013. [Online]. Available: http://www.mdpi.com/1424-8220/13/5/5406

[70] T. Babb, "How a kalman filter works, in pictures," August 2015. [Online]. Available: http://www.bzarg.com/p/how-a-kalman-filter-works-in-pictures/#mjx-eqn-kalpredictfull

[71] R. Faragher, "Understanding the basis of the kalman filter via a simple and intuitive derivation [lecture notes]," *Signal Processing Magazine, IEEE*, vol. 29, no. 5, pp. 128–132, Sept 2012.

[72] C. Burnett, "Serial peripheral interface bus," November 2015. [Online]. Available: http://bit.ly/1I6eIP0

[73] C. Cereske, "Learn spi - serial peripheral interface," November 2015. [Online]. Available: http://support.saleae.com/hc/en-us/articles/200895130-Learn-SPI-Serial-Peripheral-Interface

[74] M. Cunha, J. Cunha, and T. Oliveira e Silva, "Sigif: a digital signal interchange format with application in neurophysiology," *Biomedical Engineering, IEEE Transactions on*, vol. 44, no. 5, pp. 413–418, May 1997.

[75] O. S. . H. Administration, "Osha technical manual (otm) section iii: Chapter 4," November 2015. [Online]. Available: http://1.usa.gov/1P43cX5

[76] Code::Blocks, "The open source, cross platform, free c, c++ and fortran ide." November 2015. [Online]. Available: http://www.codeblocks.org/

[77] A. P. Welles, M. J. Buller, C. L. Margolis, C. D. Economos, R. W. Hoyt, and M. M. W. Richter, "Thermal-work strain during marine rifle squad operations in afghanistan," *Military Medicine*, vol. 178, pp. 1141–1147, 2013. [Online]. Available: http://publications.amsus.org/doi/pdf/10.7205/MILMED-D-12-00538

[78] Y. Seo, T. DiLeo, J. B. Powell, J.-H. Kim, R. J. Roberge, and A. Coca, "Comparison of estimated core body temperature measured with the bioharness and rectal temperature under several heat stress conditions," *Journal of Occupational and Environmental Hygiene*, To be published.

[79] R. Niedermann, E. Wyss, S. Annaheim, A. Psikuta, S. Davey, and R. M. Rossi, "Prediction of human core body temperature using non-invasive measurement methods," *International Journal of Biometeorology*, vol. 58, no. 1, pp. 7–15, 2014. [Online]. Available: http://dx.doi.org/10.1007/s00484-013-0687-2

[80] C. Engineering, "Heat flux sensors and radiometers," November 2015. [Online]. Available: http://conceptheatsensors.com/products.html

[81] greenTEG, "Products for r&d," November 2015. [Online]. Available: http://shop.greenteg.com/shop/products-rd/

[82] G. Welch and G. Bishop, "An introduction to the kalman filter. 2006," *University of North Carolina: Chapel Hill, North Carolina, US*, 2006.

Appendix A

Undergraduate Internship at CMU - Evaluation Report

Carnegie Mellon University
Office of International Education

5000 Forbes Ave, Warner Hall 3rd Floor, Pittsburgh, PA 15213
Phone: (412) 268-5231 ▪ **Email:** oie@andrew.cmu.edu ▪ **Web:** www.cmu.edu/oie

Evaluation - J-1 Student Intern

Guidelines

In accordance with US Department of State regulations, the hosting professor of a Carnegie Mellon University Student Intern must provide an evaluation of the Student Intern's program progress. The Office of International Education (OIE) is required to keep these evaluations on file for at least 3 years. Failure to submit these evaluations could jeopardize the department's ability to bring J-1 Student Interns in the future.

- Programs shorter than six months require only one evaluation be submitted near the conclusion of the internship and before the Student Intern leaves the US.
- Programs longer than six months require a mid-point evaluation and another at the conclusion of the intern's program, before the Student Intern leaves the US.
- If an extension request is made on behalf of the intern, a completed Student Intern evaluation must be submitted with the request for program extension. Extensions will not be granted to interns whose program evaluations have not been submitted. **A Student Intern program can only be extended for a maximum of 12 months.**
- Host professors must be current on intern evaluations for all interns under their sponsorship to have J-1 applications processed for new Student Interns.

Instructions

- The hosting professor must fill out Section I completely and review the evaluation with the Student Intern.
- The Student Intern must fill out Section II.
- The evaluation must be completed and returned to OIE before the Student Intern departs the US.

Section I ***(to be completed by the host professor)***

Student Intern's last name: Silva Student Intern's first name: João

Professor's name: Fernando De la Torre Title: Research Associate Professor

Hosting department: Robotics Institute

Check one: Mid program Evaluation: _____ End of program Evaluation: X

Evaluate the Student Intern's performance related to the specific objectives as outlined in the training plan.

Excellent X Above average _____ Average _____ Below Average _____

Comments: João got initialized in the machine learning. In particular, to Kalman filter techniques.

Updated 7/2014

Were there any deficiencies or problem areas that should be addressed?

Yes _____ No X

If yes, comment:

How would you rate the overall training program and its benefits to you?

Excellent X Above average _____ Average _____ Below Average _____

Comments: João did a fantastic job. He contribute to the activities in the lab.

Professor's signature: _____ **Date:** November 9, 2015

Section II ***(to be completed by the Student Intern)***

Student Intern's last name: SILVA Student Intern's first name: JOÃO
Student Intern's e-mail: JFIGUEIR@ANDREW.CMU.EDU
Dates of current training program: 21 OF AUGUST, 2015 to 13 OF NOVEMBER, 2015

How would you rate the overall training program and its benefits to you?

Excellent X Above average _____ Average _____ Below Average _____

Comments: The program was great, as it gave me the opportunity to work in an incredible environment with amazing people. I feel that I grew a lot both professionally, by working in such diverse environment, and at the personal level, as I experienced a new culture, that is enormously different from the one I am used to.

Would you recommend this program to other students in your field of study?

Yes X No _____

If no, comment:

Provide recommendations you may have to improve this internship program.

My only recommendation is to "advertise" the program more, as only a minority gets to know of this incredible opportunity.

Student Intern's signature: João Manuel Figueira da Silva **Date:** November 9, 2015

Updated 7/2014